FINAL PROGRESS REPORT

DERMAL ABSORPTION OF CHEMICALS FROM LIQUID MIXTURES

AWARD NUMBER: 5 R01 OH007493-03 REVISED

Project Period: September 1, 2004 – March 31, 2009

Principal Investigator: Annette L. Bunge, Ph.D.
Professor Emeritus
Chemical Engineering Department
Colorado School of Mines (CSM)
Golden, CO 80401
abunge@mines.edu
Phone: (303) 273-3722
FAX: (303) 273-3730

Submitted to:

NATIONAL INSTITUTE OF OCCUPATIONAL SAFETY AND HEALTH (NIOSH)

Program Official: Joan F. Karr, PhD
Scientific Program Administrator
Office of Extramural Programs
National Institute for Occupational Safety and Health
Atlanta, GA 30333
404.498.2506
jkarr@cdc.gov

Grants Management Specialist: Peter E. Grandillo Jr.
PGO/Acquisition & Assistance Field Branch, CDC
P.O. Box 18070
Pittsburgh, PA 15236
412.386.6429
png2@cdc.gov

Submitted by:
Annette L. Bunge, Principal Investigator
Colorado School of Mines (CSM)
Golden, Colorado 80401

△ COLORADOSCHOOLOFMINES

6 August 2009

TABLE OF CONTENTS

LIST OF TERMS AND ABBREVIATIONS

A	exposed skin area
AC	alternating current
ACGIH	American Conference of Governmental Industrial Hygienists
ACT	acetone
a_{BE}	thermodynamic activity of 2-butoxyethanol (unitless)
a_j	thermodynamic activity of chemical species j (unitless)
$a_{j,v}$	thermodynamic activity of chemical species j in vehicle v (unitless)
$a_{j,v}\vert_{REL}$	thermodynamic activity of solute j in vehicle v at the dermal REL
$a_{j,vy}$	thermodynamic activity of solute j in a binary mixture of solvents v and y (unitless)
$a_{v,vy}$	thermodynamic activity of solvent v in a binary mixture of solvents v and y (unitless)
$a_{y,vy}$	thermodynamic activity of solvent y in a binary mixture of solvents v and y (unitless)
a_w	thermodynamic activity of water (unitless)
BAEE units	indication of trypsin enzymatic activity characterized by the Benzoyl-L-Arginine Ethyl Ester assay
BAP	benzo(a)pyrene
BE	2-butoxyethanol
C	capacitance of a capacitor
CAS No.	Chemical Abstracts Service registry number
C_{eff}	effective skin capacitance derived from the R-CPE equivalent circuit model applied to the impedance data from skin as specified by Eq. (61)
$C_{j,sc}$	concentration of chemical species j in the stratum corneum
$C_{j,v}$	concentration of chemical species j in the vehicle v
$C_{j,v}{}^o$	constant concentration of chemical species j in a vehicle v (i.e., the concentration of j does not change during the skin exposure)
$C_{j,v}\vert_{REL}$	the concentration of solute j in vehicle v that is equal to the dermal REL
$C_{j,w}$	concentration of chemical species j in water
$C_{j,vy}$	concentration of chemical species j in the a binary mixture of vehicles v and y
C_k	capacitance of the kth Voigt element in the measurement model as described by Eq. (58)

CN	4-chloronitrobenzene (also called p-chloronitrobenzene)
CP	4-cyanophenol
CPE	constant phase element
CYC	cyclohexane
DC	direct current
DMSO	dimethyl sulfoxide
$D_{j,sc/v}$	effective diffusion coefficient for solute j in the stratum corneum from a vehicle v in which the heterogeneous stratum corneum is treated as if it were a homogeneous membrane with the same thickness
E	applied oscillating potential (voltage) in the measurement of impedance
E_o	amplitude of the oscillating potential (voltage) in the determination of impedance
EIS	electrochemical impedance spectroscopy
EPA	Environmental Protection Agency
f	frequency of the potential (voltage) perturbation in the measurement of impedance
F	Farad, units of capacitance;
$F_{j,sc/v}$	the steady-state rate of chemical permeation through the stratum corneum per area from a vehicle v (in mg hr^{-1} cm^{-2}); the steady-state flux of chemical permeation through the stratum corneum from vehicle v
HAID	highest-acceptable-internal dose
H2O	water
Hz	Hertz, unit of frequency (cycles per sec)
I	current response to the applied oscillating potential in the measurement of impedance
I_o	amplitude of the current response to the applied oscillating potential in the measurement of impedance
IPM	isopropyl myristate
j	$\sqrt{-1}$, unity in the complex plane
K_a	acid dissociation constant
$K_{j,sc/v}$	equilibrium partition coefficient of chemical species j between the stratum corneum and the *vehicle v*
$K_{o/w}$	octanol-water partition coefficient
LOAEL	lowest-observed-effect level
L_{sc}	thickness of the stratum corneum

m	number of skin samples from each subject
$M_{in,j,v}$	total absorption of chemical species j into the skin from a vehicle v across an exposed area A for an exposure time t_{exp}; the dermal systemic dose (also called internal dose) absorbed for chemical species j from a vehicle v assuming all of the absorbed chemical penetrates through the skin to enter the systemic circulation
$M_{in\,j,v}\big|_{for\ a_{j,v}=1}$	total absorption of chemical species j into the skin from a vehicle v across an exposed area A for an exposure time t_{exp} when the thermodynamic activity of j in vehicle v is equal to one (i.e., the vehicle v is saturated with j)
$M_{in\,j,v}\big|_{for\ C_{j,v}=S_{j,v}}$	total uptake of chemical species j into the skin from a vehicle v across an exposed area A for an exposure time t_{exp} when the vehicle v is saturated with j
$m_{j,sc/v}$	mass of chemical species j in a fixed area of isolated and hydrated stratum corneum that has been equilibrated with a vehicle v that is saturated with chemical species j
$m_{j,sc/vy}$	mass of chemical species j in a fixed area of isolated and hydrated stratum corneum that has been equilibrated with a binary mixture of vehicles v and y that is saturated with chemical species j
$m_{j,sc/w}$	mass of chemical species j in a fixed area of isolated and hydrated stratum corneum that has been equilibrated with water that is saturated with chemical species j
MP	methyl paraben
MW_{BE}	molecular weight of 2-butoxyethanol
MW_j	molecular weight of chemical species j
MW_v	average molecular weight of the vehicle v
MW_w	molecular weight of water
n	the number of Voigt elements in the measurement model; also the number of skin samples from different subjects
N_v	number of chemical components in a vehicle v
NIOSH	National Institute for Occupational Safety and Health
NOAEL	No-observed-adverse-effect level; equivalent to the NOEL
NP	naphthalene
OCT	1-octanol
OEL	occupational exposure limit, equivalent to the REL

PBS	phosphate buffered saline
p^*	vapor pressure
p_j	partial pressure of chemical species j in the air
p_j^*	vapor pressure of chemical species j
$p_{j,\alpha\beta}^*$	vapor pressure of chemical species j from solvent phase α saturated with solvent β
$P_{j,sc/v}$	permeability coefficient for a chemical species j transferring through the stratum corneum from a vehicle v
$P_{j,sc/w}$	permeability coefficient for a chemical species j transferring through the stratum corneum from water
$P_{j,skin/w}$	permeability coefficient for a chemical species j transferring through the skin (including the stratum corneum and viable epidermis) from water
pK_a	negative of the logarithm of the acid dissociation constant, K_a
Q	parameter characterizing the constant phase element (CPE) in the equivalent circuit model of the stratum corneum
Q_{eff}	effective Q parameter characterizing the constant phase element (CPE) as defined by Eq.(60)
QSAR	quantitative structure activity relationship
R	resistance of a resistor
R_e	resistance of the electrolyte solution surrounding the skin sample
R_k	resistance of the kth Voigt element in the measurement model as described by Eq. (58)
R_m	resistance of a resistor in the equivalent circuit model representing the stratum corneum
R_t	total resistance; sum of the resistances through the skin and the electrolyte solution surrounding the skin sample (i.e., $R_m + R_m$)
$RD_{j,v/w}$	ratio of the effective diffusion coefficients in the stratum corneum from a vehicle v and from water; equal to $D_{j,sc/v}/D_{j,sc/w}$
$RD_{j,v/y}$	ratio of the effective diffusion coefficients in the stratum corneum from vehicles v and y; equal to $D_{j,sc/v}/D_{j,sc/y}$
REL	recommended exposure limit

$Rm_{j,v/w}$ ratio of the saturated masses of chemical species j in a fixed area of isolated and hydrated stratum corneum that are in equilibrium with a vehicle v and water; equal to $m_{j,sc/v}/m_{j,sc/w}$

$Rm_{j,v/y}$ ratio of the saturated masses of chemical species j in a fixed area of isolated and hydrated stratum corneum that are in equilibrium with a vehicle v and y; equal to $m_{j,sc/v}/m_{j,sc/y}$

$Rm_{j,with/without}$ ratio of the saturated masses of chemical species j (where j is either MP or CP) in a fixed area of isolated and hydrated stratum corneum that are in equilibrium with water that is saturated with both MP and CP compared to either MP or CP alone; equal to $m_{j,sc/v}/m_{j,sc/y}$ where v is water saturated with both MP and CP and y is water saturated with either MP or CP alone

$Rm_{j,v/y}$ ratio of the saturated masses of chemical species j in a fixed area of isolated and hydrated stratum corneum that are in equilibrium with a vehicle y and v; equal to $m_{j,sc/y}/m_{j,sc/v}$

S   siemans, units of conductance (1 S = $1/\Omega$)

SC   stratum corneum

$SF_{j,sc/v}$ steady-state flux through the stratum corneum from a saturated solution of chemical species j in a vehicle v (i.e., $C_{j,v} = S_{j,v}$, which is equivalent to $a_{j,v} = 1$); maximum steady-state flux through the stratum corneum of chemical species j from a vehicle v

$SF_{j,sc/vy}$ steady-state flux through the stratum corneum from a saturated solution of chemical species j in a binary mixture of vehicles v and y (i.e., $C_{j,vy} = S_{j,vy}$, which is equivalent to $a_{j,vy} = 1$); maximum steady-state flux through the stratum corneum of chemical species j from a vehicle v

$SF_{j,sc/w}$ steady-state flux through the stratum corneum from a saturated solution of chemical species j in water (i.e., $C_{j,w} = S_{j,w}$, which is equivalent to $a_{j,w} = 1$); maximum steady-state flux through the stratum corneum of chemical species j from a vehicle w

SI Ratio   ratio of the skin dose to the inhalation dose

$S_{j,o}$ saturation concentration of chemical species j in 1-octanol

$S_{j,sc/v}$ saturation concentration of chemical species j in the stratum corneum equilibrated with a vehicle v reported as mass of chemical j per volume of hydrated SC

$\hat{S}_{j,sc/v}$	saturation concentration of chemical species j in the stratum corneum equilibrated with a vehicle v reported as mass of chemical j per mass of dry SC
$S_{j,sc/w}$	saturation concentration of chemical species j in the stratum corneum equilibrated water reported as mass of chemical j per volume of hydrated SC
$S_{j,v}$	saturation concentration of chemical species j in the vehicle
$S_{j,vy}$	saturation concentration of chemical species j in a binary mixtures of vehicles v and y
$S_{j,w}$	saturation concentration of chemical species j in water
$S_{y,\alpha}$	saturation concentration of chemical species y in solvent phase α
$S_{y,\alpha\beta}$	saturation concentration limit of chemical species y in solvent phase α saturated with solvent β
SM	safety margin
SRM	silicone rubber (polydimethyl siloxane) membranes
t	time
t^{*}	steady-state time
t_{exp}	exposure time
T_b	boiling point
T_m	melting point
TOL	toluene
UNIQUAC	UNiversal QUAsiChemical is an activity coefficient model for calculating activity coefficients based on empirical data
UNIFAC	UNIversal Functional Activity Coefficient; a semi-empirical system for the prediction of non-electrolyte activity estimation in non-ideal mixtures using a functional group approach
US	United States
V	volts (units of electric potential or voltage)
VE	viable epidermis
W	water
w_j	weight fraction of chemical species j
w_{jv}	weight fraction of species j in a multicomponent vehicle v
x_j	mole fraction of chemical species j in a solution
$x_{j,sat}$	mole fraction of chemical species j at its saturation concentration in a solution
x_{jv}	mole fraction of species j in a multicomponent vehicle v

Z	measured impedance; for an Ohmic material, the ratio of the current and potential by Ohms law (i.e., $Z = E/I$); Z is a complex number
$\hat{Z}$	model value of the impedance
Z_j	imaginary component of the impedance
$|Z|$	modulus (i.e., the magnitude) of the impedance at a given frequency $|Z|$
Z_r	real component of the impedance
$Z_r(\infty)$	real-component of the impedance at an infinitely large frequency

Greek

α	parameter characterizing the constant phase element (CPE) in the equivalent circuit model of the stratum corneum
γ_j	activity coefficient of chemical species j in a vehicle
ε_{bias}	frequency-dependant systematic experimental (i.e., bias) error in the measured impedance data
ε_{fit}	frequency-dependant systematic error due to lack of fit of the measured impedance data by the equivalent circuit model
ε_{res}	frequency-dependant residual error defined as the difference between the measured and modeled impedance
$\bar{\varepsilon}_{res,Z_r}(f)$	mean of the residual errors measured at frequency f for n scans
$\varepsilon_{res,Z_r,k}(f)$	frequency dependent residual error of the real part of the impedance measured at frequency f of scan k, as defined by Eq. (54)
ε_{stoch}	frequency-dependant stochastic error in the measured impedance data
ρ	density
σ_{Z_j}	standard deviation of the imaginary component of the stochastic error
σ_{Z_r}	standard deviation of the real component of the stochastic error
ϕ	phase-shift of the current response to the oscillation potential in the measurement of impedance
Ω	ohms, units or resistance

Subscripts

BE	2-butoxyethanol
j	chemical species j
sc	stratum corneum
skin	skin
v	vehicle
vy	a mixture of vehicles *v* and *y*
w	water
y	a second vehicle distinguished from vehicle *v*

ABSTRACT

The workplace is one of the most common venues for hazardous chemical contact with skin. Recognition of the dermal exposure hazard is essential for its control. Unfortunately, the present identification of chemicals as skin absorption hazards is inconsistent, poorly documented, and qualitative. Although a new skin notation strategy, announced by NIOSH July 2009, will designate the type(s) of skin hazard potential (e.g., systemic toxicity, direct irritant, corrosive, and sensitizing) for a given chemical and improve documentation for the hazard designation, it will provide no information about the effect of concentration or the solution containing the potentially hazardous chemical. As a result, those charged with protecting human health and safety in the workplace are forced to make judgments about safe or dangerous levels, and the type of personal protection required, with little or no information. The ultimate goal of this research effort is to provide occupational safety and health practitioners with improved guidance regarding potentially dangerous levels of skin exposure to chemicals.

While most occupational exposures of skin involve mixtures of chemicals, the interactions between multiple components and skin has received little study. This research was directed toward identifying and understanding the effect of exposures to chemical mixtures and especially non-aqueous solutions. The approach was to develop fundamental understanding of the underlying mechanisms by combining data with mathematical models of skin absorption and phase equilibrium thermodynamics. Specifically, we (i) examined experimentally the extent to which several test solutes (4-cyanophenol, methyl paraben, naphthalene, and 4-chloronitro-benzene) in water and in four non-aqueous solutions (toluene, 1-octanol, cyclohexane and isopropyl myristate) interact with each other or skin to alter the rate and/or amount of chemical absorption, (ii) developed computational procedures for estimating dermal absorption from aqueous and non-aqueous solutions containing two or more organic compounds including the effects of thermodynamic activity in the vehicle, and (iii) developed and used a new method for measuring electrochemical impedance to characterize skin barrier function and the effect of chemical or mechanical insult compared with skin permeation measurements. The results of this research are new experimental data from non-aqueous solvents and solvent mixtures and a framework for relating dermal absorption measurements and predictions for liquid mixtures to industrial health scientists in the form of useful guidelines. Outcomes from this study include: (i) preliminary guidelines for acquiring, interpreting and using data related to dermal absorption from chemical mixtures, and (ii) preliminary methods for making estimates of dermal absorption of toxic chemicals from chemical mixtures including the limits of applicability.

SECTION 1

Highlights / Significant Findings

The results generated in this project are some of the first experimental measurements of dermal absorption from solutions with two or more absorbing solutes and from mixtures of solvents. These results represent a first step towards the goal of generating recommended exposure limits (RELs) for dermal exposure to chemicals in liquids and liquid mixtures, including the effects of chemical composition of the liquid solution. In addition, we have generated electrochemical impedance spectroscopy (EIS) measurements from *in vitro* skin samples and developed methods for analyzing the measurements to extract parameters that meaningfully characterize the resistive and capacitive components of the skin.

The study of flux through skin and uptake into stratum corneum from saturated solutions of two model solutes, methyl paraben (MP) and 4-cyanophenol (CP), tested individually and in combinations with each other from water have shown that these two compounds, neither of which is considered a skin enhancer, do interact synergistically to increase the flux through skin. Additional experiments comparing uptake into stratum corneum that had and had not been delipidized suggest that CP changes MP solubility in the corneocytes.

Measurements of flux through skin and uptake into stratum corneum from saturated solutions of three model compounds (4-cyanophenol, methyl paraben, and naphthalene) from water and three model organic solvents (toluene, 1-octanol, cyclohexane) alone and in binary mixtures have been characterized for solvent-skin and solvent-solute interactions affecting the rate of solute permeation. The results include examples of solvents that do and do not increase flux and/or uptake. The uptake of naphthalene into the stratum corneum was increased significantly compared with water, whereas the solvent effect compared with water was much smaller for 4-cyanophenol and methyl paraben.

Measurements of flux through skin from saturated solutions of four model compounds (4-cyanophenol, methyl paraben, naphthalene, and 4-chloronitrobenzene) from water and isopropyl myristate (IPM) were similar supporting the recommendation that IPM be used as an alternative to water for determining skin permeation of highly lipophilic chemicals.

A thermodynamic model developed for estimating dermal absorption from non-ideal solutions was applied to solutions of 2-butoxyethanol (BE) and water. These computations show that the apparently anomalous permeation behavior of BE is predictable, and, except for nearly pure solutions of BE, due to thermodynamic activity of BE in the solution.

Thermodynamic models of the solvent mixtures have been developed for interpreting the measurements of solute permeation and uptake into skin from binary mixtures of solvent compared with determinations from the pure solvents. These calculations indicate that permeation and uptake into skin of a solute in a solvent mixture can be predicted from measurements of solute j made in the pure solvents.

Methods were developed for analyzing electrochemical impedance spectroscopy (EIS) data to obtain values for the skin resistance and effective skin capacitance.

EIS measurements and skin permeation determinations have been collected on several pieces of human skin to assess the hypothesis that the capacitive character of the skin is correlated with permeability of nonpolar solutes. The results appear to demonstrate that this is generally not the case, although further data analysis is still underway.

EIS measurements and skin permeation determinations of a nonpolar model compound (either 4-chloronitrobenzene or 4-cyanophenol) have been collected before and after treatments that alter the skin barrier function, including mechanical damage to the skin (i.e., holes added using a needle) and treatment with dimethyl sulfoxide (DMSO) or solvents. The results indicate that the electrical measurements (especially the skin resistance) are generally more sensitive to the treatments than permeation of the model compound.

EIS measurements have been collected on two layers of skin positioned with the stratum corneum (SC) of each layer in contact with each other and with a conducting solution separating the two SC layers. The results of these study show that resistance is greater when there is SC-SC contact, suggesting that channels or holes in the SC may be the primary route of charge transfer. This is consistent with previously published measurements of skin permeation through a single piece of SC compared with the SC layered on top of an epidermal membrane (Essa *et al.*, 2002).

Translation of Findings

The identification of chemicals as skin hazards has been inconsistent, poorly documented, and qualitative. In July 2009, NIOSH proposed a new *skin notation* strategy that will more clearly designate the type(s) of skin hazard potential (e.g., systemic toxicity, direct irritant, corrosive, and sensitizing) for a given chemical and improve documentation for the hazard designation. Skin notations only indicate that skin contact with a chemical could be potentially hazardous. Unlike the recommended exposure limits (RELs) for inhalation exposures, neither the old nor new skin notations provide quantitative information about the effect of concentration or the solution containing the potentially hazardous chemical. As a result, those charged with

protecting human health and safety in the workplace are forced to make judgments about safe or dangerous levels, and the type of personal protection required, with little or no information. This research effort represents the first steps toward the ultimate goal of providing occupational safety and health practitioners with improved guidance regarding potentially dangerous levels of skin exposure to chemicals. The strategy is to develop a dermal equivalent to the REL, which would be the chemical-specific concentration below which a dermal exposure could be considered safe. This REL would depend on the time and skin area exposed as well as the concentration and the solution containing the chemical. The findings of this project form a framework for developing dermal RELs. Experimental and theoretical strategies for acquiring the scientific knowledge needed to generate the desired dermal RELs have been developed and demonstrated for an initial set of model chemicals and solvents. These include methods for extrapolating the dermal REL for a given chemical: (i) in one solution to another solution (e.g., from phenol in water to phenol in toluene), (ii) from one concentration to another concentration in a non-ideal solution (i.e., when dermal absorption is not proportional to concentration), and (iii) in two pure solvents to their binary mixture. With respect to improving the quality of exposure assessment, this information allows one to screen for commonly used chemicals, of known toxicological risk, for which more detailed experimental measurements of dermal absorption are warranted.

Outcomes / Relevance / Impact

The outcomes from this study include: (i) preliminary guidelines for acquiring, interpreting and using data related to dermal absorption from chemical mixtures, (ii) preliminary methods for making estimates of dermal absorption of toxic chemicals from chemical mixtures including the limits of applicability, and (iii) methods for deriving and reporting measures of the skin barrier function (i.e., the electrical resistance and effective capacitance of the skin) from electrochemical impedance data that have been assessed for suitable quality. The findings of this study form the framework for developing a methodology to produce guidelines for skin exposure to chemicals that are more quantitative than both the old and new skin notation strategies.

SECTION 2

Scientific Report

Introduction

The workplace is one of the most common venues for hazardous chemical contact with the skin. According to NIOSH (NIOSH, 2000, 2007a), more than 13 million workers in the US are potentially exposed to chemicals that can absorb into skin. Given this, it is not surprising that skin disease is the second most common occupational illness in the United States accounting for 15-20% of all reported occupational disease (NIOSH, 2009). NIOSH estimates that occupational skin disease costs (including the cost of lost workdays and productivity) approach $1 billion dollars annually (NIOSH, 2009).

Systemic toxicity following dermal exposure is also a significant concern. Because systemic toxicity (and also progressive dermal disease such as skin cancer) manifest slowly, recognition of harm may not be recognized for months or even years. As a result, workers may be inadequately protected from dermal exposures that are not recognized as harmful.

The likelihood for health risk from a chemical exposure depends on the magnitude of the exposure as well as toxicological potency. If the exposure is small enough, often there is no toxicity. As a consequence, chemical exposure below certain levels is considered safe for nearly all workers and NIOSH has developed time-weighted average (up to 10 h/day and 40 h/wk) and short-term (usually 15 min) recommended occupational exposure limits (RELs) for inhalation, which are reported as concentration in air. A chemical's REL indicates its toxicity. Highly toxic chemicals have low REL values compared to those for less toxic chemicals. Guidelines, perhaps in the form of a dermal REL, would be useful for classifying a chemical's potential to cause dermatitis or systemic toxicity after dermal exposure.

Developing meaningful RELs for dermal exposures presents several challenges. First, experimental data for systems relevant to occupational exposures and relevant field observations are extremely limited and of dubious quality. When local toxicity has occurred, the magnitude of the dermal exposure is seldom known, and when dermal exposure is the suspected source of systemic toxicity, the contribution of skin exposure relative to other exposure routes (i.e., inhalation or ingestion) is not usually documented. Based on the data that do exist, we know that the amount of toxic chemical on the skin surface (i.e., the *exposed dose*) and the amount of chemical that penetrates through skin during the exposure (i.e., the *absorbed dose*) can be substantially different. We also know that the magnitude of this difference varies

13

significantly depending on the properties of the absorbing chemical and the exposure conditions (i.e., the length of the exposure time, the composition of the solution, and the volume of the solution). Since the potential health risks from dermal exposures depends on both absorbed dose and toxicological potency, then estimating safe limits for dermal exposure must consider the difference between absorbed and exposed doses. Adverse health effects will only occur when enough chemical absorbs through skin.

Presently, the only indication that a chemical presents a potential dermal risk is a *skin* designation in the listings of REL values by NIOSH (NIOSH, 2007b) and threshold limit values (TLVs) by the American Conference of Governmental Industrial Hygienists (ACGIH) (ACGIH, 2009). (Like RELs, TLVs are the air borne concentrations of substances at which nearly all workers may be repeatedly exposed day after day without adverse health effects (ACGIH, 2009).) Generally, this skin designation is consistent in the NIOSH and ACGIH listings and based on the ACGIH document, which states that the skin designation is given "to chemicals having potential significant contribution to the overall exposure by the cutaneous route." The process by which chemicals have been identified as skin absorption hazards has been criticized for its inconsistencies and poor documentation (Fiserova-Bergerova *et al.*, 1990; Grandjean *et al.*, 1988; Scanseti *et al.*, 1988). Significantly, a skin notation is not necessarily assigned to materials capable of causing irritation, dermatitis, and sensitization in workers (ACGIH, 2009; NIOSH, 2009). Consequently, the absence of a skin notation in these documents does not mean there is no risk from skin exposure to a particular chemical.

Recognizing that the skin notations issued by NIOSH for the past 20 years: (i) were intended to indicate only systemic toxicity (and not local toxicity to skin), (ii) have not been assigned on the basis of a standardized methodology, and (iii) do not reflect current scientific knowledge and recommendations, NIOSH announced on July 17, 2009 (http://www.cdc.gov/niosh/updates/upd-07-17-09.html) an updated and formalized strategy for skin notations that: (i) can be assigned consistently, and (ii) are capable of distinguishing the hazard potential among systemic, direct, and sensitizing effects caused by exposures of the skin to chemicals (NIOSH, 2009). In the new strategy, the potential for local dermal toxicity (i.e., direct irritant or corrosive effects to the skin itself) are notated differently from systemic toxicity, and also distinguished from the potential to cause or contribute to allergic contact dermatitis. In the absence of health effect indicators from human exposure or empirical data (either *in vivo* or *in vitro*), the new skin notation strategy (NIOSH, 2009) recommends assessing the hazard potential for systemic toxicity using a quantitative approach that is similar to that proposed by Fiserova-Bergerova (Fiserova-Bergerova *et al.*, 1990; Fiserova, 1993).

14

This quantitative estimate is based on the assumption that the mechanism of toxicological action is the same for both dermal and inhalation exposures. In this scheme, the ratio of the estimated dermal and inhalation absorbed doses (the skin-inhalation or SI ratio) is calculated. A notation indicating potential systemic hazard is assigned if the SI ratio is greater than or equal to 0.1 (NIOSH, 2009). The inhalation dose is calculated by multiplying the OEL (i.e., the recommended occupational exposure limit, which is the same as the REL) by the inhalation volume for a continuous 8-hour exposure (i.e., 10 m^3) and an inhalation retention factor of 75% (NIOSH, 2009). The calculated skin dose is the estimate of the maximum amount of dermal absorption that could occur if both hands (with an area of approximately 360 cm^2) are exposed to a saturated solution in water for 8 hours. It is calculated by multiplying the hand area by the aqueous solubility limit and an experimentally based algorithm for estimating the dermal absorption from water (a procedure that will be discussed further below).

While an improvement over the original skin notation scheme, the new strategy for assessing systemic dermal exposure hazard is limited in two important ways. First, this method fails for chemicals that may absorb dermally but have no REL because they are not sufficiently volatile to be an inhalation hazard. Second, it identifies chemicals with potential for systemic toxicity but provides no guidance regarding safe levels of exposure. For example, phenol would be designated as a potential dermal risk for systemic toxicity because its SI ratio calculated using the aqueous solubility limit of 83,000 ppm is greater than 15. (In fact, in the new skin notation strategy, phenol would be given a systemic hazard notation based on the large number of well documented poisonings from phenol exposure. The SI criteria are used only for chemicals for which information on the potential for dermal absorption hazard is inadequate.) Like the old skin notation strategy, there is no guidance of the potential hazard from systemic toxicity for exposures to aqueous solutions containing phenol below the saturation limit (e.g., to solutions with phenol concentrations of 10,000 ppm, 1,000 ppm or 100 ppm).

An important need, therefore, is to develop reliable *assessment methods* for identifying dermal exposures likely to produce local and/or systemic toxicity, and if possible, for estimating dose-response relationships to facilitate the establishment of RELs for skin.

The efforts of this project were to develop and demonstrate experimental and theoretical strategies for acquiring the scientific knowledge that is needed to generate the desired dermal RELs. To keep the problem manageable, the estimation procedures need to be fundamental enough in their development to allow for reasonable extrapolation of data from one chemical and vehicle to other chemicals and vehicles. The exposure assessment approach must represent separately the exposure situation (e.g., the concentration of all constituents in the

solution, the exposure time) and the properties of the chemical constituents (e.g., lipophilic character, molecular size, vapor pressure, and melting point). The starting goal is the ability to extrapolate the dermal REL for a given chemical in one solution to the same chemical in another solution (e.g., from phenol in water to phenol in toluene). Ultimately we seek computational procedures that allow confident extrapolation of dermal RELs for chemicals in one exposure scenario to other chemicals in the same or different exposure scenarios. Our goal is the ability to identify, based only upon structure-activity information of the chemical constituents in the solution, those chemicals or solutions of greatest concern for dermal exposure. At the level of risk evaluation, such information is important for identifying new chemicals (or new formulations) that have the potential to present significant health risk following dermal exposure. With respect to improving the quality of exposure assessment, this information allows one to screen for commonly used chemicals, of known toxicological risk, for which more detailed experimental measurements of dermal absorption are warranted.

Background

In this project we used *in vitro* testing to investigate the magnitude and mechanisms of the interactions by selected model compounds in aqueous and non-aqueous solutions to alter significantly the rate and extent of skin absorption. In addition, we studied the use of electrochemical impedance spectroscopy for characterizing skin barrier function. To put the results of this study into context, we provide In the next few page background information on the process of dermal absorption and its measurement and prediction, and on electrochemical impedance spectroscopic measurement and its interpretation and application to skin.

In-Vivo and *In-Vitro* Measurements of Dermal Absorption

It is only occasionally possible to study chemical absorption in humans, and consequently, *in vitro* measurements are often used as surrogates. Besides avoiding the risks to human subjects, *in vitro* experiments are simpler to conduct and the data are easier to interpret. The relevance of in vitro measurements to the *in vivo* situation remains controversial, although many different studies (for example, Bronaugh and Franz, 1986; Bronaugh and Maibach, 1985; Hadgraft et al., 1993; Hadgraft and Wolff, 1998; Scott et al., 1992; Scott and Ramsey, 1987; Tojo and Lee, 1989 have indicated that the two are at least qualitatively, and often quantitatively related. Rather than attempt to mimic the *in vivo* exposure, the well-designed *in vitro* study measures physicochemical parameters that control dermal absorption. Parameters determined *in vitro* are then used in mathematical models that mechanistically describe the *in vivo*

exposure. Pirot et al. (1997) and Silcox et al. (1990) are two examples of studies that demonstrate the process of using *in vitro*-derived data to predict *in vivo* observations . Pirot et al. (1997) showed that *in vivo* absorption of 4-cyanophenol into human subjects was predicted reasonably well by data from *in vitro* diffusion cell experiments. Similarly, Silcox et al. (1990) found that *in vivo* absorption of benzoic acid across human skin grafted onto congenitally nude rats could be reliably estimated using *in vitro* diffusion cell measurements from Parry et al. (1990).

Although easier and less costly than *in vivo* techniques, *in vitro* experiments still require considerable resources. Consequently, it is impossible to experimentally investigate chemical absorption for all toxic chemicals from all types of media in which they are found and experimentally tested methods for extrapolating dermal absorption data to other chemicals and exposure scenarios are needed. The goal then is to acquire experimental results for several model systems that could be extrapolated to predict behavior for other systems.

Figure 1. Schematic of human epidermis.

Origins of Skin Barrier Function

Skin's effectiveness as a chemical barrier results primarily from its composite structure (Roberts and Walters, 1998), illustrated schematically in Figures 1 and 2). The outermost layer, the stratum corneum (SC), is composed of dead, essentially impermeable keratinized cells (corneocytes) piled about 10 - 40 cells deep. As indicated in Figure 2, the intercellular space is filled with highly organized lipid bilayers (~ 10-15% of the dry SC weight), primarily consisting of ceramides, saturated free fatty acids and cholesterol with a molar ratio of 1:2:2 (Wertz, 2000; Wertz and van den Bergh, 1998). X-ray diffraction measurements and transmission electron microscopy have established repeat distances of 6 and 13 nm for the lipid bilayers. Water
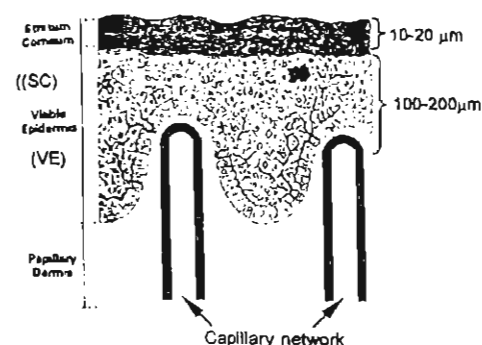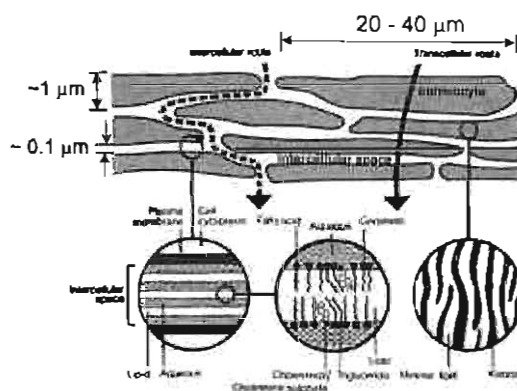

Figure 2. Schematic of SC showing intercellular and transcellular pathways; (taken from Moghimi, 1996).

within the intercellular space associates with the polar groups of the lipid constituents. Thus, the *aqueous regions* depicted in Figure 2 are most probably not literal layers and even in fully hydrated SC, there is little evidence of continuous phase water.

The viable epidermis (VE), a layer of differentiating nucleated cells, is located beneath the SC. Like the SC, the VE is avascular. The cells at the base of the VE proliferate at a rate of ~1 cell layer/day. At the same time, the outermost layer of the SC falls off at an equal rate and thus, the skin's thickness remains relatively constant. A hydrated, essentially non-cellular layer, the dermis, lies beneath the VE. Since the dermis is vascularized, chemicals only need to diffuse through the SC and VE to enter the systemic circulation. While sweat glands and hair follicles can act as diffusive *shunts* through the SC, their contribution to transport is small for most organic chemicals of moderate size (< ~ 500 Da) because they occupy only 0.1-1% of the total skin surface area (Scheuplein and Blank, 1973). In most dermal exposure situations, blood concentrations of absorbing chemicals remain small, meaning the systemic circulation acts as a sink for chemical absorption.

Compared to other biological tissues, chemical transport across skin is a relatively simple process. Chemical penetration through the SC and VE occurs via passive Fickian diffusion (Barry, 1999). There is no convection (unless large electrical currents are applied) and no evidence of active or facilitated transport. In addition, diffusion coefficients through the highly organized SC are significantly smaller than that through the much less organized VE. Thus, except for highly lipophilic solutes (which have difficulty transferring from the SC to the hydrophilic VE), the SC controls chemical penetration through skin. Consequently, in the following discussion we will refer to penetration through skin as penetration through the SC.

Mass transfer across the SC appears to follow either polar or nonpolar pathways, depending upon the hydrophilic-lipophilic character of the penetrating molecule (Barry and Bennett, 1987). Evidence for this is provided in Figure 3 (taken from Peck et al., 1995), which compares measurements in human SC of electrical resistance with steady-state rates of chemical penetration for urea, a polar chemical (i.e., $\log K_{o/w}$ = -2.11, where $K_{o/w}$ is the octanol-water partition coefficient) and corticosterone, a nonpolar chemical (i.e., $\log K_{o/w}$ = 1.94). Since electrical resistance measures the inverse of ionic mobility, decreasing values of resistance should correspond with easier penetration through the aqueous polar pathway. Furthermore, because ionic migration through the lipid pathway is small, electrical resistance measurements should be insensitive to changes in the nonpolar pathway. Thus, as Figure 3 shows, electrical resistance is correlated with permeability of the polar compound (urea) but independent of permeability for the nonpolar compound (corticosterone). This distinction between polar and

nonpolar pathways and the potential for alteration one or both pathways in the presence of chemical mixtures was an important element in the research strategy of this project.

Multicomponent solutions may consist of one or more toxic chemicals along with other non-toxic components, all of which may absorb dermally and perhaps alter the absorption properties of each other. Many dermal exposures in the workplace are of this type. Skin contact with petroleum distillates (including gasoline, kerosene, fuel oils, and naphtha), cutting fluids, cleaning/degreasing products, paints and coatings, automotive fluids, pesticides, and aircraft de-icing formulations, are just a few examples. Sometimes one or more of the components of the solution may evaporate during the exposure. However, for many exposures, the

Figure 3. Correlation between permeability (cm s^{-1}) and electrical resistance (kΩ cm^2) for (a) urea and (b) corticosterone (from Peck *et al.*, 1995.

solution is modestly volatile and evaporation only moderately affects dermal absorption. In other exposure situations, the evaporation of volatile components may be prevented by some degree of occlusion (e.g., gloves or clothing). Consequently, the focus of this project has been liquid solutions that do not evaporate or are prevented from evaporating during the skin exposure.

Penetration of a chemical through skin often is characterized by the *permeability coefficient*, which is the ratio of the steady-state flux (i.e., the area normalized rate of transfer through the skin) of the chemical from a given vehicle divided by the concentration of the chemical in the vehicle. Flux through skin is a *solution-diffusion* process. That is, the penetrating chemical must first *dissolve* into the outermost layer of the SC before it can *diffuse* across the SC. Diffusion coefficients in the SC depend primarily on molecular size and chemicals of similar size usually have similar diffusion coefficients. Significantly, chemicals with similar sizes can exhibit skin permeability coefficients that differ by 3 or 4 orders of magnitude. For example, although trichloroethylene and 5-fluorouracil have essentially the same *MW*, their
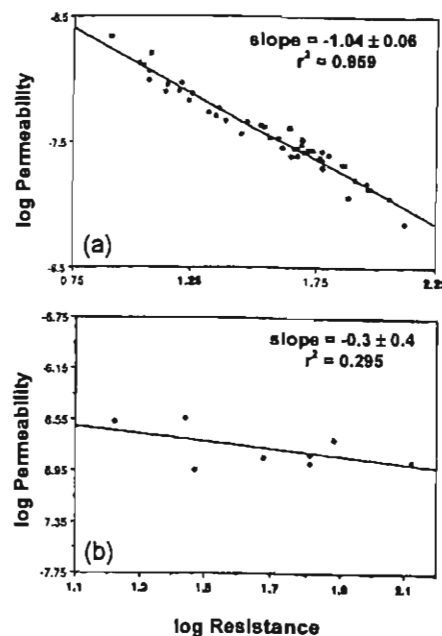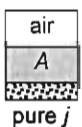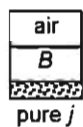
19

permeability coefficients into human skin differ by a factor of 12,000 (Nakai *et al.*, 1995; Rigg and Barry, 1990)! This is because more trichloroethylene dissolves into human SC than does 5-fluorouracil. Penetration through skin is slow compared to diffusion in liquids. Consequently, when a liquid solution contacts skin, all components in the solution rapidly establish equilibrium with the outermost layer of the SC. Equilibrium between phases limits the amount and rate of dermal absorption. In the next sections, we review the pertinent aspects of phase equilibrium.

<u>Phase Equilibrium Thermodynamics</u>

When two phases brought into contact have exchanged their constituents until the composition of each phase is constant, we say that the phases are in *equilibrium*. Generally, the compositions of two phases in equilibrium are different from one another and this difference is linked directly to the chemical nature of all components present in the two phases. Table 1 illustrates phase equilibrium in 5 systems relevant to the mechanisms of dermal absorption and to methods for experimentally studying dermal absorption. In the simplest system, a pure solid *j* is in equilibrium with air, and consequently, the partial pressure of *j* in the air (p_j) is equal to the

Table 1. Phase equilibrium in example systems relevant to dermal absorption mechanisms and experiments

Equilibrium System	1	2	3	4	5
Schematic Diagram	air pure *j*	air A pure *j*	air B pure *j*	air B A pure *j*	air B A pure *j*
Phase(s) in Equilibrium with Pure Solid *j* and Air	None	A	B	Not Miscible A & B	Partly Miscible A & B
Pressure of *j* in air [a]	p_j^*	p_j^*	p_j^*	p_j^*	$p_{j,A/B}^* = p_{j,B/A}^*$
$ Concentration of: [b]					
Solute *j* in A	no A	$S_{j,A}$	no A	$S_{j,A}$	$S_{j,A/B}$
Solute *j* in B	no B	no B	$S_{j,B}$	$S_{j,B}$	$S_{j,B/A}$
B in A	no A	no B	no A	$S_{B,A} = 0$	$S_{B,A} \neq 0$
A in B	no B	no B	no A	$S_{A,B} = 0$	$S_{A,B} \neq 0$

[a] p_{j^*} = vapor pressure of solute *j*; $p_{j^*,\alpha/\beta}$ = vapor pressure of solute *j* from phase α saturated with β

[b] $S_{y,\alpha}$ = solubility limit of *y* in phase α alone; $S_{y,\alpha/\beta}$ = solubility limit of *y* in phase α saturated with β

20

vapor pressure of j (p_j^*). In systems 2 and 3, a pure solid j is in equilibrium with air and either phase A (in system 2) or phase B (in system 3). The concentrations of j in systems 2 and 3 are then at the solubility limit in A and B, which we will designate as $S_{j,A}$ and $S_{j,B}$, respectively. Unless phases A and B are chemically similar, the concentration of solute j in each will be different (i.e., $S_{j,A} \neq S_{j,B}$). Despite this, the partial pressure of j in the air of systems 2 and 3 is exactly the same as in system 1 (i.e., $p_j = p_j^*$). This is because air in equilibrium with another phase that is in equilibrium with j is thermodynamically the same as air in equilibrium with j alone. For example, the partial pressure of naphthalene (j) in air that is equilibrium with either water (A) or toluene (B) is the same ($p_j = p_j^* = 0.085$ mm Hg) even though the concentration of naphthalene in toluene is almost 10,000 times larger than its concentration in water (i.e., $S_{j,B} = 286$ mg mL^{-1} and $S_{j,A} = 0.031$ mg mL^{-1} at 25°C).

In systems 4 and 5, a pure solid j is in equilibrium with air and both phases A and B. In system 4, A and B have no solubility in each other (i.e., $S_{A,B} = 0$ and $S_{B,A} = 0$), and the concentrations of j in phases A and B and the partial pressure in air (p_j) are the same as in systems 2 and 3. This is because contact between phases A and B does not change the composition of either phase A or B. Often, as illustrated by system 5, A and B will be partially miscible and, at equilibrium, phase A will be saturated with respect to B (i.e., $S_{B,A} \neq 0$) and phase B will be saturated with A (i.e., $S_{A,B} \neq 0$). Equilibrium between water and 1-octanol is one example of system 5. At 25°C, the solubility of 1-octanol in water is 0.54 mg mL^{-1} and the solubility of water in 1-octanol is 41.7 mg mL^{-1}.

In system 5, j is in equilibrium with phase A that contains B. As a result, the equilibrium concentration of j in A (designated as $S_{j,A/B}$ to represent that it is the solubility limit of j in A that is saturated with respect to B) is not the same as the concentration of j in A of systems 2 or 4 (i.e., the solubility limit of j in A alone, $S_{j,A}$). For the system of naphthalene, water and 1-octanol, the concentration of naphthalene in 1-octanol saturated water is larger than in pure water, because octanol-saturated water is more attractive to naphthalene than pure water alone. The magnitude of the difference between $S_{j,A/B}$ and $S_{j,A}$ will depend on the amount of B dissolved into A (more B means a bigger effect) and the chemical nature of A and B relative to j. If species j is chemically similar to B, then the presence of B in phase A might significantly increase $S_{j,A/B}$ compared to $S_{j,A}$. If species j is chemically dissimilar to B, then the presence of B in phase A might significantly decrease $S_{j,A/B}$ compared to $S_{j,A}$ or have no effect at all (as long as B does not interfere with interactions between j and A).

The equilibrium distribution of solute j between two phases is often represented quantitatively by a partition coefficient $K_{j,B/A}$, defined is the ratio of the equilibrium concentrations

of j in phases B and A (i.e., $K_{j,B/A} = C_{j,B}/C_{j,A}$). When water and toluene and excess naphthalene are equilibrated, the concentration of naphthalene is 285 mg mL^{-1} in toluene and 0.031 mg mL^{-1} in water, and the toluene-water partition coefficient is 92,000 (= 285/0.031). Often, the equilibrium partition coefficient is constant for all concentrations of j. Figure 4 illustrates the equilibrium concentration of solute j in the SC as a function of the concentration of j in a solvent vehicle v, assuming the relationship is linear.

Figure 4. Equilibrium concentration of solute j in SC as a function of its concentration in vehicle v.

Unless the solvent vehicle changes the SC in a significant way (e.g., by dehydrating the SC), the maximum concentration of j in the SC usually occurs when the solvent vehicle v is saturated with j. If partitioning of j between the SC and v is constant, then $K_{j,sc/v} = S_{j,sc/v}/S_{j,v}$.
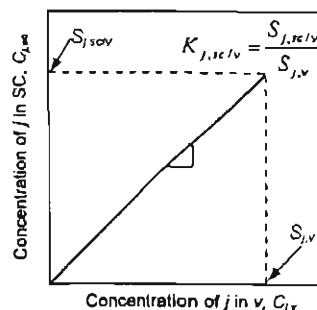
Thermodynamic Activity

Thermodynamic activity is helpful for comparing concentrations of a given solute in different solutions. As described already, while naphthalene solubility in water is much smaller than in toluene (i.e., 0.031 compared to 286 mg mL^{-1} at 25°C), at equilibrium both solutions produce the same naphthalene pressure in air. It is common to say that these solutions have the same *thermodynamic activity*. Furthermore, because these concentrations are solubility limits (the maximum concentration that can be achieved at equilibrium) the *thermodynamic activity* is a *maximum*. To a first approximation, a solute j in different phases will be at the same thermodynamic activity whenever its concentration is at the same fraction of the solubility limit (also given as the mole fraction) in that phase. For example, a naphthalene concentration of 28.6 mg mL^{-1} in toluene has the same thermodynamic activity as 0.0031 mg mL^{-1} in water (i.e., $C_{j,A}/S_{j,A} = C_{j,B}/S_{j,B} = 0.1$) and consequently, the naphthalene pressure in air equilibrated with either solution is expected to be 0.0085 mm Hg, which is 10% of its vapor pressure (i.e., $p_j = 0.1$ p_j^*). (Strictly speaking, this description of the relationship of thermodynamic activity to concentration applies to solutions that are ideal and for which the concentrations are sufficiently small so that concentration of solute j given on a weight basis is proportional to the mole fraction of solute j in the solution of j in the vehicle v. Descriptions of thermodynamic activity for scenarios when this is not true are described below.)

For comparing dermal absorption of solute j from different liquid solutions, thermodynamic activity is meaningful when concentration is not. Dermal absorption of j at the same concentration from two different liquids A and B (i.e., $C_{j,A} = C_{j,B} = C_j$) is almost always different, simply because the thermodynamic activity of j is different (i.e., $C_j / S_{j,A} \neq C_j / S_{j,B}$). However, absorption of j at the same thermodynamic activity in two different liquids (i.e., for $C_{j,A}/S_{j,A} = C_{j,B}/S_{j,B}$) would be the same as long as A and B are completely immiscible with the skin (i.e., neither A nor B dissolves into skin) and neither A nor B extracts components from the skin. If the absorption of solute j from liquids at the same thermodynamic activity is different, then interaction between the skin and either A or B is indicated.

Based on the concept of thermodynamic activity, modifications in vehicle composition that change the solubility of solute j in the vehicle (i.e., $S_{j,v}$) will affect dermal absorption. The effects of altering drug solubility in topical vehicles has been recognized and discussed extensively in the pharmaceutical literature (Chiang et al., 1989; Ostrenga et al., 1971a; Ostrenga et al., 1971b; Ostrenga et al., 1971c; Poulsen, 1972, 1973). With respect to occupational dermal exposures, increasing vehicle solubilization of a toxic chemical (in the absence of other alterations to the skin barrier or concentration of the toxic chemical) will reduce dermal absorption and consequently, the health risk. For example, the time for onset of erythema following dermal exposure to the same dose of methyl nicotinate is significantly shorter from water than from water-glycerol solutions that exceed 60% glycerol (Hadgraft et al., 1972). On the surface, these results might suggest that glycerol acts to antagonize (or that water acts to synergize) the erythemic effect of methyl nicotinate. However, changes in thermodynamic activity are sufficient to explain the observations. Glycerol delays erythema by increasing methyl nicotinate solubility in the vehicle, which decreases the thermodynamic activity of methyl nicotinate (Hadgraft et al., 1973). When glycerol-water solutions are prepared with methyl nicotinate at the same thermodynamic activity (i.e., 0.07 M for 0% glycerol, 0.1 M for 80% glycerol, and 0.2 M for 100% glycerol), then erythema occurs at the same time for all formulations (Hadgraft et al., 1973).

Differences in thermodynamic activity also explain the benzo(a)pyrene (BAP) experiments reported by Booth et al. (1999). In their study, CD1 mice that were dermally exposed to benzo(a)pyrene (approximately 0.01 to 7 µg/animal) in tetrahydrofuran manifested a larger number of DNA adducts in lung and skin than the animals exposed to the same BAP doses in dodecane. They argued that dodecane moderated the genotoxicity of BAP. This is possible, but it is more likely that DNA adduct formation are greater for the same amount of BAP applied in tetrahydrofuran than in dodecane simply because BAP, which has a $\log K_{o/w}$ of 6.13, is

23

more soluble in dodecane, which has a $\log K_{o/w}$ of 6.10, than in tetrahydrofuran, which has a $\log K_{o/w}$ of 0.46.

Thermodynamic activity alone will not explain all vehicle effects. For example, adding 0.035 M 1,2-octanediol to PBS increases corticosterone solubility by 1.7 (Warner et al., 2001). As a result, based on thermodynamic activity alone, dermal absorption rates for a given corticosterone concentration should be 1.7-fold less from PBS with than without 1,2-octanediol. Instead, the absorption rate is 50-fold greater with than without 1,2-octanediol (Warner et al., 2001)! Thus, adding a small amount of 1,2-octanediol reduced the skin barrier resistance to corticosterone by almost 100-fold (i.e., 1.7 x 50). Furthermore, this effect was reversible (i.e., corticosterone flux from PBS was restored when 1,2-octanediol was removed). Similar results are reported for several 1,2-alkanediol and also N-N-dimethylalkanamide additives (Warner et al., 2001). It is vehicle effects such as these that were the focus of the experimental and theoretical efforts of this project. In the next section we describe the strategy we used for relating the experimental observations of chemical flux through the SC and uptake into the SC to identify and characterize vehicle effects on skin barrier function.

Vehicle Effects on Steady-State Penetration Rate of Chemicals through Skin

Once compounds have partitioned into the outermost layer of the SC, they diffuse across the SC and then the VE. If the solute concentration difference between the outermost and innermost layers of the skin is kept constant, eventually the rate of chemical penetration through skin will also be constant (i.e., the penetration rate will be at *steady state*). The time required to reach steady state can be a few minutes (e.g., < 15 min for benzoic acid (Parry et al., 1990) and chloroform (Islam et al., 1995; Islam et al., 1996)) or more than a day (e.g., > 45 h for phenobarbitone (Hadgraft and Ridout, 1987)). According to Fick's law, the steady-state flux through the SC of a solute j from a liquid solution (i.e., the vehicle, v), can be described by the following equation:

$$F_{j,sc/v} = \left(C_{j,v}\ K_{j,sc/v}\right) D_{j,sc/v}/L_{sc} \tag{1}$$

where $F_{j,sc/v}$ represents the steady-state rate of chemical penetration per area in mg hr^{-1} cm^{-2}. In Eq. (1), $C_{j,v}$ is the concentration of solute j in the vehicle, $K_{j,sc/v}$ is the equilibrium partition coefficient of solute j between the SC and the vehicle. Therefore, $(K_{j,sc/v}\ C_{j,v})$ is the concentration in the outermost layer of the SC, which is in equilibrium with the solvent vehicle v. The remaining parameters are the thickness of the SC (L_{sc}) and the *effective* diffusion coefficient for solute j in the SC ($D_{j,sc/v}$) from vehicle v in which the heterogeneous SC is treated as if it were a homogeneous membrane with the same thickness. As shown in Figure 4, $K_{j,sc/v}$ can be

represented by the ratio of saturation concentrations in vehicle ($S_{j,v}$) and in the SC equilibrated with the vehicle ($S_{j,sc/v}$) and Eq. (1) can be rewritten as follows:

$$F_{j,sc/v} = \left(C_{j,v}/S_{j,v}\right) S_{j,sc/v} \, D_{j,sc/v}/L_{sc} \tag{2}$$

The mass of solute j in a fixed area of isolated and hydrated SC that has been equilibrated with a vehicle saturated with j ($m_{j,sc/v}$) is equal to $S_{j,sc/v} L_{sc}$. Based on Eq. (2), $F_{j,sc/v}$ is related to $m_{j,sc/v}$ as:

$$F_{j,sc/v} = \left(C_{j,v}/S_{j,v}\right) m_{j,sc/v} \, D_{j,sc/v}/L_{sc}^2 \tag{3}$$

Thus, the flux of j through skin from a given vehicle depends on three components: (i) the thermodynamic activity of the solute j in the vehicle (i.e., approximately $C_{j,v}/S_{j,v}$ for solutes with low solubility in ideal solutions), (ii) the saturated mass of solute j in the vehicle-saturated SC (i.e., $m_{j,sc/v}$), and (iii) the diffusion rate of j through the vehicle-saturated SC (i.e., $D_{j,sc/v}/L_{sc}^2$). Changing vehicles can change the penetration rate of j by changing any of these three components. However, except for vehicles that irreversibly damage skin by extracting components from the SC lipids, changes in saturated mass and diffusion rate will be small if vehicle constituents do not partition significantly into the SC lipids. If $D_{j,sc/v} L_{sc}^2$ and $m_{j,sc/v}$ do not change (or change only a little), then $F_{j,sc/v}$ would be the same from all vehicles with the same thermodynamic activity (i.e., the same value for $C_{j,v}/S_{j,v}$ for solutes with low solubility in ideal solutions). This has been observed experimentally (e.g. see (Barry et al., 1985a; Barry et al., 1985b; Hadgraft et al., 1973)).

For many vehicles in occupational exposures, significant solubility within the SC lipids is probable, meaning that the saturated mass and the diffusivity of j will be different for different vehicles. This situation is illustrated by system 5 in Table 1, in which the vehicle (A) absorbs into the SC (B). In this case, the flux of j from a vehicle y ($F_{j,sc/y}$) could be estimated from the saturated flux of j from a different vehicle v as follows:

$$F_{j,sc/y} = SF_{j,sc/v} \, Rm_{j,y/v} \, RD_{j,y/v} \left(C_{j,y}/S_{j,y}\right) \tag{4}$$

in which $SF_{j,sc/v}$ represents the flux through the SC from a *saturated* solution of solute j in a vehicle v (i.e., $C_{j,v} = S_{j,v}$), defined as:

$$SF_{j,sc/v} = S_{j,sc/v} \, D_{j,sc/v}/L_{sc} = m_{j,sc/v} \, D_{j,sc/v}/L_{sc}^2 \tag{5}$$

Thus, $SF_{j,sc/v}$ is the maximum flux for solute j in vehicle v. The factors, $Rm_{j,y/v}$ and $RD_{j,y/v}$, adjust respectively for the saturated mass and the diffusion of j in the SC in the presence of y instead of v. These two factors, defined as:

$$Rm_{j,y/v} = m_{j,sc/y}/m_{j,sc/v} = S_{j,sc/y}/S_{j,sc/v} \tag{6}$$

$$RD_{j,ylv} = \left(D_{j,scly}/L_{sc}^2\right)/\left(D_{j,sclv}/L_{sc}^2\right) \tag{7}$$

relate the saturated fluxes of solute j in vehicle v and y as follows:

$$SF_{j,scly} = SF_{j,sclv}\, Rm_{j,ylv}\, RD_{j,ylv} \tag{8}$$

If both vehicles v and y have little or no solubility in the SC, then $Rm_{j,ylv}$ and $RD_{j,ylv}$ will equal one and $SF_{j,scly} = SF_{j,sclv}$. When $SF_{j,scly} \neq SF_{j,sclv}$, most often the adjustment for the saturated mass of solute is larger than the adjustment for solute diffusivity. This is because making an appreciable change in solubility is generally easier than changing the solute diffusivity significantly. Vehicles v and y may be different pure liquids (e.g., water compared to toluene) or the same liquid but containing other solutes (e.g., water alone compared to water containing naphthalene). For example, dermal absorption of phenanthrene (a 3-ring polyaromatic hydrocarbon, PAH) might be different from either toluene (an aromatic solvent) or water containing naphthalene (a 2-ring PAH with significant solubility in skin) as compared to water alone.

By the scheme quantified in Eq. (4), we can estimate the steady-state flux of solute j through the SC from a vehicle y with a concentration $C_{j,y}$ knowing $SF_{j,sclv}$, and the two adjustment factors, $Rm_{j,ylv}$ and $RD_{j,ylv}$. The saturated flux of solute j from a vehicle v has to be determined experimentally or estimated using predictive quantitative structure activity relationships (QSAR) developed from a vehicle for which there are substantial amount of dermal absorption data (e.g., water, which is discussed below). Likewise, the adjustment factors for a solute j in different vehicles, $Rm_{j,ylv}$ and $RD_{j,ylv}$, have to be measured or estimated. Presently, there are almost no experimental observations from which to estimate $Rm_{j,ylv}$ and $RD_{j,ylv}$. An important goal of this project was to experimentally determine $Rm_{j,ylv}$ and $RD_{j,ylv}$ in several model systems that might be extrapolated to other systems.

The experimental strategy of this project is based on Eqs. (6) and (8). $Rm_{j,ylv}$ was measured by equilibrating isolated SC in water and non-aqueous vehicles containing solute j alone and in the presence of other solutes. The steady-state flux of solute j from vehicles saturated with j was determined in standard diffusion cells experiments. $RD_{j,ylv}$ was then calculated by dividing the ratio steady-state saturated flux measurements in vehicles y and v ($SF_{j,scly}/SF_{j,sclv}$) by $Rm_{j,ylv}$. That is,

$$RD_{j,ylv} = \left(SF_{j,scly}/SF_{j,sclv}\right)/Rm_{j,ylv} \tag{9}$$

This approach of measuring both flux and solubility in the SC was used to identify the mechanism by which ethanol increases estradiol flux through the SC. Specifically, it was determined that estradiol solubility in SC containing ethanol was larger and primarily responsible for its greater flux in SC containing ethanol (Ghanem et al., 1987). Unfortunately, there are few

other examples of this approach in the literature. Nearly always, studies of vehicle effects have measured flux alone (e.g., corticosterone in PBS with various alkanol, 1,2-alkanediol or N,N-dimethylalkanamide additives (Warner et al., 2001)), making it impossible to know why penetration rates changed. To predict dermal absorption from liquid mixtures, we must know whether the barrier function has changed, and when it does change, we need to know why.

<u>Flux vs. Permeability Coefficients for Representing Dermal Absorption from Different Vehicles</u>

In the dermal absorption literature, it is common to report permeability coefficients rather than flux. The permeability coefficient for a solute j transferring through the SC from a vehicle v ($P_{j,sclv}$) is the concentration normalized steady-state flux. As long as the solute j does not damage the SC (and the saturation concentration is low and the solution ideal), $P_{j,sclv}$ measurements from saturated and sub-saturated solutions should be the same, i.e.:

$$P_{j,sclv} = F_{j,sclv}/C_{j,v} = SF_{j,sclv}/S_{j,v} \qquad (10)$$

While useful for comparing different solutes from a single vehicle (e.g., from water), $P_{j,sclv}$ is a confusing parameter for representing the effect of different vehicles on penetration of a given solute. This is because $P_{j,sclv}$ varies with $S_{j,v}$ and consequently, different values of $P_{j,sclv}$ in different vehicles reflect differences in the solubility of solute j in these vehicles rather than differences in dermal absorption rates. For example, as reported below, at 32°C naphthalene solubility in water was approximately 0.04 mg mL^{-1} compared to about 300 mg mL^{-1} in toluene. If the steady-state saturated flux of naphthalene through the SC is similar for toluene and water, the permeability coefficient for naphthalene from water would be almost 7,500 times larger than from toluene (i.e., 300/0.4). In fact, the saturated flux of NP was determined in this study to be approximately 3-fold larger from toluene compared with water. Therefore, the permeability coefficient from water is only 2,500 times larger than from toluene.

There is prior experimental evidence that $P_{j,sclv}$ changes even when flux does not. Methyl nicotinate flux is the same from aqueous and glycerol solution with the same thermodynamic activity (i.e., 0.07 M in water and 0.2 M in glycerol), while $P_{j,sclv}$ from water is nearly 3 times larger than from glycerol (Hadgraft et al., 1973). In another example, the flux of benzyl alcohol from a 50 mole percent solution of benzyl alcohol in butanol (300 ± 62 μg cm^{-2} s^{-1}) is nearly the same as from a 11.8 mole percent solution of benzyl alcohol in isopropyl myristate (380 ± 140 μg cm^{-2} s^{-1}) (Barry et al., 1985b), although $P_{j,sclv}$ from the isopropyl myristate solution was 8 times larger than from butanol solution. Consequently, for purposes of comparing dermal absorption of a solute j from multiple vehicles, flux normalized to saturation (i.e., the maximum flux) is a more useful quantity than the permeability coefficient.

27

Dermal Absorption Parameters for Single Solutes in Water

Dermal absorption from one vehicle, water, has been studied extensively. Measurements from many hundreds of *in vitro* diffusion cell experiments have been reported in the literature for human and animal skins. Nearly 20 years ago Flynn (Flynn, 1990) assembled almost 100 measurements, primarily from aqueous solutions into human skin. Using a semi-theoretical approach proposed by Kasting and others (Kasting *et al.*, 1987), Potts and Guy (Potts and Guy, 1992, 1995) used Flynn's database to develop the following simple QSAR for estimating permeability coefficient values for penetration of a single solute *j* through human skin from aqueous solutions:

$$\log_{10}\left[P_{j,skin/w}\ (cm/hr)\right] = -2.72 + 0.71\log_{10} K_{j,o/w} - 0.0060\ MW_j \tag{11}$$

in which $K_{j,o/w}$ and MW_j are the octanol-water partition coefficient and molecular weight, respectively for solute *j*. Several other investigators have developed similar equations and these are summarized by Vecchia and Bunge (Vecchia, 1997; Vecchia and Bunge, 2002a). They concluded that Eq. (11) was among the better algorithms for representing data for a broad range of chemicals.

The database used to develop Eq. (11) contains few compounds for which the VE probably contributes a noticeable resistance (i.e., compounds with $\log_{10} K_{j,o/w} > 4$) and thus, $P_{j,skin/w}$ in Eq. (11) is really the permeability coefficient for the SC alone (i.e., $P_{j,sc/w}$). The VE should present a resistance to dermal penetration by highly lipophilic chemicals (i.e., those with $\log_{10} K_{o/w} >$ about 4). Bunge and Cleek (Bunge and Cleek, 1995) recommended estimating $P_{j,skin/w}$ from $P_{j,sc/w}$:

$$P_{j,skin/w} = P_{j,sc/w}/(1+P_{j,sc/w}\sqrt{MW_j}/2.6) \tag{12}$$

in which $P_{j,skin/w}$ calculated from Eq. (11) is used as $P_{j,sc/w}$ in Eq. (12). Published data support this strategy (Vecchia, 1997; Vecchia and Bunge, 2002a). In a smaller number of studies, equilibrium distribution of solutes between isolated SC (i.e., all other skin layers have been removed) and water have been measured (i.e., the partition coefficient, $K_{j,sc/w} \cong S_{j,sc/w}/S_{j,w}$ as shown in Figure 4). Cleek and Bunge (Cleek and Bunge, 1993) examined these results and showed that they could be reasonably represented by:

$$\log_{10} K_{j,sc/w} = 0.71\log_{10} K_{j,o/w} \tag{13}$$

By combining Eqs. (11) and (13) as indicated by Eq. (10), we obtain the following equation:

$$\log_{10}\left[D_{j,sc/w}/L_{sc}\ (cm/hr)\right] = -2.72 - 0.0060\ MW_j \tag{14}$$

which can be used to estimate the diffusion rate of solute j across the SC when this barrier is equilibrated with an aqueous solution. If absorption of water has not greatly disturbed the diffusion pathway through the SC, then Eq. (14) would also represent diffusion rates for hydrated SC in the presence of other vehicles that do not greatly disturb the SC.

The newly released strategy for assigning NIOSH skin notations (NIOSH, 2009) recommends using Eq. (15), which is called the revised Robinson model, for estimating the permeability coefficient for skin from water ($P_{j,skin/w}$):

$$P_{j,skin/w} = P_{j,sc/w} \bigg/ \left[\frac{1}{1 + 1.59 \times 10^{-4} \big/ \left(P_{j,sc/w} \sqrt{MW_j} \right)} + P_{j,sc/w} \sqrt{MW_j} \big/ 2.5 \right] \tag{15}$$

where $P_{j,sc/w}$ is calculated using Eq. (16):

$$\log_{10} \left[P_{j,skin/w} \, (\text{cm/hr}) \right] = -1.326 + 0.6097 \log_{10} K_{j,o/w} - 0.1786 \sqrt{MW_j} \tag{16}$$

Notably, Eqs. (12) and (15) are essentially the same as long as the first term in the denominator of Eq. (15) is approximately 1. This occurs when the product of $P_{j,sc/w}$ and the square-root of MW_j is larger than approximately 1.59×10^{-3}, which is the case for chemicals that are not so hydrophilic or large that $P_{j,sc/w}$ is very small.

Estimating Dermal Absorption of Single Solutes

Methods for estimating chemical absorption from dermal exposures consist of a mathematical description of: (i) the exposure situation (e.g., the concentration of the absorbing solute, the length of time of the exposure, the vehicle volume), and (ii) the solution-diffusion steps of dermal penetration, which are characterized by chemical-dependent parameters such as partition coefficients and permeability coefficients. We have developed several mathematical models of dermal absorption as part of previous research projects, which are described in detail elsewhere (e.g., see Bunge and Cleek, 1995; Bunge et al., 1995a; Bunge et al., 1994; Bunge and Parks, 1997, 1998; Cleek and Bunge, 1993; McCarley and Bunge, 1998, 2000, 2001; Parry et al., 1990; Reddy et al., 1998; Reddy et al., 2002; Silcox et al., 1990; Vecchia, 1997). The purpose of all of these models is to describe the dermal absorption process (e.g., the mass of chemical absorbed into and across the skin layers) based on fundamental descriptions of skin: its physical dimensions (e.g., the thickness of each skin layer) and its physicochemical parameters (e.g., diffusion coefficients, partition coefficients and permeability coefficients for absorbing solutes in each skin layer). Significant to the research described here, in all of these previously published models, absorption of only a one solute is considered. Absorption by the vehicle itself and its effect on solute penetration was not considered.

While conceptually simple, many dermal absorption models are mathematically complicated (e.g., see Reddy *et al.*, 1998). Sometimes relatively simple equations can provide good approximations. However, before recommending simpler equations, their appropriateness (and limitations) must be demonstrated by comparing calculations to a more accurate (and complex) mathematical description of the dermal absorption process. For example, Cleek and Bunge (Cleek and Bunge, 1993) showed that a more complicated mathematical model (i.e., consisting of an infinite series) describing the total uptake of solute j into skin from a vehicle v ($M_{in,j,v}$) across an exposed area (A) from a vehicle with constant concentration of solute j ($C_{j,v}^{o}$) could be represented with reasonable accuracy by one of two simple equations that apply for short (unsteady-state) and long (steady-state) exposure times (t_{exp}), respectively:

$$M_{in,j,v} = A C_{j,v}^{o} \sqrt{4(K_{j,sc/v} \, L_{sc}) P_{j,sc/v} \, t_{exp}/\pi} \qquad\qquad \text{for } t_{exp} < t^{*} \qquad (17)$$

$$= A\left(C_{j,v}^{o}/S_{j,v}\right)\sqrt{4 m_{j,sc/v} \, SF_{j,sc/v} \, t_{exp}/\pi}$$

$$M_{in,j,v} = A C_{j,v}^{o} \left[P_{j,sc/v} \, t_{exp} + (K_{j,sc/v} \, L_{sc})/3 \right] \qquad\qquad \text{for } t_{exp} \geq t^{*} \qquad (18)$$

$$= A\left(C_{j,v}^{o}/S_{j,v}\right)\left[SF_{j,sc/v} \, t_{exp} + m_{j,sc/v}/3 \right]$$

$$t^{*} \approx K_{j,sc/v} \, L_{sc}/\left(2 P_{j,sc/v}\right) = m_{j,sc/v}/\left(2 SF_{j,sc/v}\right) \qquad (19)$$

The right hand side of these equations are written in terms of the saturated flux ($SF_{j,sc/v}$) and saturated mass ($m_{j,sc/v}$) which are related to ($K_{j,sc/v} \, L_{sc}$) and $P_{j,sc/v}$ as follows:

$$m_{j,sc/v} = (K_{j,sc/v} \, L_{sc}) S_{j,v} \qquad (20)$$

$$SF_{j,sc/v} = P_{j,sc/v} \, S_{j,v} \qquad (21)$$

Written this way, the contribution of thermodynamic activity in the vehicle (i.e., $C_{j,v}^{o}/S_{j,v}$) is apparent. Eqs. (18) and (19) represent absorbing solutes that are not so lipophilic that the mass transfer resistance from the VE is no longer small. Small adjustments to Eqs. (18) and (19) are required for more lipophilic compounds (e.g., see Cleek and Bunge, 1993).

Eqs. (17) and (18) provide much better estimates of absorption than the commonly suggested equation:

$$M_{in,j,v} = A C_{j,v}^{o} P_{j,skin/v} \, t_{exp} \qquad (22)$$

while adding little additional complexity. Bunge *et al.* (1995b) showed that calculations made using Eq. (22) will always underestimate the amount of dermal absorption, sometimes significantly. However, Eq. (22) should provide a good estimate or overestimate the amount of chemical that would enter the systemic circulation during the exposure time. This is because there will be chemical left in the skin at the end of the exposure time that can be absorbed into

the systemic circulation after the exposure has ended. Dermal absorption estimates made using Eqs. (17) and (18) include all of the chemical left in the skin at the end of the exposure; estimates made with Eq. (22) include only a portion of the chemical that is left in the skin at the end of the exposure. The new NIOSH skin notation strategy recommends using Eq. (22) to estimate the dermal dose, using the saturation concentration of the chemical in water for $C_{j,v}^{o}$ and $P_{j,skin/v}$ is calculated using Eqs. (15) and (16).

Comparison of several experiments with predictions made using dermal absorption models have generally validated the basic theoretical approach. For example, the studies by Pirot et al. (Pirot et al., 1997) and Silcox et al. (Silcox et al., 1990), demonstrated that mathematical models using permeability coefficients and partition coefficients determined *in vitro* can provide reasonable predictions of *in vivo* experiments.

The development of QSAR equations for estimating permeability and partition coefficients (as described above for organic non-electrolytes in water) makes dermal absorption estimates possible without new experimental measurements. Dermal absorption of solutes in aqueous solutions can be estimated by combining Eqs. (17) and (18) with equations for estimating the physicochemical parameters of the SC, Eqs. (11) and (13). When tested against experiments, this strategy has provided generally reasonable results. Figure 5 shows predictions made with no adjustable parameters for chloroform absorption into frozen cadaver skin (Bogen et al., 1998). Overall, predictions of the experimental results are quite adequate.

We note that the ratio of concentration to saturation, $C_{j,v}^{o}/S_{j,v}$, is often a good representation of thermodynamic activity for a solute j with limited solubility ($\sim$ less than 5 mole percent) in the vehicle v. For a species j that has a larger saturation concentration in vehicle v or is completely miscible in a vehicle (or the solution of j in a vehicle v is a non-ideal solution) then thermodynamic activity must be deduced from experimental measurements or by methods for estimating phase equilibrium that have been developed in the chemical engineering literature. These approaches have been utilized in this study and are discussed further in the Results and Discussion section below.

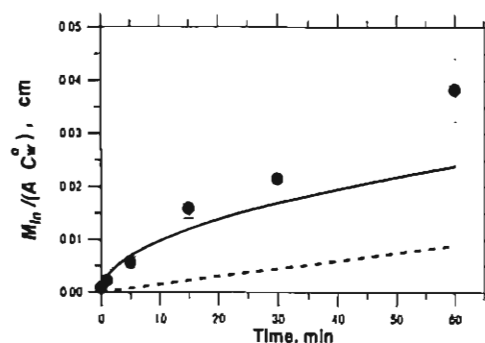In many respects, dermal absorption of single solutes from water is understood and the

Figure 5. Comparison of predictions (solid curve, Eqs. 11, 13, and 17; dashed line, Eq. 22) with dermal absorption measurements of chloroform into excised human skin from dilute aqueous solutions.

methods for estimating absorption (Eqs. (11), (13). and (17)-(19)) are well-developed and accepted by most investigators in the field (Bunge and McDougal, 1999). For example, the US EPA has adopted this approach for estimating absorption from dermal exposure to aqueous solutions (US EPA, 1992, 1998c). In occupational settings, however, exposure to a single solute in water is the exception in occupational settings. The majority of occupational exposures involve non-aqueous solutions and solutions with several components. The ultimate goals of this research are computational approaches for estimating dermal absorption from multi-component aqueous and non-aqueous solutions that are analogous to Eqs. (17) through (19). The strategy of this study was to measure the effects of the selected vehicle (either a pure solvent or water containing another solute) relative to a single compound in water.

<u>Estimating Dermal Absorption of Chemicals from Aqueous Mixtures and Non-Aqueous Vehicles</u>

In general, methods for estimating the amount of chemical dermally absorbs from aqueous mixtures and non-aqueous vehicles must include the thermodynamic activity in the vehicle of all components, mass balances for all components, chemical-dependent dermal absorption parameters (i.e., $SF_{j,sclv}$ and $m_{j,sclv}$) and relate how these parameters change as concentration of the components change in the SC and vehicle. If the saturation concentration of solute j in the vehicle is not too large, the thermodynamic activity will be approximately the concentration relative to saturation (i.e., $C_{j,v}°/S_{j,v}$).

Our strategy is to calculate the steady-state maximum flux of solute j in vehicle v ($SF_{j,sclv}$) and the equilibrium uptake from a vehicle v saturated with solute j ($m_{j,sclv}$) by adjusting the existing and tested methods described above (e.g., Eqs. (11) and (13) combined with the aqueous solubility limit of solute j, $S_{j,w}$ and L_{sc}) for estimating saturated flux and saturated mass of single solutes j from water. That is,

$$SF_{j,sclv} = Rm_{j,vlw} \, RD_{j,vlw} \, SF_{j,sclw} = Rm_{j,vlw} \, RD_{j,vlw} \, P_{j,sclw} \, S_{j,w} \tag{23}$$

$$m_{j,sclv} = Rm_{j,vlw} \, m_{j,sclw} = Rm_{j,vlw} \, K_{j,sclw} \, L_{sc} \, S_{j,w} \tag{24}$$

The rationale for this approach is that Eqs. (11) and (13) have been developed from large databases and water solubility data are readily available for a large number of compounds. If the vehicle v has little effect on skin compared to water then $Rm_{j,vlw} = 1$ and $RD_{j,vlw} = 1$, and if concentration of solute j remains constant during the exposure, then total uptake of solute j into skin ($M_{in,j,v}$) can be estimated using Eqs. (17) and (18). When vehicles alter the SC lipids, then Eqs. (17) and (18) only apply approximately if the solvent vehicle absorbs quickly compared with solute j or the skin has been pre-equilibrated with the vehicle. If neither of these conditions are met, then the effect of the vehicle, which is itself absorbing into the SC, would not

immediately be described by $Rm_{j,v/w}$ and $RD_{j,v/w}$. To account for changes in $Rm_{j,v/w}$ and $RD_{j,v/w}$ as the vehicle components absorb in the SC would require mass balances on all components in the vehicle and estimates for how $Rm_{j,v/w}$ and $RD_{j,v/w}$ vary with concentration of vehicle components in the SC. However, for making preliminary estimates, it might be sufficient to use $Rm_{j,v/w}$ and $RD_{j,v/w}$ values that are averages of $Rm_{j,v/w}$ and $RD_{j,v/w}$ at the starting and at the final concentrations of vehicle components in the SC.

Many occupational exposures to liquids involve small enough volumes that components can be depleted by dermal absorption. This factor must be included into strategies for developing dermal RELs for different vehicles. For example, the saturated flux and saturated mass of naphthalene is the same from an aqueous solution with a concentration of 0.031 mg mL^{-1} and a toluene solution of 286 mg mL^{-1}. However, if the exposure is to 1 mL of each solution distributed over 100 cm^2 of skin for approximately 30 minutes, a mathematical model that includes the vehicle volume predicts that only 0.031 mg of naphthalene would dermally absorb from water (which is all of the naphthalene in the water) while approximately 140 mg would absorbed from toluene (about half of what was there). As stated earlier, dermal absorption estimates must include information about the exposure condition.

Electrochemical Impedance Spectroscopy (EIS)

We investigated the use of electrochemical impedance spectroscopy (EIS) to characterize each skin sample so that measurements of flux of nonpolar compounds through different skin samples can be more meaningfully compared. The next few paragraphs describe how EIS is measured and how the measurements are related to skin properties.

For ohmic materials, electrical resistance (R) is related to the resulting direct current that arises when a constant voltage drop (E) is applied (or vice versa) according to Ohm's law ($R = E$ divided by I). Electrochemical impedance spectroscopy (EIS) involves imposing an oscillating current or voltage perturbation to a system and measuring the resulting voltage or current signal, respectively. If a current perturbation is imposed on the system and the resulting voltage signal is measured, the process is called a galvanostatic EIS. If a voltage perturbation is imposed on the system and the resulting current signal is measured, the process is called potentiostatic EIS.

For potentiostatic EIS the time oscillation of the potential (or voltage) E can be described as:

$$E(t) = E_o \cos(2\pi f t) \tag{25}$$

where t is time, E_o is the amplitude and f is the frequency of the potential perturbation. In a linear system (i.e., an ohmic material), the current response to the oscillating potential is expressed as:

$$I(t) = I_o \cos(2\pi f t - \phi)$$ (26)

where ϕ is the phase-shift and I_o is the amplitude of the measured current response signal. Like the resistance in a DC circuit, for ohmic materials the impedance (Z) in an AC circuit is related to the potential and current by Ohms law (i.e., $Z = E/I$). Thus,

$$Z = \frac{E_o \cos(2\pi f t)}{I_o \cos(2\pi f t - \phi)} = \frac{E_o}{I_o} e^{j\phi} = |Z| e^{j\phi}$$ (27)

in which $|Z|$ is the frequency-dependent magnitude (i.e., the modulus) of the impedance and $j = \sqrt{-1}$. Using Euler's relationship,

$$e^{j\phi} = (\cos\phi + j\sin\phi)$$ (28)

the impedance can be written as the sum of real and imaginary components (Z_r and Z_j, respectively):

$$Z = Z_r + j Z_j$$ (29)

where

$$Z_r = |Z|\cos\phi \quad \text{and} \quad Z_j = |Z|\sin\phi.$$ (30)

are related to the modulus and phase angle as follows:

$$|Z| = \sqrt{Z_r^2 + Z_j^2}.$$ (31)

$$\phi = \arctan\frac{Z_j}{Z_r}$$ (32)

In electrochemical impedance *spectroscopy* (EIS), the impedance is measured over a range (i.e., a *spectrum*) of frequencies (e.g., a range of 1 to 10^5 Hz is common for skin). A limitation of the data analysis described above is that it assumes the output signal is proportional to the input signal (i.e. linear response). In practice, the polarization curve of skin, and most electrochemical systems, is non-linear. To minimize bias errors from the non-linearity of the system, the amplitude of the perturbation signal is kept small enough to confine the impedance scan to a pseudo-linear region of the polarization curve. Failure of the system to behave linearly can be assessed by testing for Kramers-Kronig consistency, which is described in the Results and Discussion section below.

EIS measurements from physical systems like skin are commonly interpreted by relating them to the impedance that would arise from an electrical circuit, called an equivalent circuit

model, comprised of simple current elements that represent the physical attributes of the system. Circuit elements that are commonly used in models applied to skin are a resistor (with resistance R), a capacitor (with capacitance C), and a constant-phase element (CPE, which is characterized by the parameters Q and α). The functional form of the impedance that arises from each of these elements is summarized in Table 2. The impedance of the resistor is independent of the frequency, while the impedance for the capacitor and constant phase element (CPE) vary with frequency. Thus, the system resistance affects the magnitude of the impedance signal while components that behave like a capacitor or CPE affect the phase shift of the signal. EIS has been used in investigations of a wide variety of electroactive systems including ceramic, polymeric, and biological membranes (Macdonald, 1987). Its use on skin has been more limited, but recent results show that EIS may be useful for characterizing the skin barrier function.

Often, the equivalent circuit model required to represent the observed impedance-frequency response involves two or more circuit elements connected in either series or parallel. For circuits containing elements in series, the total impedance is the sum of the impedances:

$$Z = Z_1 + Z_2 + ... + Z_n \tag{33}$$

For circuits with elements in parallel, the reciprocal of the total impedance is the sum of reciprocals of the impedances:

$$\frac{1}{Z} = \frac{1}{Z_1} + \frac{1}{Z_2} + ... + \frac{1}{Z_n} \tag{34}$$

It is convenient (and common) to present impedance-frequency results on an *impedance-plane* plot (also called a Nyquist plot), which displays the negative of the imaginary part of the impedance ($-Z_j$) versus the real part of the impedance (Z_r) determined for each frequency.

Table 2. Typical circuit elements and corresponding impedance
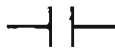
Element	Symbol	Impedance
Resistor	—\/\/\—	R
Capacitor	—||—	$\dfrac{1}{2\pi f C j}$
Constant Phase Element	—[CPE]—	$\dfrac{1}{Q(2\pi f j)^{\alpha}}$

Figure 6 shows the impedance-plane plot that would be measured for a simple circuit (also shown in Figure 6) consisting of a resistor with resistance R_e that is in series with a resistor (with resistance R_m) and a capacitor (with capacitance C) that are in parallel. The real and imaginary parts of the impedance for this circuit are described by the following expressions:

$$Z_r = R_e + \frac{R_m}{1+\left(2\pi f R_m C\right)^2} \tag{35}$$

$$Z_i = -\frac{2\pi f C R_m^2}{1+\left(2\pi f R_m C\right)^2} \tag{36}$$

which represent a semi-circle on the impedance-plane plot. For a circuit with a resistor and capacitor in parallel (e.g., R_m and C in Figure 6), the product of the resistance and capacitance (i.e., $R_m \cdot C$) has units of time. It follows that $R_m \cdot C$ represents the characteristic time constant for a parallel circuit of R_m and C and the reciprocal (i.e., $(R_m \cdot C)^{-1}$) is the characteristic frequency.

An important characteristic of the impedance-plane plot is that for many systems (including skin) the impedance at high frequency appears on the left side of the Z_r axis, near the intercept, and the low frequency data appear on the right side of the Z_r axis. Furthermore, for
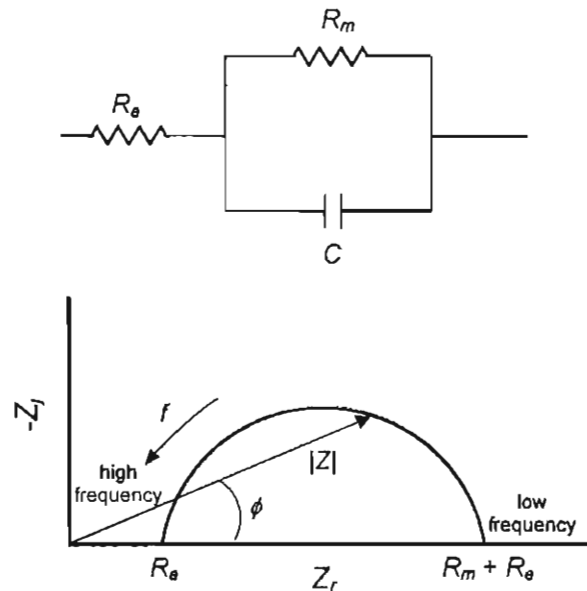

Figure 6. A schematic diagram of the impedance-plane plot for parallel resistor-capacitor circuit in series with a resistor shown illustrating the key features of the impedance measurement.

the simple circuit shown in Figure 6, the high and low frequency intercepts on the Z_r axis respectively correspond to R_e (the electrolyte resistance) and $R_m + R_e$ (which is the total resistance, R_t).

In Figure 7, a typical skin impedance spectrum measured in this study is compared to an R-C equivalent model circuit, which predicts a semi-circular function. The R-C equivalent model circuit poorly represents the skin data, which resemble a depressed semi-circle. Specifically, for this skin sample (which is typical skin samples), the maximum value of Z_j is less than half the maximum value of Z_r, which is equal to $R_m + R_e$.

In a circuit commonly used to model skin impedance, the capacitor in the R-C circuit is replaced by a CPE as shown in Figure 8 (and represented by two parameters, Q and α, as specified in Table 2). The impedance for the R-CPE circuit in series with a resistor of resistance R_e is described by Eq. (37):

$$Z = R_e + \frac{R_m}{1 + R_m Q (2\pi f \, j)^\alpha} \tag{37}$$

which can be written in terms of its real and imaginary parts as follows:

$$Z_r = R_e + \frac{R_m \left(1 + R_m Q (2\pi f)^\alpha \cos(\alpha\pi/2)\right)}{1 + \left(R_m Q (2\pi f)^\alpha\right)^2 + 2R_m Q (2\pi f)^\alpha \cos(\alpha\pi/2)} \tag{38}$$
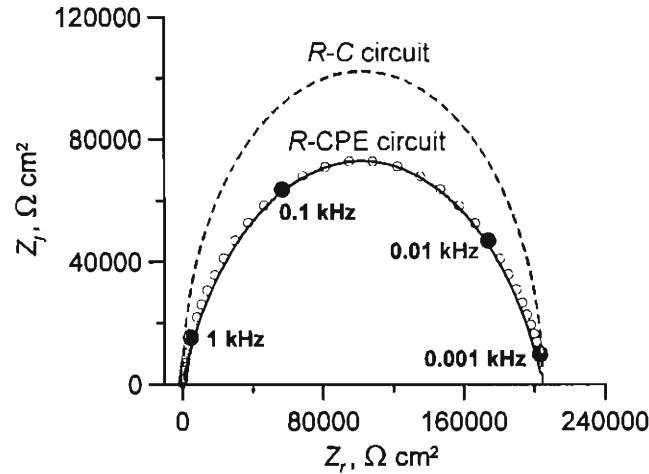

Figure 7. Impedance-plane plot of typical skin impedance data (circles) compared with equivalent circuit models: R-C circuit (dashed curve) and R-CPE circuit (solid curve). Filled symbols designate measurements collected at the indicated frequencies.
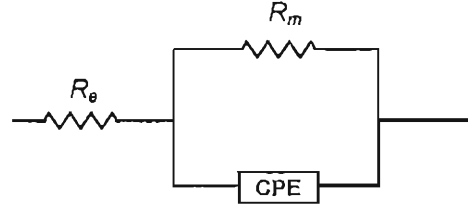
Figure 8. An equivalent model circuit of R-CPE in series with a resistance R_e that is commony used to model skin impedance.

$$Z_I = -\frac{R_m^2 Q(2\pi f)^\alpha \sin(\alpha\pi/2)}{1 + \left(R_m Q(2\pi f)^\alpha\right)^2 + 2R_m Q(2\pi f)^\alpha \cos(\alpha\pi/2)}$$ (39)

The R-CPE equivalent model circuit fits the data in Figure 6 well. This might be expected since the R-CPE circuit is characterized by a distribution of time constants (Kontturi and Murtomaki, 1994) rather than a single time constant, which characterizes a simple R-C circuit. Certainly the pathway for ions (and current) through skin consists of multiple paths of varying length and area, and thereby, multiple time constants (Yamamoto and Yamamoto, 1976).

Measurements of electrical resistance and tritiated water permeation have been used to evaluate skin integrity. Commonly, these measurements are used only to identify samples that are deemed unacceptable. For example, based on recommendations by Bronaugh et al. (1986), many study protocols reject skin samples if the measured water permeability is larger than 2.5×10^{-3} cm/hr, claiming the sample is probably physically damaged. For samples with acceptable values of water permeability, permeability coefficients of nonpolar organic solutes from water generally do not correlate with either water flux or electrical resistance (e.g., see Peck et al., 1995 and Green and Brain, 2006). This lack of correlation is attributed to a different pathway for skin permeation by organic non-electrolytes (i.e., the nonpolar pathway) compared to the pathway for electrons, water, or highly polar compounds (i.e., the polar pathway). Like urea (Figure 3) the flux of water and other highly polar compounds (e.g., mannitol (Sims et al., 1991)) usually do correlate with electrical resistance, even for different subjects. For example, the data shown in Figure 3 include measurements from 5 different subjects determined at two different temperatures over a period of 5 days (Peck et al., 1995).

The results shown in Figure 3 suggest that electrical resistance measurements might be used to control for both intra- and inter-subject variations in permeation for polar solutes. Instead of comparing mean values of solute flux from various solutions measured in one or

38

more subjects, the flux of the specified solute through all skin samples would be regressed with the electrical resistance and then the regression results for different solutions would be compared. While promising, this strategy would not be helpful for nonpolar compounds. We hypothesized that electrochemical impedance, which characterizes the skin capacitive elements in addition to resistance, might be used to characterize the nonpolar pathway.

In the application for this project, we hypothesized that the physicochemical origin of skin capacitance arises from the SC lipids, which act as the dielectric material separating charge (DeNuzzio and Berner, 1990; Oh et al., 1993). Two different studies were cited as evidence supporting this hypothesis. In their study of treatment with oleic acid, Kim and Oh (Kim and Oh, 2000) observed increased skin capacitance. This behavior is consistent with increased fluidity (and decreased crystallinity) within the highly organized SC lipids, which oleic acid is known to effect (Barry and Bennett, 1987; Bond and Barry, 1988; Williams and Barry, 1998). Kim and Oh (Kim and Oh, 2000) also found that surfactant treatment enhanced penetration of a nonpolar drug, ketoprofen (log $K_{o/w}$ = 3.2), suggesting that capacitance may characterize the lipid pathway. In a different study, Curdy et al. (Curdy et al., 2000) measured the recovery of human skin impedance in vivo after iontophoresis, a technique by which ionized drugs are forced through skin by the application of a steady electrical current (usually less than ~ 0.5 mA cm^{-1}). Iontophoresis is thought to affect and proceed through the polar pathway with almost no effect on the lipid pathway. Consistent with this, from impedance measured immediately after and 30 min after iontophoresis ceased, Curdy et al. found that the skin resistance increased by almost 2 fold, while there was no statistically discernible change in skin capacitance.

Specific Aims

This project had the following four specific aims:

- Determine the extent to which selected model compounds in aqueous solutions interact with each other or with skin to alter significantly the rate and/or extent of chemical absorption, and identify the underlying mechanisms.
- Determine the extent to which selected model compounds in non-aqueous solutions interact with each other or with the skin to alter the rate and/or extent of chemical absorption, and identify the underlying mechanisms.
- Develop electrochemical impedance spectroscopy (EIS) as a method for characterizing skin barrier function and to assess whether EIS can be used to reduce uncertainty in dermal absorption measurements.
- Develop, based on the accumulated experimental information, computational procedures

for estimating dermal absorption from aqueous and non-aqueous solutions containing one or more organic nonelectrolytes, which could be used to derive dermal exposure limits.

The first two aims were address using two types of experiments: measurements of permeation rates through the skin (also called diffusion cell measurements), and determination of the amount of chemical uptake into the stratum corneum (SC) at equilibrium. In the last aim, the results of our permeation and uptake experiments (as well as data published by others) have been compared with phase equilibrium thermodynamic data and predictions. This approach is shown to provide a promising strategy for extrapolating skin permeation data measured in one solvent (e.g., water) to other solvents or data measured in pure solvents to their mixtures. In the third aim, we developed and applied the electrochemical impedance spectroscopy (EIS) technique to non-invasively characterize the skin. The EIS results were then compared with measurements of skin permeation of nonpolar model compounds.

Procedures and Methodology

This project represents an initial step toward the ultimate goal of being able to predict dermal absorption of multiple solutes from water and single or multiple solutes from non-aqueous vehicles. To keep the project tractable and focused, we limited the scope in two significant ways: (i) the absorbing solutes were organic chemicals that are not known to damage skin at the concentrations studied, and (ii) the concentrations of the liquid solutions did not change during the dermal absorption study (i.e., solutions were be saturated with excess chemical and evaporation prevented). While inorganic chemicals, solvent evaporation and irreversible damage of skin by solutes and vehicles are important in occupational exposures, each of these issues introduces substantial complications that were left for future studies.

Chemicals

Three different model compounds (4-cyanophenol, methyl paraben, and naphthalene), all solids at skin temperature (i.e., at 32°C), were studied in 5 pure vehicles (i.e., water, 1-octanol, toluene, cyclohexane, and isopropyl myristate). The three model compounds were also studied in binary mixtures of 1-octanol, toluene, and cyclohexane. In addition, 4-chloronitrobenzene was studied in water and isopropyl myristate. Several physicochemical properties of these solutes and vehicles are summarized in Table 3. Experimental and estimated values of parameters describing dermal absorption (i.e., permeability coefficients, partition coefficients and estimates of maximum flux through the SC and the saturation limit in the SC) are listed in

Table 4. The experimental values of permeability and partitioning in SC (i.e., $P_{j,sc/w}$ and $K_{j,sc/w}$) listed in Table 4 are from steady-state *in-vitro* measurements on human skin from aqueous solutions of single solutes that were reported in earlier studies.

Reagent grade 4-cyanophenol (CP) and methyl paraben (MP) were purchased from Aldrich (Milwaukee, WI) and Sigma-Aldrich (St. Louis, MO), respectively. Scintillation grade naphthalene (NP) was from Sigma-Aldrich; 4-chloronitrobenzene (99%) was from Aldrich . HPLC grade toluene (T) and 1-octanol (O) were from Mallinckrodt, Baker (Phillipsburg, NJ) and Sigma-Aldrich, respectively. Reagent grade cyclohexane (C) was from Fisher (Fair Lawn, New Jersey). Isopropyl myristate (also known as 1-tetradecanoic acid, isopropyl ester) labeled as 98% pure was from Aldrich. Chloroform and methanol were all at least HPLC grade and acquired from various sources over the course of the study; HPLC grade acetonitrile was from Pharmaco-Aaper (Brookfield, CT). ACS certified dimethyl sulfoxide (DMSO) was from Fisher Scientific (Fair Lawn, NJ).

Water was de-ionized and polished with a Millipore MILLI-Q water system (Bedford, MA). The receptor fluid in the diffusion cell experiments was 0.01 M phosphate buffered saline (PBS, from Sigma P-3813, 0.138 M NaCl; 0.0027 M KCl; pH 7.4 at 25°C), which was degassed by vacuum filtration through a 0.45-μm pore size Nylaflo® nylon membrane filter (Pall Gelman Sciences, Ann Arbor, MI) to prevent bubbles in the receptor chamber and the flow lines. Methyl paraben is susceptible to biodegradation. Therefore, unless indicated differently, the receptor fluid in diffusion cell experiments with MP was treated with a small amount of chloroform (approximately 0.05 to 0.15 mg/mL) and sodium azide (0.02 mg/mL).

The total number of solutes and vehicles that could be studied in the project was small compared to all solutes and vehicles of concern for occupational dermal exposures. Solvent vehicles and solutes were selected to have similar and dissimilar chemical structures, which were expected to cause more or less interaction. For example, naphthalene (a polyaromatic hydrocarbon) was expected to interact more with toluene than with 1-octanol or cyclohexane. While most of the selected chemicals are not themselves significant occupational dermal hazards, they represent classes of chemicals that are and meaningful extrapolation to hazardous compounds in these classes should be justified. Other practical considerations included: (i) availability of HPLC analytical methods for analyzing the solutes in the various vehicles and receptor solution, (ii) skin penetration rates that will produce measurable concentrations of solutes in the diffusion cell receptor solution, (iii) solutes that will not produce significant irreversible damage to skin, and (iv) solutes and vehicles that do not pose significant health risk to laboratory personal conducting the experiments.

Table 3. Chemical properties of the model solvent vehicles and model solutes studied[a,b]

Chemical	ID	CAS No.	Formula	MW	ρ (g mL^{-1})	$\log K_{o/w}$	pK_a	$S_{j,w}$ (g L^{-1})	$S_{w,v}$ (g L^{-1})	$S_{j,o}{}^c$ (g L^{-1})	T_m (°C)	T_b (°C)	p^* (mm Hg)
water	H2O	7732-18-5	H2O	18.0	0.996	-1.38	7.0	1000	1000	41.7	0.0	100	23.8
1-octanol	OCT	111-87-5	C8H18O	130.2	0.826	3.00	--	0.54	41.7	miscible	-15.5	195	0.0794
toluene	TOL	108-88-3	C7H8	92.13	0.866	2.73	--	0.53	0.43	miscible	-95	111	28.4
cyclohexane	CYC	110-82-7	C6H12	84.16	0.779	3.44	--	0.055	--	151	6.6	80.7	96.9
isopropyl myristate	IPM	110-27-0	C17H34O2	270.5	0.853	7.17^d	--	1.35 x 10^{-5}	--	200	3	--	9.4 x 10^{-5}
naphthalene	NP	91-20-3	C10H8	128.2	1.145	3.30	--	0.031	--	61.9	80.2	218	0.085
4-cyanophenol	CP	767-00-0	C7H5NO	119.1	1.000	1.60	7.97	12.5	--	498	112	--	0.00665
methyl paraben	MP	99-76-3	C8H8O3	152.1	1.209	1.96	--	2.5	--	228	131	275	0.000237
4-chloronitrobenzene	CN	100-00-5	C6H4ClNO2	157.6	1.298	2.39	--	0.225	--	55.2	83.5	242	0.0219

[a] ID = identification as solvent vehicle (H2O, OCT, TOL, CYC, IPM) or solute (NP, CP, MP, CN); MW = molecular weight; ρ = density; $K_{o/w}$ = octanol-water partition coefficient; pK_a = -log$_{10}$[acid dissociation constant, K_a]; $S_{j,w}$ and $S_{j,o}$ = solubility limit of the solvent or chemical in water and octanol, respectively; $S_{w,v}$ = solubility of water in solvent vehicle j; T_m = melting point; T_b = boiling point; p^* = vapor pressure;

[b] properties listed are at 25 °C; most properties are from the Syracuse PhysProp database

[c] estimated as $S_{j,o} = S_{j,w} K_{o/w}$

[d] This value for $\log K_{o/w}$ is estimated because an experimental value is not available for IPM; other values are calculated using other calculators. Estimates from 5 different calculators available for estimating $\log K_{o/w}$ at the two URLs listed below were 6.37, 6.89, 7.02, 7.07, 7.17, and 7.18.
http://146.107.217.178/lab/aloqps/start.html
http://www.chemexper.com/tools/propertyExplorer/main.html

Table 4. Estimated and measured dermal absorption parameters for model chemicals and solvents in this study

Chemical	$P_{j,skin/w} \times 10^3$ (cm h^{-1})[a]	$SF_{j,skin/w}$ (μg/cm^{-2} h^{-1})[b]	$K_{j,sc/w}$[a]	$m_{j,sc/w}$ (μg cm^{-2})[c]	$\hat{S}_{j,sc/w}$ (mg g^{-1})[d]
	Eq. (11)	$= P_{j,sc/w}\, S_{j,w}$	Eq. (13)	$= \dfrac{K_{j,sc/w}\, S_{j,w}}{L_{sc}}$	$= \dfrac{K_{j,sc/w}\, S_{j,w}}{L_{sc}}$
water	0.16 (0.5)	156	0.10 (0.2)	160	390
1-octanol	36 (25, 61)	19	130 (12.5)	110	270
toluene	40 (83)	21	87	69	170
cyclohexane	104	5.7	280	23	56
isopropyl myristate	154	0.0021	1.2×10^5	2.5	6.2
naphthalene	55	1.7	220	10	25
4-cyanophenol	5.0	62 (170)	14	260	630
methyl paraben	5.6	14 (91)	25	92	230
4-chloronitrobenzene	10.2	2.3	50	17	41

[a] $P_{j,skin/w}$ calculated using Eqs. (11) and (12); $K_{j,sc/w}$ calculated using Eq. (13); values in parenthesis are experimental (Romonchuk and Bunge, 2006; Vecchia and Bunge, 2002b; 2002c).

[b] $SF_{j,skin/w}$ is the product of the saturation concentration in water and the calculated value of $P_{j,skin/w}$.

[c] $m_{j,sc/w}$ is the product of the saturation concentration in water and the calculated value of $K_{j,sc/w}$.

[d] $\hat{S}_{j,sc/w}$ is the saturation concentration per mass of dry SC calculated from $m_{j,sc/w}$ assuming 3.7 mL of hydrated SC per g of dry SC (Vecchia and Bunge, 2002b) and L_{sc} = 15 μm.

Rationale for Selection of Non-Aqueous Vehicles

The most common liquids in occupational skin exposures are water, hydrocarbons from a few chemical classes (e.g., saturated, aromatics, unsaturated non-aromatics, alcohols, ketones and ethers) and chlorinated hydrocarbons. Petroleum distillates, perhaps the most common hydrocarbon solvent encountered in occupational settings, consist predominantly of alkanes. While vehicles within a given class will behave differently, these differences will be smaller than differences between vehicles from different chemical classes. Thus, in this first systematic study of non-aqueous vehicles, we focused on differences between classes by studying water compared with one vehicle from each of four common classes: saturated alcohols (1-octanol), aromatic hydrocarbon (toluene), saturated hydrocarbon (cyclohexane), and a carboxylic acid ester lipid (1-tetradecanoic acid, isopropyl ester, which is identified in this report as isopropyl myristate). Because occupational skin exposures frequently involve solvent mixtures, binary mixtures of 1-octanol (OCT), toluene (TOL), and cyclohexane (CYC) were also studied.

In addition to representing an important chemical class, isopropyl myristate (IPM) was chosen because it is specified in the test rule issued by EPA in 2004 (US EPA, 2004) as an alternative vehicle to water for chemicals with low water solubility that cannot be applied neat (because they are solids or damage the skin). The test rule, issued under TSCA Section 4, required in vitro skin testing for 34 chemicals for which more than one million pounds are produced annually or handled by more than 1000 workers. The strategy behind the test rule is that the flux from saturated solutions of IPM and water are the same and therefore, a permeability coefficient from water could be estimated by multiplying the permeability coefficient measured from IPM by the ratio of the saturation concentrations in IPM and water (US EPA, 1992). Despite its inclusion in the 2004 EPA test rule, the thesis that flux from saturated solutions of IPM and water are the same is largely untested.

Rationale for Model Chemical Selection

All selected model chemicals were solids at experimental temperature (i.e., 32°C) and studied at their saturation concentration in each vehicle. Notably, the saturation concentrations are large for some of the solutes in the non-aqueous vehicles (e.g., naphthalene solubility in toluene is approximately 30 wt %). In addition, the selected solutes are: (i) known to primarily penetrate skin through the nonpolar pathway (i.e., compounds are non-ionized at experimental conditions and $K_{j,o/w} > 0$); (ii) similar to some but not all of the other solutes in ways that might be important to dermal absorption from the selected vehicles, (iii) similar to at least one hydrocarbon vehicle and dissimilar to another, (iv) exhibit a range of values in log $K_{j,o/w}$ without being so lipophilic that mass transfer resistances in aqueous solutions may be significant (i.e., log$K_{o/w} < 4.5$), and (v) are reasonable surrogates for those used in previous dermal investigations, so that mechanistic understandings gained in this study may be related to these earlier results.

Naphthalene (2 benzene rings) is an important component in occupational exposures and a relevant surrogate for other important components in fuels, petroleum distillates, coal liquids, feed stocks for many chemical syntheses (e.g., dyes, pesticides, carbon fibers, pharmaceuticals, and rubber), and in products used to seal roads, wood and roofs. As an aromatic hydrocarbon, we expected it might interact differently with skin containing toluene compared to skin with 1-octanol (or cyclohexane). 4-Cyanophenol is similar in structure and properties to munitions, such as trinitrotoluene and its metabolites; it is also similar to a number of precursors used the chemical processing industry. Methyl paraben is widely used in many commercial and consumer products and represents a common class of chemical in industrial

production. Because they are similar to each other, 4-cyanophenol and methyl paraben were expected to affect solubility of each in skin and solutions, although the direction of the effect (increased solubility because the solutes interact with each other or diminished solubility because they compete in a saturable process) was unknown until this study. 4-Chloronitro-benzene is used in the manufacture of p-nitrophenol, p-nitroaniline, p-aminophenol, phenacetin, acetominophen, parathion and other agricultural chemicals, rubber chemicals, antioxidants, oil additives and dapsone (an antimalarial drug). It is one of 34 compounds for which *in vitro* skin permeation data were required by the test rule, issued under TSCA Section 4, by EPA in 2004.

Skin

Split-thickness human skin (approximately 350-μm thick) collected within 24-hours post mortem was purchased from National Disease Research Interchange (NDRI, Philadelphia, PA) and stored at approximately minus 70°C until use. Prior to a permeability experiment, skin was removed from the freezer and cut into square pieces of about 1 cm^2. In most permeability experiments, the epidermis was separated from the dermis by heating for 60 seconds at 60°C (Peck *et al.*, 1993). In some permeability experiments and most EIS-diffusion cell experiments, split-thickness skin was used without further treatment. Isolated stratum corneum (SC) was used in the uptake experiments. This was prepared by enzymatically digesting the dermis and viable epidermis from 1.5 cm x 1.5 cm pieces of split-thickness skin in a 1% trypsin solution (from bovine pancreas, essentially salt free, 8.060 BAEE units/mg solid and 9.060 BAEE units/mg of protein, T-8915, Sigma, St. Louis, MO) for approximately 36 hrs at 32°C as described elsewhere (Liron *et al.*, 1994a; 1994b). After the SC is carefully peeled from the digested skin tissues, it is rinsed with distilled water, dried and stored in a desiccator for later use. In a few experiments, the contribution of the SC lipids on uptake of MP and CP alone and in combination from aqueous solutions was assessed by measuring uptake into SC with the lipids removed. In these experiments, the lipids of each weighed piece of dry isolated SC were extracted by soaking with gentle agitation for approximately 20 hours in 10 mL of 2:1 v:v chloroform:methanol. After rinsing three times in fresh samples of the chloroform:methanol solution, the remaining solvent was removed by evaporation at room temperature for at least 48 hours. The mass fraction of the lipids removed from the delipidized SC was determined gravimetrically.

<u>Permeation Experiments</u>

Permeation through skin of the selected compounds from the selected vehicles was determined in vertical flow-through Neoflon™ diffusion cells (9 mm, Series 1, in-line) from Permegear (Bethlehem, PA). The diffusion area of these cells is 0.64 cm^2 and the volumes of the donor and receptor chambers are approximately 1.0 and 0.5 mL, respectively. The skin membrane was clamped into each of the 14 cells with SC facing the donor chamber. The receptor chambers were then filled with PBS, connected to a peristaltic pump (Ismatec, Cole Parmer Instrument Company, Chicago, IL) and the cells were placed onto one of two cell holders (Permegear, Bethlehem, PA), which accommodated seven cells each. A short tube from the receptor chamber outlet directs the receptor fluid into a liquid scintillation vial positioned in a fraction collector (Retriever IV, ISCO Inc, Lincoln, NE). The cells and collection system are contained in an environmental chamber in which temperature and humidity can both be controlled.

In many experiments, skin was mounted in the diffusion cells with a receptor solution flowing at 0.6 mL h^{-1} and equilibrated overnight (approximately 12 hours) with deionized water in the donor chamber overnight and the environmental chamber set at 32°C. In other experiments, the skin surface was left exposed to air at 50% relative humidity in the chamber. After this, the donor chamber was emptied and dried (if filled with water overnight) and then was filled with a saturated solution of the selected compound(s) in the selected solvent solution. The receptor solution flow rate was adjusted be between 1 and 6 mL hr^{-1}, depending on the permeation rate (i.e., a lower flow rate was used from compounds that permeated at a lower rate). Excess chemical was added to saturated donor solutions to ensure that they remained saturated during the entire exposure time. In most experiments of a selected compound, the 14 diffusion cells were divided between the selected solvent and water (the reference vehicle), providing a direct comparison on the skin from the same subject measured on the same day. In a few experiments, chemical was applied to the skin surface as a neat powder or in a small volume of acetone that quickly evaporated. In these experiments, the skin surface was exposed overnight to air at controlled relative humidity varying from 10% to 90% to evaluate the effect of skin hydration. In most cases, receptor solution samples were collected hourly and the flow rate to each cell was determined by the weight change in the collection vials. Concentrations of the selected compound in the receptor fluid were determined by HPLC.

Equilibrium Uptake Concentration

Uptake was determined by measuring the amount of the test chemical in pieces of hydrated SC that were equilibrated in the selected solvent saturated with respect to water and chemical at 32°C. Pieces of dry isolated SC were weighed (2-4 mg) using a semi-microgram balance (Mettler Toledo AX26DR Delta Range, Columbus, OH) and equilibrated for at least 24 hours and usually 48 hours. In most experiments, saturation of the solution was maintained during equilibration by adding excess chemical, while preventing the possibility that particles of chemical might adhere to the SC samples. In most of these experiments, uptake was measured in two-chamber micro-dialysis cells (1.0 mL total volume from Harvard Apparatus, Holliston, MA), in which the SC sample in one chamber was separated from the solution with excess chemical in the other chamber by a porous membrane that was compatible with the solvent solution. In a less elegant version of this experiment, the solution with excess particles was contained in a dialysis bag that was submerged along with the SC sample in a saturated solution without excess chemical. In some studies, excess chemical was not included and the uptake results were adjusted for equilibrium concentrations that were measurably lower than saturation.

After equilibration, a sample of the solution containing the SC sample was collected and the SC sample was removed and adhering solution removed by quickly rinsing the sample three times in either acetonitrile or the same solvent used in the experiment but without any test chemical. The SC sample was then extracted 2 or 3 times in acetonitrile. Concentrations of the extracts were determined by HPLC using appropriate dilutions and the amount of uptake per mass of dry SC calculated. Concentration of chemical in the last extraction of each SC sample was always small (typically, less than 5% of the total mass of chemical extracted). The solute concentration in the solutions equilibrated with the SC was determined by HPLC. A chemical uptake experiment typically consisted of 16 dialysis cells divided to study one test chemical in 4 SC samples ($m = 4$) from each of two subjects ($n = 2$) in each of two solvents (8 cells each). When possible, the SC used in chemical uptake experiments was from the same subject studied in diffusion cell experiments of the same chemical and solvent.

The equilibrium uptake concentration of a solute j from saturated solutions reported as the mass of j per mass of dry SC from a vehicle v is represented in this report as $\hat{S}_{j,sdv}$. This saturation concentration per mass of dry SC is related to the saturation concentration reported as the mass of j per volume of hydrated SC ($S_{j,sdv}$) by the dry weight per volume of hydrated SC, which is estimated to be approximately one gram per 3.7 mL (Vecchia and Bunge, 2002b); i.e., $\hat{S}_{j,sdv} / S_{j,sdv} \approx 3.7$.

A small study was conducted to check that the uptake measurements determined chemical that was absorbed into the SC and not chemical that was in the solution adhering to the SC. Specifically, hydrated SC samples were swirled using forceps in a sub-saturated solution of NP in 1-octanol (50 mg/mL) for 0.5 min and then allowed to sit in the solution for an additional minute. The SC samples were then removed and the standard cleaning process used followed by extraction into acetonitrile. The apparent uptake after 1.5 minutes of exposure to the NP solutions was normalized by the solution concentration and compared with the equilibrium uptake results (also normalized for solution concentration). These showed that that residual adherence accounted for less than 10% of the measured uptake of NP from 1-octanol; no more than 0.5 mL of 1-octanol adhered per g of dry SC. The contribution of liquid adhering to the SC surface will vary with the concentration of chemical in the solution. Most probably the contribution of adhering liquid is not more than the equilibrium solution concentration multiplied by 0.5 mL/g. For all of the experiments in this study, this contribution was not more than 10% of the measured uptake.

Saturation Concentration

Solute concentrations in solutions saturated at 32°C were determined by determining dissolved concentration from a solution equilibrated with excess amounts of the test chemical. Various methods were employed over the course of the study to prevent particles from contaminating the samples of saturated solution. In several experiments, the micro-dialysis cells used in a procedure that was similar to the uptake experiments but without any SC. The submerged dialysis bag with excess chemical was also used. It was found that equally good results could be obtained from solutions containing particles by carefully collecting the solution sample after allowing the excess chemical to settle. Precipitation of naphthalene onto interior and exterior walls of the pipette tip was a problem in solutions of toluene and cyclohexane. Loss of naphthalene by this mechanism was reduced by using pipette tips that had been warmed to 32°C. Concentrations of the collected samples were determined by HPLC using appropriate dilutions.

EIS-Diffusion Cell Experiments

Potentiostatic EIS measurements (Gamry model PCI4/300) are collected on split-thickness human cadaver skin in glass, side-by side diffusion cells from Permegear (Hellertown, PA). The cells have been modified so that the skin is mounted inside a frame that can be removed from the cells as illustrated schematically in Figure 9. This design allows the skin to be removed from
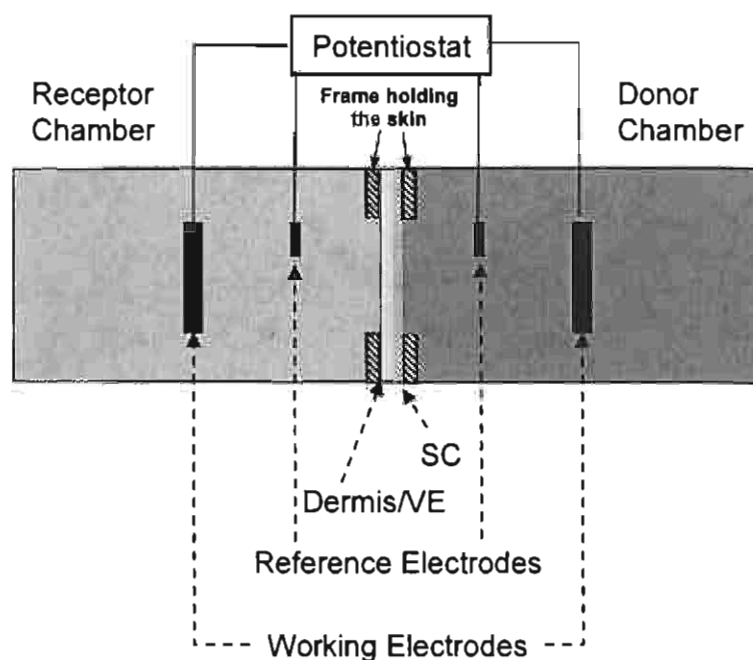
Figure 9. Schematic showing cross-sectional view of diagram of the EIS-diffusion cell apparatus

the cell for a chosen treatment and then returned to the cell for further measurements. The frame containing the skin, with a 1.77-cm^2 exposed area, is mounted inside the diffusion cell so that the outer surface of the SC is oriented toward the donor solution. The working electrodes are 12 mm diameter discs oriented parallel to the skin surface and the reference electrodes are cylinders 1.5 mm in diameter and 3 mm long oriented such that the long axis is vertical. The reference and working electrodes, which are all made from Ag/AgCl electrodes (In Vivo Metric, Healdsburg, CA), are located 18 and 32 mm from the skin surface, respectively in both chambers of the diffusion cell. Experiments can be conducted simultaneously on four diffusion cell-EIS systems, which are contained in an environmental chamber (ETS Model 5518, Glenside, PA) controlling the temperature at 32 °C.

In a typical EIS-diffusion cell experiments, split-thickness skin was clamped between the donor and receptor chambers, which were filled with chemical-free 0.01 M phosphate buffered saline solution (PBS, 0.138 M NaCl, 0.0027 M KCl, pH 7.4, from Sigma) and allowed to equilibrate with the skin for eight to ten hours. To minimize a pressure difference across the skin sample, the donor and receptor chambers were filled to the same height. EIS scans were

49

collected hourly during the equilibration period to establish a baseline for the electrical properties of the skin as well as to verify that the skin was at equilibrium before beginning the diffusion experiment. The chosen frequency range varied over the course of the study within a maximum range of 0.1 Hz to 300 kHz. The minimum frequency range was 1 Hz to 10 kHz (i.e., 4 orders of magnitude) and the maximum range was 1 Hz to 300 kHz. Each scan takes less than 5 minutes to complete. A small amplitude AC potential, 10 mV root mean squared, is applied to minimize skin damage during the scan and to confine the scan to a pseudo-linear region of the current versus voltage curve. The analysis of the EIS data, which was developed over the course of this project, is described in the Results and Discussion section. Briefly, the data, which were shown to be Kramers-Kronig consistent, were analyzed to determine the R-CPE parameters (R_e, R_m, Q, α, and C_{eff}, which were explained in the Background section of this report).

Once the skin was equilibrated (as indicated by stable EIS scans over a few hours), the donor solution (pre-equilibrated at 32°C) is replaced with the selected solution. Excess chemical was included if the donor solution was saturated. If the volume of solution in the receptor chamber was insufficient to maintain sink conditions over the course of the experiment (i.e. the concentration in the receptor chamber might exceed 10% of the solubility limit of the permeating solute), then the receptor chamber solution (pre-equilibrated at 32°C) was replaced as needed for sink conditions to be insured. Periodically, samples from the receptor solution were collected and replaced with fresh receptor solution. In most cases, the duration of the diffusion portion of the experiment was long enough for at least four receptor solution samples to be collected after steady state was reached (i.e., the elapsed time after the donor solution containing chemical was introduced was great than or equal to 2.4 times the lag time (Bunge *et al.*, 1995b)).

In several experiments, the effect of a chemical treatment on permeation of a model chemical and the resistance and effective capacitance of the skin was determined. These experiments were conducted in two different ways. In the first, EIS and permeation was measured before and after treatment on the same piece of skin. In the second, EIS and permeation was determined in parallel experiments on two cells containing skin from the same source subjected to the same protocol except that one cell was treated and one was not. Unless indicated otherwise, EIS scans were collected hourly during the period of the permeation measurements.

Results and Discussion

A large body of experimental data and computational results has been generated as part of this project. It is our intention to publish all of the work in refereed journal papers, which will insure the widest possible use of these results. Some results have been published already. However, as many of the final measurements have only been made in the past year, we are still preparing and submitting manuscripts at this time. Also, although support from NIOSH is now completed, some experimental work and further data analyses (especially related to Eric White's PhD thesis, which describes the EIS experiments but is not completely written yet) are continuing with institutional support. A summary of the main results of this research are listed next, after which more detailed results are provided. We note that changes in the detailed results may occur during the data review that will occur in finalizing the results for publication.

Summary of Main Results

1. Flux through skin and uptake into stratum corneum were measured from saturated solutions of two model solutes (methyl paraben and 4-cyanophenol) tested individually and in combinations with each other from water. These studies have shown that these two compounds, neither of which is considered a skin enhancer, do interact synergistically to increase the flux through skin. Additional experiments comparing uptake into stratum corneum that had and had not been delipidized suggest that CP changes MP solubility in the corneocytes.

2. Flux through skin and uptake into stratum corneum were measured for two model solutes (methyl paraben and 4-cyanophenol) presented to skin as pure powders in air at different levels of relative humidity, or as saturated aqueous solutions prepared with different amounts of LiCl salt or K_2CO_3 salt (to produce different hydration levels in the skin). Permeation is reduced significantly through desiccated skin. Permeation from neat powders is increased in the presence of humidified air and similar to measurements from saturated solutions of deionized water.

3. Flux through skin and uptake into stratum corneum were measured from saturated solutions of three model compounds (4-cyanophenol, methyl paraben, and naphthalene) from water and three model organic solvents (toluene, 1-octanol, cyclohexane) representing aromatic, aliphatic, and aliphatic alcohol solvents. From these results, we have characterized solvent-skin and solvent-solute interactions affecting the rate of solute permeation.

4. Flux through skin and uptake into stratum corneum were measured from saturated solutions

of three model compounds (4-cyanophenol, methyl paraben, and naphthalene) from water and mixtures of three model organic solvents (toluene, 1-octanol, cyclohexane) representing aromatic, aliphatic, and aliphatic alcohol solvents. From these results, we have characterized the solvent-solvent mixture effects as well solvent mixture-skin and solvent mixture-solute interactions affecting the rate of solute permeation.

5. Flux through skin and uptake into stratum corneum were measured from saturated solutions of four model compounds (4-cyanophenol, methyl paraben, naphthalene, and 4-chloronitrobenzene) from water and isopropyl myristate (IPM), which has been recommended as an alternative to water for determining skin permeation of highly lipophilic chemicals, especially chemicals of concern in the workplace. Generally, the results from water and IPM were similar supporting the use of IPM as an alternative vehicle to water.

6. A thermodynamic model was developed for estimating dermal absorption from non-ideal solutions, applied specifically to 2-butoxyethanol (BE) and water. This model framework is the basis of the computational effort of Aim 4. These computations show that the anomalous permeation behavior of BE is predictable.

7. Thermodynamic models of the solvent mixtures have been developed for interpreting the measurements of solute permeation and uptake into skin from mixtures of solvents compared with determinations from the pure solvents. These calculations indicate that solute permeation and uptake into skin from a solvent mixture can be predicted from measurements of solute j made in the pure solvents.

8. The electrochemical impedance spectroscopy (EIS) instrument and diffusion cell assembly was acquired, assembled, modified (based on results), and demonstrated as useful for assessing skin barrier function. Methods were developed for deriving from qualified data the electrical resistance and effective capacitance of the skin. Data were qualified by assessment for Kramers-Kronig consistency.

9. EIS measurements and skin permeation determinations have been collected on several pieces of human skin to assess the hypothesis that the capacitive character of the skin is correlated with permeability of nonpolar solutes. The results appear to demonstrate that this is generally not the case, although further data analysis is still underway.

10. A review was completed of the existing skin literature reporting electrical resistance, impedance measured at a single frequency, and EIS data. It is evident from this review that these measurements have been reported inconsistently (and often incorrectly) and

sometime misunderstood. Some data from this literature is being reanalyzed using the new methods for analyzing EIS data and a review paper of impedance measurements in skin is being prepared.

11. EIS measurements have been collected on two layers of skin positioned with the stratum corneum (SC) of the two layers in contact with each other and with a conducting solution separating the two SC layers. The results of these study show that resistance is greater when there is SC-SC contact, suggesting that channels or holes in the SC may be the primary route of charge transfer. This is consistent with previously published measurements of skin permeation through a single piece of SC compared with the SC layered on top of an epidermal membrane (Essa *et al.*, 2002).

12. EIS measurements and skin permeation determinations of a nonpolar model compound (either 4-chloronitrobenzene or 4-cyanophenol) have been collected before and after treatments that altered the skin barrier function, including mechanical damage the skin (i.e., holes added using a needle) and treatment with dimethyl sulfoxide (DMSO) or solvents. The results indicate that the electrical measurements (especially the skin resistance) are generally more sensitive to the treatments than permeation of the model compound.

Permeation and Equilibrium Uptake Concentration

Permeation through human skin and uptake into isolated human SC was determined for the model compounds and vehicles listed in Table 5. Data collected on SC that was delipidized or treated with DMSO are also summarized in Table 5. The main results from these studies are described in the next few paragraphs.

Mixtures of methyl paraben (MP) and 4-cyanophenol (CP) in Water

The steady-state saturated flux through heat separated human epidermis and equilibrium uptake concentrations in the SC from saturated aqueous solutions are listed in Table 6 for MP and CP alone and in combination. Because the saturated solutions were in equilibrium with the pure CP and MP, the thermodynamic activity of the compounds was the same whether or not the other solute was present. Although there is nothing in the chemical structures of MP or CP that suggests either would be a penetration enhancer (other than their similarities to each other), the dermal permeation rates as well as SC uptake for both compounds are increased when the other is present. The increase in MP flux in the presence of CP is primarily due to increases in MP uptake in the SC (i.e., the saturated mass uptake ratio when CP is present,

Table 5. Permeation (P) through skin or uptake (U) into isolated stratum corneum (SC) from saturated solutions of the indicated model compounds have been measured from the indicated vehicles for the designated treatment of the SC [a]

Vehicle	Treatment [b]	CP	MP	NP	CN	MP-CP mixed
H2O	None	P, U	P, U	P, U	P, U	P, U
TOL	None	P, U	P, U	P, U		
OCT	None	P, U	P, U	P, U		
IPM	None	P	P	P	P, U	
OCT-TOL mixed	None	P, U	P, U	P, U		
CYC-TOL mixed	None	P, U	P, U	P, U		
OCT-CYC mixed	None	P, U	P, U	P, U		
H2O	DMSO	P, U			P, U	
H2O	delipidized SC				U	U
ACT (evaporate)	humidified air	P	P	P		

[a] Vehicles: water (H2O), toluene (TOL), cyclohexane (CYC), 1-octanol (OCT), isopropyl myristate (IPM), acetone (ACT) allowed to evaporate

Model compounds: 4-cyanophenol (CP), methyl paraben (MP), naphthalene (NP), 4-chloronitrobenzene (CN)

[b] Skin treated with: 100% dimethyl sulfoxide (DMSO), chloroform:methanol to extract lipids (delipidized SC), skin surface exposed to air controlled at relative humidity values varying from about 20-90% (humidified air)

Table 6. Steady-state flux through heat separated human epidermis and silicone rubber membranes and equilibrium uptake concentrations in the SC from saturated aqueous solutions of MP and CP alone or in combination [a]

Quantity	Stratum corneum (SC)				Silicone rubber membrane			
	MP alone	MP with CP	CP alone	CP with MP	MP alone	MP with CP	CP alone	CP with MP
$SF_{j,sclv}$ (μg/cm²·h)	26 ± 7.8%	135 ± 6.2%	123 ± 11%	325 ± 7.3%	48.9 ± 12.3%	51.3 ± 4.3%	91.4 ± 6.0%	96.8 ± 6.0%
$\hat{S}_{j,sclv}$ (μg/mg of dry SC)	33.9 ± 25%	218 ± 17%	274 ± 18%	451 ± 4.5%				
$SF_{j,sclv} / \hat{S}_{j,sclv}$ (mg of dry SC/cm²·h)	0.77 ± 26%	0.62 ± 18%	0.45 ± 21%	0.72 ± 8.6%				
$SF_{j,sclwith} / SF_{j,sclwithout}$ [b]		5.19 ± 10%	±	2.64 ± 13%		1.05 ± 13%	±	1.06 ± 8.0%
$RM_{j,with/without}$		6.43 ± 30%	±	1.65 ± 19%				
$RD_{j,with/without}$ [c]		0.81 ± 32%	±	1.61 ± 23%				

[a] Mean ± 95% confidence interval. All measurements were made at 32°C. All SC measurements were made on a total of 10 to 16 samples that were collected from two subjects. For the silicone rubber measurements n = 4 for MP or CP alone and n=6 for MP and CP combined.

[b] $Rm_{j,with/without} = S_{j,sclwith} / S_{j,sclwithout}$ as specified by Eq. (6); note that $S_{j,sclwith} / S_{j,sclwithout} = \hat{S}_{j,sclwith} / \hat{S}_{j,sclwithout}$

[c] $RD_{j,y/v} = \left(SF_{j,scly} / SF_{j,sclv} \right) / Rm_{j,y/v}$ as specified by Eq. (9)

$RM_{MP,with/without}$, is 6.43 ± 30% compared with a negligible change in the diffusion ratio when CP is present, $RD_{MP,with/without}$ = 0.81 ± 32%). In contrast, the increase in CP flux in the presence of MP is due to changes in both the CP uptake as well as diffusion rates as indicated by similar increases in the ratio of saturated mass uptake and diffusion (i.e., 1.65 ± 19% and 1.61 ± 23% for $RM_{MP,with/without}$ and $RD_{MP,with/without}$, respectively). The ratio of the saturated flux to the saturated uptake concentration ($SF_{j,sclv}/\hat{S}_{j,sclv}$), which is also listed in Table 6, should be proportional to the diffusion rate. It appears then that the diffusion rates for MP alone and in the presence of saturated CP solutions are almost the same as the diffusion rates for CP in the presence of MP.

Since the thermodynamic activities of MP and CP in saturated solutions should be the same whether or not the other solute is present, the saturated flux of MP and CP through a membrane that is unchanged by MP and CP should be the same whether or not the other solute is present. This hypothesis was tested on silicone rubber membranes (SRM), for which there was no statistically significant difference on the saturated flux of MP or CP when they were present alone or in combination (see Table 6).

To assess the contribution of the SC lipids on uptake, a second series of experiments were conducted to compare results for the saturated uptake concentration into delipidized and untreated SC. The results, listed in Table 7, indicate that the saturated uptake concentration (on a dry basis; i.e., $\hat{S}_{j,sclv}$) of CP into SC without lipids is about 70% of SC with lipids. A similar result was observed for MP in the presence of CP. However, when MP is present alone, the uptake into SC without lipids was only about 40% of SC with lipids. This suggests that CP enhances MP uptake primarily by increasing the amount of MP in the corneocytes (i.e., into the SC without lipids); whereas the effect of MP on CP is almost the same for lipids and corneocytes. Consistent with this, the saturated mass ratio of CP in the presence of MP compared to alone ($Rm_{j,with/without}$ in Table 7) is the not statistically significantly different for SC with and without lipids. However, for MP in the presence of CP, $Rm_{j,with/without}$ is large by nearly a factor of two.

Additional details on the dermal permeation and uptake of CP and MP from saturated aqueous solutions containing both solutes are provided elsewhere (Romonchuk and Bunge, 2009). This paper also describes the use of the saturated mass and diffusion ratios ($Rm_{j,y/v}$ and $RD_{j,y/v}$, respectively) to assess the effect of nicotinamide on diffusion cell data from aqueous solutions of MP and ethyl, propyl and butyl paraben. Based on this analysis, we concluded that addition of nicotinamide increased the paraben permeation through skin primarily by increasing the SC uptake, with the exception of ethyl paraben, which, due to formation of a co-crystal with

Table 7. Equilibrium uptake concentrations in untreated and delipidized SC from saturated aqueous solutions of MP and CP alone or in combination [a]

Quantity	Untreated Stratum Corneum (SC)				Delipidized Stratum Corneum (SC)			
	MP alone	MP with CP	CP alone	CP with MP	MP alone	MP with CP	CP alone	CP with MP
$\hat{S}_{j,scv}$ (μg/mg of dry SC) [a]	27.4 ± 2.5%	146 ± 11%	192 ± 5.5%	339 ± 9.9%	11.0 ± 21%	110 ± 14%	131 ± 4.0%	223 ± 11%
$RM_{j,with/without}$ [b]		5.33 ± 11%		1.77 ± 11%		10 ± 25%		1.70 ± 12%
$RM_{j,delip/untreated}$ [c]					0.40 ± 21%	0.75 ± 18%	0.68 ± 7%	0.66 ± 15%

[a] Mean ± 95% confidence interval. All measurements were made at 32°C. Measurements of MP or CP alone were made on 3 pieces of SC from each of two subjects; measurements on MP and CP combined were made on 8 pieces of SC from each two subjects. The data presented in this table were measured in the same subjects, which were different than the subjects in the study presented in Table 6.

[b] $Rm_{j,with/without} == S_{j,scwith} / S_{j,scwithout}$ as specified by Eq. (6); note that $S_{j,scwith} / S_{j,scwithout} = \hat{S}_{j,scwith} / \hat{S}_{j,scwithout}$

[c] $Rm_{j,delip/untreated} = S_{j,scdelip} / S_{j,scuntreated}$ for MP and CP alone or in combination

nicotinamide having a 1:1 molar composition, showed reduced skin uptake and flux in the presence of nicotinamide (Romonchuk and Bunge, 2009).

Permeation and Equilibrium Uptake Concentrations from Nonaqueous Solutions

The steady-state flux through human epidermis and equilibrium concentrations in the SC of CP, MP and NP was determined from saturated solutions of toluene (TOL), 1-octanol (OCT), and cyclohexane (CYC) and their mixtures. The full analysis of the complete data set is still being completed. Example results for CP and MP from binary mixtures of CYC and either TOL or OCT are presented in Figure 10 for two different subjects. While the magnitude of the flux was different between subjects, the trends within each subject were consistent with each other. For both CP and MP the steady-state saturated flux from 100% CYC was smaller than from 100% TOL and generally decreased with increasing amounts of CYC in the vehicle. By comparison, the flux of both CP and MP from 100% OCT was similar to 100% CYC, but the mixtures containing 50 and 75% (on a volume basis) CYC exhibited a statistically significant increase in flux. This distinctly different behavior for the mixture of solvents that are similar (CYC:TOL) and different (CYC:OCT) can be explained in terms of the thermodynamic activity of TOL and OCT in binary mixtures with CYC. Thermodynamic activity results for the binary systems of TOL or OCT in CYC, presented below are consistent with the flux results shown in Figure 10. The flux results shown in Figure 10 can be compared with the steady-state saturated fluxes from water (see Table 6), which were 0.026 mg/cm^2-h for MP and 0.123 mg/cm^2-h for CP. Of the three pure solvents, the largest increase in flux was from TOL. Otherwise, the increase in saturated flux from CYC and OCT was either similar to or only a little larger than from water.

Steady-state flux results for NP from saturated solutions in pure and 50:50 binary mixtures of CYC, OCT, and TOL are listed in Table 8. In this case, the saturated flux increased in the order of

Table 8. Steady-state flux of naphthalene (NP) through heat separated human epidermis from saturated solutions in pure and binary mixtures of cyclohexane (CYC), 1-octanol (OCT), and toluene (TOL) [a]

Vehicle	$SF_{j,sclv}$ (μg/cm^2·h)			n
CYC	4.93	±	46%	8
CYC:OCT (50%)	3.69	±	35%	6
OCT	3.86	±	27%	7
OCT:TOL (50%)	6.27	±	28%	7
TOL	5.40	±	43%	7
CYC:TOL (50%)	8.49	±	47%	7

[a] Mean ± one standard deviation for measurements made on 3 or 4 pieces of skin from each of two subjects (identified as subjects *AD* and *AJ*) for a total of n samples. All measurements were made at 32°C. Mixture compositions are in volume %.
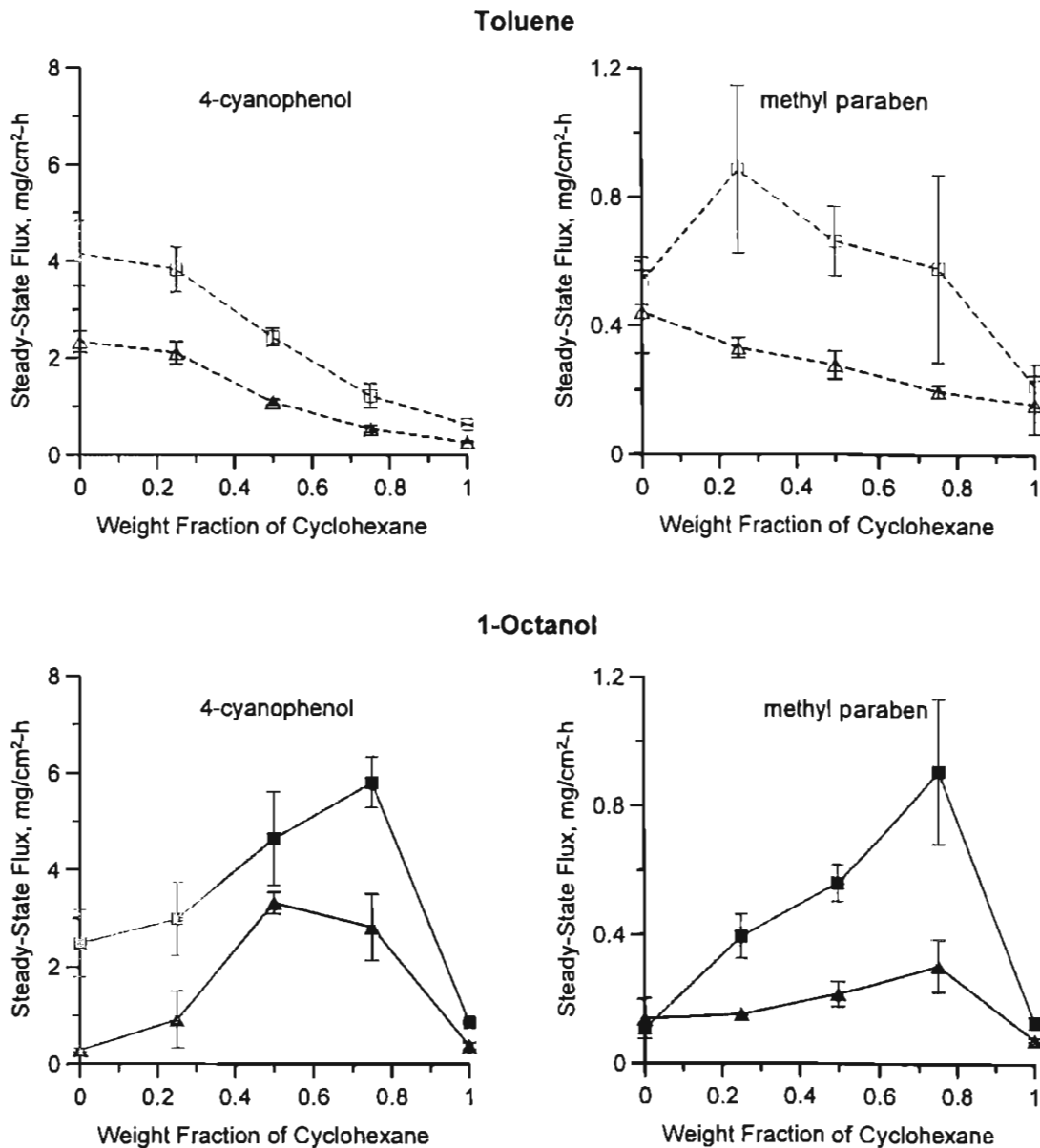
Toluene

1-Octanol

Figure 10. Steady-state flux (mean ± one standard deviation) from saturated solutions of either 4-cyanophenol (CP) or methyl paraben (MP) in either toluene (dashed line, open symbols) or 1-octanol (solid line, filled symbols) measured in heat-separated human epidermis from subjects AL (squares) and AH (triangles).

CYC:OCT:TOL but by only a small amount. Enhanced saturated flux from TOL, which is the only aromatic solvent in the study, was anticipated. Similar to the results for MP and CP, the largest increase in saturated flux occurred for the solvent mixtures; in this case, the mixtures with TOL gave the largest flux. In measurements of different subjects than those in the experiments listed in Table 8 (identified as subjects X, Y and Z), the saturated fluxes from TOL and OCT compared with water was approximately 3-fold and 2-fold larger. (The full analysis of all the solvent data is still being completed.)

Equilibrium uptake concentrations reported per dry mass of SC (i.e., $\hat{S}_{j,sclv}$) results for MP, CP, and NP into isolated stratum corneum from each of the three model solvents (TOL, OCT, and CYC) are compared with water in Table 9. Uptake results from binary mixtures of the model solvents are listed in Table 10. Compared to water, there was little or no enhancement in the saturated mass uptake for either CP or MP in TOL or CYC. However, there was a 5-fold increase for CP from OCT and more than a 20-fold increase for MP from OCT. This was surprising since there was no corresponding increase in the saturated flux for CP and MP from OCT. This suggests that either there is a corresponding decrease in the diffusion from SC containing OCT compared with water, or that OCT alters the SC in a significant way during the uptake experiments that is not observed in the diffusion cell experiments.

For NP the mass uptake ratio compared with water is significantly larger than one ((i.e., greater than 50-fold) and increases in the same order as the saturated flux results (i.e., CYC:OCT:TOL). The possibility exists that the uptake numbers for NP from solvents are confounded by adherence of small amounts of solvent, in which NP is highly soluble. However, it appears from experiments conducted with SC exposed to NP in 1-octanol for only a couple minutes that at most about 10% of the measured uptake amount is from solvent adhering to the surface of the SC samples. The magnitude of the enhanced uptake in the present of the three solvents compared with water was surprising since the increase in the saturated flux compared with water was either small or not statistically significant for the three solvents.

Solubility

Preliminary solubility values for the four model compounds in this study in water, TOL, OCT, CYC, IPM and in 50:50 mixtures of TOL, OCT, and CYC are listed in Table 11. Most of the numbers reported in Table 11 were concentrations of the solutions in the chamber of the micro-dialysis cells that contained the SC sample. Solubility determinations in independent experiments are currently underway and, based on these results, the final numbers may be revised. According to the numbers in Table 11, the smallest solubility for CP is in CYC and the

Table 9. Equilibrium uptake concentration ($\hat{S}_{j,scv}$) of three model compounds into isolated stratum corneum from selected vehicles[a]

Compound	Subject	H2O			TOL				CYC				OCT			
		mean	SD	n	mean	SD	n	Ratio[b]	mean	SD	n	Ratio	mean	SD	n	Ratio
CP	AL	218	16	4	291	44	4	1.3	137	54	3	0.63	1052	209.9	4	5.0
	AH	282	5.1	3	371	65	4	1.3	189	59	4	0.67	1397	251.0	4	5.0
	AL&AH	245	37	7	331	67	8	1.3	167	59	7	0.68	1225	282.6	8	5.0
MP	AL	33.0	0.54	4	24.3	5.6	4	0.74	31.6	5.3	4	0.96	711.2	40.3	3	22
	AH	28.5	2.4	4	45.9	13	4	1.6	31.1	6.5	4	1.1	771.6	198.2	4	27
	AL&AH	30.7	2.9	8	35.1	15	8	1.1	31.8	5.5	8	1.0	745.8	145.7	7	24
NP	X	8.19	0.82	4	861	365	4	110	448	130	4	55	521.4	126.1	4	64
	Y	7.30	1.8	3	1072		1	150	587	170	4	80	708.9	202.7	4	97
	X&Y	7.81	1.3	7	903	330	5	120	517	160	8	66	615.2	185.6	8	79
MP:CP[c]	All	0.13			0.11				0.19				0.61			
NP:CP	All	0.25			26				17				0.82			

[a] Mean ± one standard deviation (SD) for n samples from the indicated subject; all measurements were made at 32°C and are reported as μg of solute per mg of dry SC
Vehicles: water (H2O), toluene (TOL), cyclohexane (CYC), 1-octanol (OCT)
Model compounds: 4-cyanophenol (CP), methyl paraben (MP), naphthalene (NP)

[b] Ratio of uptake from solvent compared with water (i.e., $Rm_{j,v/w}$)

[c] Compound 1:Compound 2 = ratio of uptakes for compound 1 to compound 2 from each solvent

Table 10. Equilibrium uptake concentration ($\hat{S}_{j,sclv}$) of three model compounds into isolated stratum corneum from solvent mixtures compared with water[a]

Compound	Subject	H2O			50:50 CYC:TOL				50:50 CYC:OCT				50:50 TOL:OCT				IPM			
		mean	SD	n	mean	SD	n	Ratio[b]	mean	SD	n	Ratio	mean	SD	n	Ratio	mean	SD	n	Ratio
CP	AL	218	17	4	374	14	4	1.7	512	28	4	2.4	831	260	4	3.8				
	AH	282	5.1	3	328	53	4	1.2	578	140	4	2.1								
	X												971	270	4	--				
	AL&AH&X	245	37	7	351	43	8	1.4	545	98	8	2.22	901	250	8	3.7				
	AN	221	12	4													708	100	4	3.2
	AO	271	11	4													540	88	4	2.0
	AN&AO	246	29	8													620	126	8	2.5
MP	AL	33.0	0.54	4	63.7	16	4	2.0	306	36	3	9.3	499	120	4	15				
	AH	28.5	2.4	4	59.5	10	4	2.1	333	37	4	12								
	X												673	44	4	—				
	AL&AH&X	30.7	2.9	8	61.6	13	8	2.0	321	36	7	11	586	130	8	19				
	AN	34.0	3.8	4													144	15	3	4.2
	AO	34.3	3.5	4													145	19	3	4.2
	AN&AO	34.1	3.4	8													144	15	6	4.2
NP	X	8.19	0.82	4									1150	170	4	140				
	Y	7.30	1.8	3	1150	330	4	160	1170	180	4	160	822	320	4	110				
	AD				868	270	4	—	830	130	4	--								
	X&Y&AD	7.81	1.3	7	1010	320	8	130	1000	230	8	130	986	300	8	130				
MP:CP[c]	All	0.13			0.18				0.59				0.65				0.23			
NP:CP	All	0.25			16				3.1				1.7				0.62			

[a] Mean ± one standard deviation (SD) for n samples from the indicated subject; all measurements were made at 32°C and are reported as µg of solute per mg of dry SC
Vehicles: water (H2O), toluene (TOL), cyclohexane (CYC), 1-octanol (OCT)
Model compounds: 4-cyanophenol (CP), methyl paraben (MP), naphthalene (NP)

[b] Ratio of uptake from solvent mixture compared with water (i.e., $Rm_{j,v/w}$)

[c] Compound 1:Compound 2 = ratio of uptakes for compound 1 to compound 2 from each solvent

Table 11. Preliminary estimates of solubility for four model compounds in the vehicles used in this study [a]

Vehicles	CP	MP	NP	CN
H2O	16.6 ± 4.2%	2.82 ± 2.3%	0.039 ± 3.6%[b]	0.3[b]
TOL	18.9 ± 35%	8.10 ± 4.4%	304 ± 39%	
OCT	299 ± 9%	133 ± 10%	124 ± 7.2%	
CYC	0.110 ± 37%	0.144 ± 18%	211 ± 8.1%	
TOL:OCT (50%)	291 ± 18%	165 ± 5.5%	246 ± 19%	
CYC:TOL (50%)	2.32 ± 8.3%	1.84 ± 5.7%	353 ± 2.1%	
CYC:OCT (50%)	109 ± 12%	77.3 ± 13%	194 ± 3.0%	
IPM	75[b]	38.0 ± 2.4%	196 ± 3.7%	179 ± 8%

[a] Mean ± one standard deviation(%). All measurements were made at 32°C and are reported as mg/mL
Vehicles: water (H2O), toluene (TOL), cyclohexane (CYC), 1-octanol (OCT)
Model compounds: 4-cyanophenol (CP), methyl paraben (MP), naphthalene (NP), and 4-chloronitrobenzene (CN)
Unless indicated otherwise, results are concentrations measured in the chamber of the micro-dialysis cell containing the SC sample after equilibration. Most results are from 7 or 8 cells containing SC from two subjects. These results may be revised based upon separate solubility determinations that are being completed.
[b] From separate solubility study

largest in OCT. The smallest solubility for MP is also in CYC, but the largest solubility is for the 50:50 mixture of TOL and OCT. NP is most soluble in the 50:50 mixture of CYC:TOL by a factor of 10,000 compared with the smallest solubility, which is in water.

<u>Thermodynamic Activity Modeling Compared with Dermal Absorption</u>

2-Butoxyethanol and Water

To develop fundamental understanding of the underlying mechanisms of the effects of different vehicles, the steady-state flux through skin and the equilibrium uptake concentration into isolated SC from saturated solutions are compared with estimates of thermodynamic activity derived from phase equilibrium thermodynamics. As a starting point, this approach was developed and applied to published measurements for mixtures of 2-butoxyethanol (BE) and water. Specifically, a thermodynamic model was developed for estimating dermal absorption from non-ideal solutions and applied to BE and water. This model framework is the basis of the computational effort of Aim 4. These computations show that the apparently *anomalous* permeation behavior of BE are predictable.

BE is a common ingredient in commercial and residential products, many of which are aqueous solutions. Water and BE are miscible in all proportions at skin temperature and the flux of BE across skin from human (*in vitro* and *in vivo*), guinea pig (*in vivo*) and rat (*in vitro* and *in vivo*) has been reported for various concentrations in water ranging from less than 1% (on a weight basis) to neat BE (Dugard *et al.*, 1984; Jakasa *et al.*, 2004; Korinth *et al.*, 2005). While there is variability in the data, there is a consistent nonlinear variation with BE concentration, which is illustrated by the measurements made in guinea pigs *in vivo* (see Figure 11). The observations show three distinct behaviors, which are indicated in Figure 11 as Regions I, II and III. In dilute BE solutions the flux increases proportional with increasing BE concentration (Region I). At concentrations between about 20 and 90%, the flux appears to be nearly unaffected by concentration change (Region II). Finally, BE flux from neat BE is substantially smaller (Region III) than from the 50% solution and similar to that from the 10%. Despite differences in the experimental procedures, similar observations have been reported for *in vitro* and *in vivo* studies on human skin (Dugard *et al.*, 1984; Jakasa *et al.*, 2004; Johanson *et al.*, 1988; Korinth *et al.*, 2005; Traynor *et al.*, 2007a; 2007b; Wilkinson and Williams, 2002), and for *in vitro* studies on rat (Traynor *et al.*, 2007a).

Because these results violate the usual expectation that dermal absorption of chemicals increase proportional with solute concentration in the vehicle, a recent paper concluded that the "applicability of Fick's law regarding the prediction of percutaneous absorption of liquid
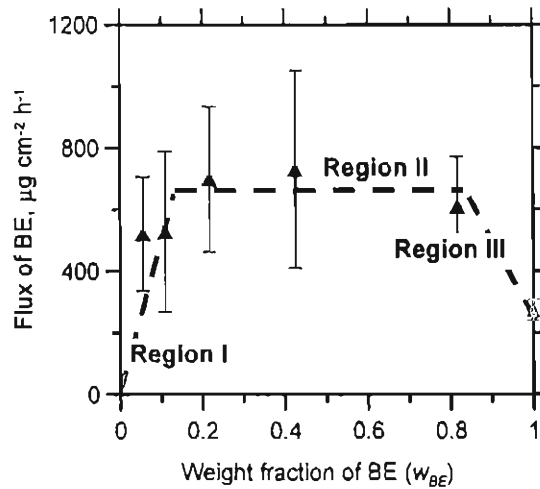
Figure 11. Flux of 2-butoxyethanol (BE) through guinea pig skin determined *in vivo* as a function of the weight fraction of BE in water (data from Johanson and Fernstrom, 1988.

compounds by modeling problematic" (Korinth *et al.*, 2005). As shown below, the apparently anomalous skin permeation of BE from water and neat solutions arises because mixtures of BE and water form thermodynamically non-ideal solutions. Thus, the problem is not with Fick's law, but with properly representing the effect of thermodynamic activity on solute permeation from the vehicle.

The approach begins with the steady-state flux of a solute *j* from vehicle *v* , which is described by Eq. (2) and rewritten here:

$$F_{j,sc/v} = S_{j,sc/v} \ D_{j,sc/v}/L_{sc} \left(C_{j,v}/S_{j,v} \right)$$ (2)

It is convenient to rewrite Eq. (2) as:

$$F_{j,sc/v} = SF_{j,sc/v} \left(C_{j,v}/S_{j,v} \right) = SF_{j,sc/v} \ a_{j,v}$$ (40)

where the fraction saturation of the chemical ($C_{j,v}/S_{j,v}$) is replaced with the symbol $a_{j,v}$ representing the thermodynamic activity of species *j* in the vehicle *v*. The parameter $SF_{j,sc/v}$, defined in Eq. (5):

$$SF_{j,sc/v} = S_{j,sc/v} \ D_{j,sc/v}/L_{sc}$$ (5)

represents the steady-state flux of chemical through the SC when it is exposed to a saturated vehicle. It follows from Eq. (4) that the steady-state flux through the SC is described by the flux from a saturated vehicle *v* (i.e., $SF_{j,sc/v}$) multiplied by the fractional saturation of chemical in any

other vehicle y (i.e., $C_{j,y}/S_{j,y}$) provided that vehicle y does not interact with the SC to change it (i.e., $Rm_{j,y/v}$ and $RD_{j,y/v}$ equal one). Thus, as long as a vehicle does not change the chemical properties of the SC, $SF_{j,scv}$ is independent of the vehicle in which the solute is dissolved. This has been supported by several experimental studies in which membrane permeation of a solute was measured from saturated solutions (i.e., $C_{j,y} = S_{j,y}$) prepared in different vehicles.

The studies by Theewes et al. (1976) and Twist and Zatz (1986) are worth noting. Theewes et al. (1976) showed that flux of progesterone through an ethylene-vinyl acetate copolymer was the same at equal fraction of saturation in three different vehicles: water, Dow 360 silicone oil, and a polyethylene glycol (PEG 600). They also coined the name transference to represent the product of the diffusion coefficient and the saturation concentration in the membrane). Twist and Zatz (1986) observed a constant flux of methyl paraben through polydimethylsiloxane (i.e., silicone rubber) membranes from saturated solutions prepared in water, propylene glycol:water mixtures, polyethylene glycol (PEG 400):water mixtures and glycerin:water mixtures. In contrast, flux of methyl paraben from saturated solutions prepared in ethanol and water mixtures containing from 0 to 100 weight percent ethanol increased with increasing ethanol (i.e., the saturated flux s not constant), because ethanol swells the polydimethylsiloxane (silicone rubber) membrane.

The ratio of concentration to saturation, $C_{j,v}/S_{j,v}$, represents thermodynamic activity $a_{j,v}$ for a solute j with limited solubility (~ less than 5 mole percent) in the vehicle v. For a species j that has a larger saturation concentration in vehicle v or is completely miscible in a vehicle v, then thermodynamic activity must be deduced from experimental measurements or by methods for estimating phase equilibrium that have been developed in the chemical engineering literature.

When the chemical components in a mixture do not interact, the solution is said to be ideal, and the thermodynamic activity a_j of each of the components is equal to its mole fraction relative to the saturation mole fraction in the solution (Prausnitz, 1969):

$$a_j = x_j / x_{j,sat} \tag{41}$$

For non-ideal solutions,

$$a_j = \gamma_j x_j / x_{j,sat} \tag{42}$$

in which solution non-idealities are described by the activity coefficient, γ_j, which will depend on x_j. Based on this definition of a_j, $\gamma_j = 1$ when $x_j / x_{j,sat} = 1$. Values of γ_j can be either larger or smaller than 1 and the magnitude relative to 1 is a measure of the extent of the non-ideal effect. If the solution is ideal at all solute concentrations, then $\gamma_j = 1$.

Often concentrations of a solute j in solution are reported in terms of weight fraction w_j rather than mole fraction. For a binary mixture of solute j in a vehicle v, the mole and weight fractions of j, designated as x_j and w_j, respectively, are related as follows:

$$x_j = \frac{w_j MW_v}{w_j MW_v + (1 - w_j) MW_j} \tag{43}$$

$$w_j = \frac{x_j MW_j}{x_j MW_j + (1 - x_j) MW_v} \tag{44}$$

where MW_j is the molecular weight of species j and MW_v is the average molecular weight of the vehicle. For a multicomponent vehicle, MW_v depends on the molecular weight of components in the vehicle (MW_{vj}) and either the mole fraction (x_{vj}) or weight fraction (x_{vj}) of components in the vehicle as given by Eq. (45)

$$M_v = \sum_{j=1}^{N_v} x_{vj} M_{vj} = 1 \Big/ \sum_{j=1}^{N_v} \left(w_{vj} / M_{vj} \right) \tag{45}$$

and

$$\sum_{j=1}^{N_v} x_{vj} = \sum_{j=1}^{N_v} w_{vj} = 1 \tag{46}$$

where N_v is the number of components in the vehicle.

Lacking other information for a chemical of interest in a given vehicle, it is often appropriate to obtain initial estimates by assuming the solution is ideal. Even then, flux is proportional to concentration, only if the concentration is reported as a mole fraction (see Eq. (42) for the case of $\gamma_j = 1$). Flux will not be proportional to concentration reported as a weight fraction or mass of chemical per volume, unless the concentration is small or $MW_j \approx MW_v$.

Generally, ideal solutions can be expected when the solute and vehicle components are chemically similar (e.g., decane dissolved in octane). Ideal behavior would not be expected for solutions, such as BE in water, which probably exhibits significant hydrogen bonding. Fortunately, experimental thermodynamic data are available for BE in water from which values of a_j can be calculated for both BE and water (Bunge, 2006; Koga, 1991). In Figure 12, the thermodynamic activity values for BE and water (a_{BE} and a_w, respectively) at 25°C are plotted as a function of the weight fraction of BE in water (w_{BE}). The estimated values of a_{BE} and a_w calculated assuming the BE-water solution is ideal (i.e., $\gamma_{BE} = 1$ and $MW_{BE} = 118$ and $MW_w = 18$) are also shown in Figure 12.

The results for a_{BE} are consistent with the flux measurements designated in Figure 11 as Regions I and II, but not Region III. The activity of water (a_w), which is also the relative

humidity, is nearly unity for w_{BE} as large as 0.8. For $w_{BE} > 0.9$ (Region III), a_w rapidly drops to zero. Thus, skin exposed to solutions with $w_{BE} > 0.95$ will become desiccated because there will be a significant driving force for water to transfer to the BE solution. This may be why BE permeation from neat BE is reduced relative to aqueous solutions. For w_{BE} < about 0.1, BE activity increases approximately proportionately to w_{BE}; for 0.1 < w_{BE} < 0.8, BE activity is nearly constant.

Figure 12. Thermodynamic activity of 2-butoxyethanol (BE) and water (W) in the binary mixture at 25°C (Bunge, 2006).

In Figure 13, the flux of BE presented in Figure 11 as a function of the weight fraction of BE are shown divided by the weight fraction (Figure 13a) and also by the thermodynamic activity of BE (Figure 13b). Clearly, the ratio of the flux to the weight fraction is not constant, whereas the ratio of flux to the thermodynamic activity of BE is except for the flux from neat BE. The ratio of the flux of BE to thermodynamic activity of BE, which is approximately 2 mg cm^{-2} h^{-1}, is the steady-state saturated flux that would be expected if the SC was not altered (most likely by desiccation) in the presence of neat BE (see Eq. (40)). For neat BE, the saturated flux decreases nearly 10-fold to 0.28 2 mg cm^{-2} h^{-1}, which is a reasonable number for desiccated SC.

Binary Mixtures of Cyclohexane with Toluene or 1-Octanol

We considered the skin uptake and permeation from saturated solutions selected model chemical in mixtures of two non-aqueous vehicles, specifically 1-octanol mixed with either toluene or cyclohexane, and toluene mixed with cyclohexane. To varying degrees, each of these pure solvents affected the skin uptake and permeation results (see Figure 10 and Table 10). To understand the results from the binary solvent mixtures compared with the pure solvents, it is essential to know how the thermodynamic activity of each of the solvents varies in the binary mixture. We have estimated the activity of each component of the binary solvent mixtures using the Aspen Engineering Suite process modeling software (Aspen Plus 2006, Aspentech, Cambridge, MA) at 25°C. The results for mixtures of cyclohexane with either 1-octanol or toluene are shown in Figure 14. The cyclohexane/toluene binary mixture was
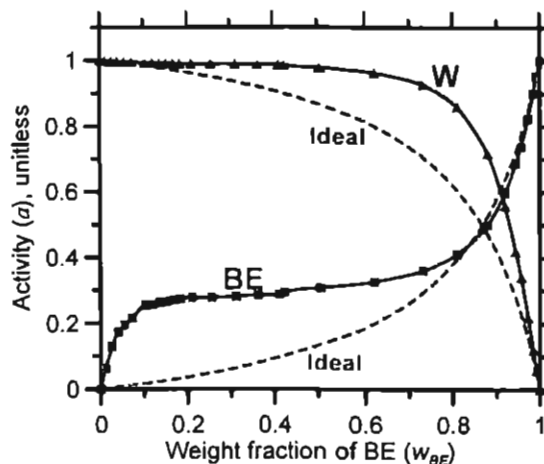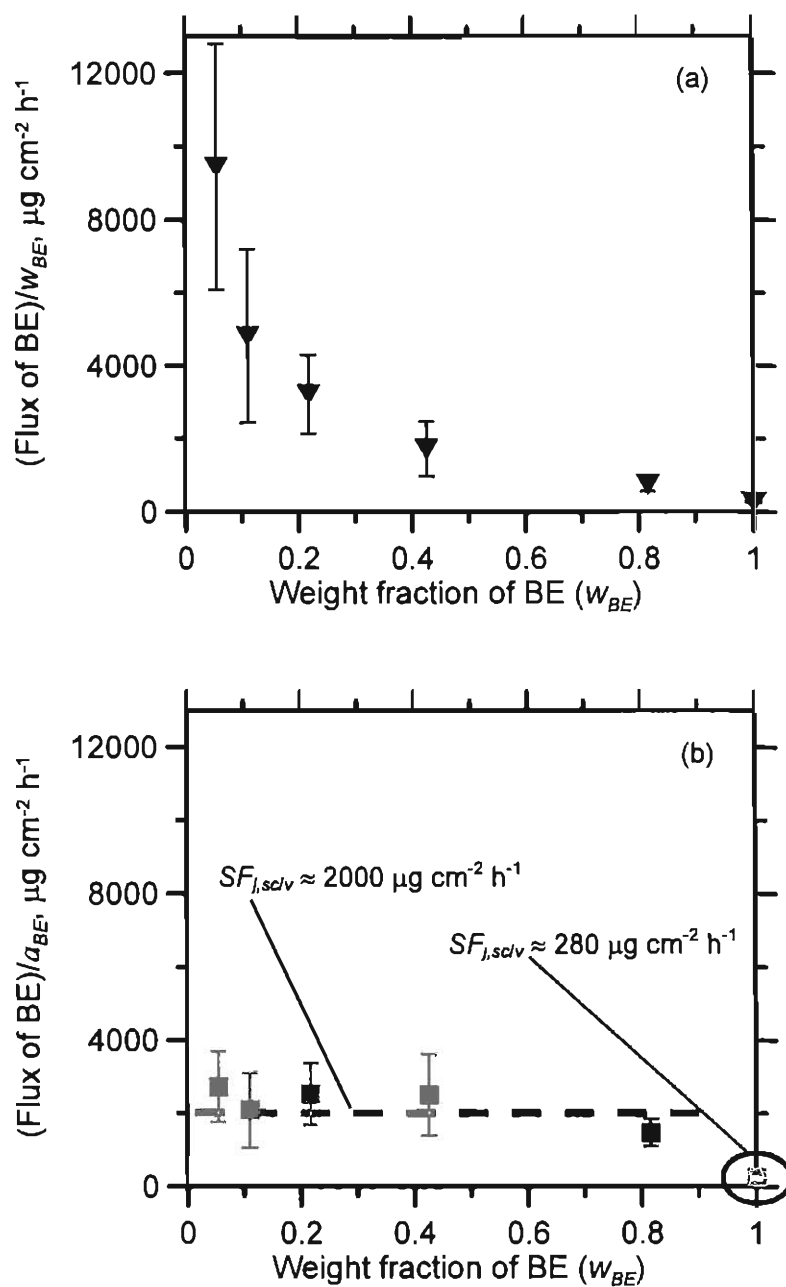
Figure 13. Flux of 2-butoxyethanol (BE) through guinea pig skin determined *in vivo* as a function of the weight fraction of BE in water (data from Johanson and Fernstrom, 1988) normalized with respect to: (a) the weight fraction of BE, and (b) the thermodynamic activity of BE (a_{BE}). The results show that, except for neat BE, the flux of BE is proportional to the thermodynamic activity of BE.
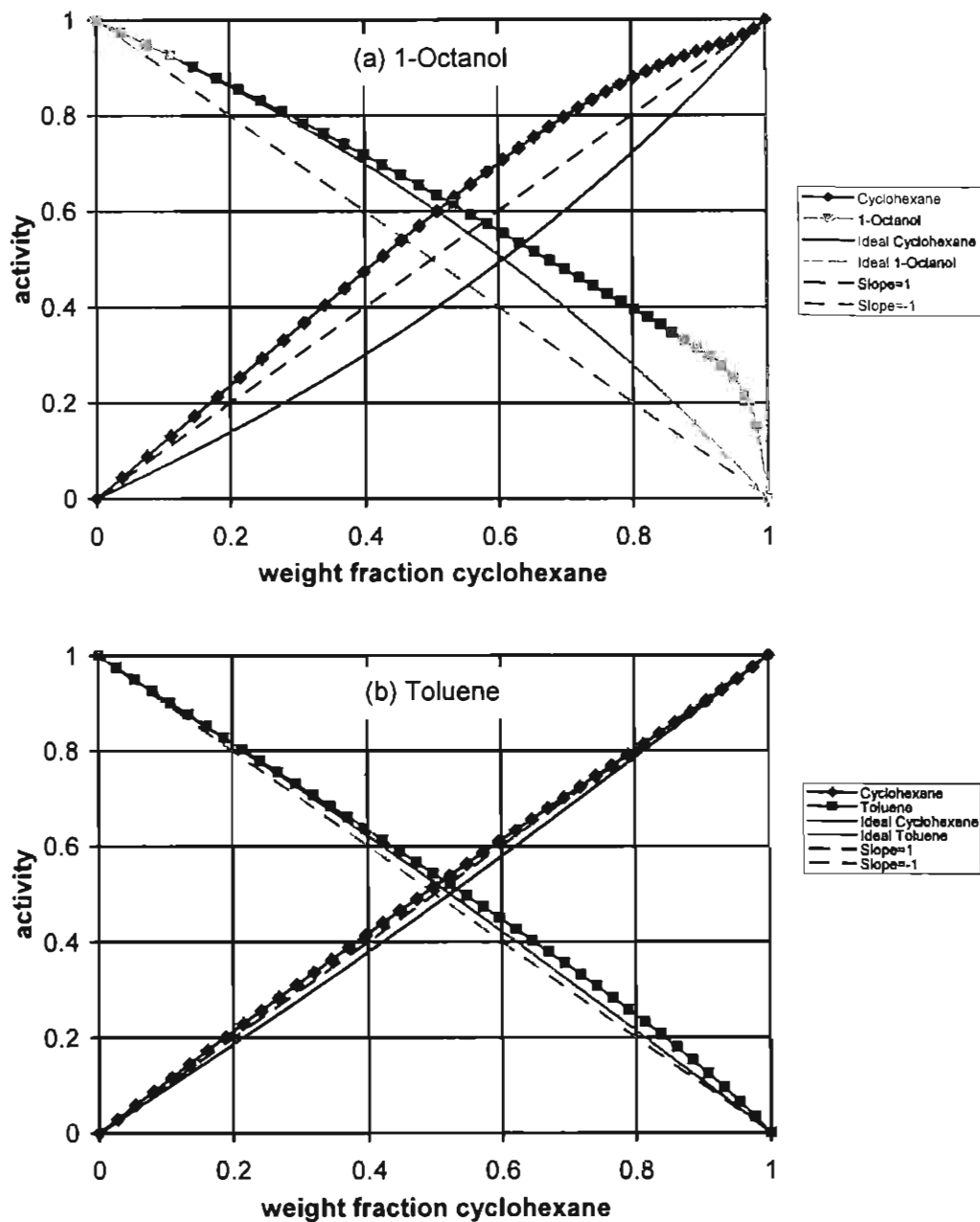
Figure 14. The calculated thermodynamic activity a binary mixture of cyclohexane with either 1-octanol (a) or toluene (b) plotted as a function of the weight fraction of cyclohexane. The calculated thermodynamic activity (represented by the symbols) is compared with the ideal solution estimate (solid curves without symbols) and the assumption that activity of a given component is proportional to its weight fraction (dashed lines).

calculated using UNIQUAC parameters (A_{12} = 360.53 and A_{21} = -237.053). The cyclohexane/1-octanol binary mixture was calculated by the UNIFAC method.

As shown in Figure 14, the binary solution of cyclohexane with toluene behaves nearly ideally. As expected, the mixture of cyclohexane with 1-octanol, which can hydrogen bond, is non-ideal, exhibiting positive deviations from the ideal solution. Based upon the thermodynamic activity for 1-octanol in a solution with cyclohexane, we expect that for cyclohexane concentrations greater than about 70 weight %, the amount of 1-octanol in skin will be larger than the 1-octanol fraction in solution.

The results shown in Figures 10 and 14 indicate that it might be possible to use the uptake and flux results of a solute j measured in pure solvents v and y to predict the uptake and flux of solute j from a mixture of solvents v and y. According to this scheme, the saturated flux of j through skin from a mixture of solvents v and y ($SF_{j,sc/vy}$) would be related to the saturated fluxes from the pure solvents v and y (i.e., $SF_{j,sc/v}$ and $SF_{j,sc/y}$, respectively) weighted by the thermodynamic activity of each solvent in the mixture of solvents v and y (i.e., $a_{v,vy}$ and $a_{y,vy}$).

$$SF_{j,sc/vy} = SF_{j,sc/v}\, a_{v,vy} + SF_{j,sc/y}\, a_{y,vy} \qquad (47)$$

A similar expression can be written for the saturated mass (uptake) of solute j from a mixture of solvents v and y ($m_{j,sc/vy}$):

$$m_{j,sc/vy} = m_{j,sc/v}\, a_{v,vy} + m_{j,sc/y}\, a_{y,vy} \qquad (48)$$

This can be written in terms of the mass ratio for the mixture of solvents v and y to pure solvent y ($Rm_{j,vy/y}$) and the mass ratio from pure solvents v and y ($Rm_{j,v/y}$) as follows:

$$Rm_{j,vy/y} = \frac{m_{j,sc/vy}}{m_{j,sc/y}} = Rm_{j,v/y}\, a_{v,vy} + a_{y,vy} \qquad (49)$$

It is important to note that this scheme is based upon the assumption that the saturated flux and saturated mass uptake of solute j depend on the amount of each solvent that absorbs into the SC, which in turn is predictable using the thermodynamic activities of each solvent v and y in the mixture of the solvents v and y. This will not always be the case.

Assessing the Potential for Harm from Skin Exposure to Chemicals

The results described above provide a framework for extending the new NIOSH skin notation strategy to a method for estimating dermal RELs. Like the new skin notation strategy, calculation of a dermal REL will require an estimate of the internal dose that produces no adverse effect. In the new skin notation strategy, the dermal dose is estimated from the REL for inhalation exposure. For chemicals that are insufficiently volatile to have a REL, alternative

sources of data for relating internal dose and toxicity (i.e., the dose response) should be considered. For example, lacking dermal toxicity data, EPA uses the RfD (i.e., the maximum acceptable oral dose of a toxic substance) or the no-observed-adverse-effect-level (i.e., the NOAEL) or the lowest-observed-adverse-effect-level (LOAEL) for ingestion exposures to assess whether the internal dose from dermal exposure to a given chemical in a given exposure scenario is likely (or unlikely) to be hazardous (US EPA, 1998a; 1998b, 2005). While necessary for estimating a dermal REL, methods for estimating the maximum acceptable internal dose was not addressed in this research.

To develop a dermal REL, three types of information are needed in addition to an estimate of the highest acceptable internal dose (HAID). The first is a safety margin, which the ratio of the highest-acceptable-internal dose to the dermal internal dose must exceed. The new NIOSH skin notation strategy (NIOSH, 2009) uses a safety margin of 10 (i.e., a skin notation is assigned when the ratio of the inhalation dose to the dermal dose is larger than 10). The second is the estimated mass absorbed from the solution containing the chemical (i.e., the vehicle v) if it were saturated with the chemical (i.e., $M_{in,j,v}\big|_{\text{for } C_{j,v}=S_{j,v}}$, which is $M_{in,j,v}$ calculated for $C_{j,v} = S_{j,v}$). The last piece of needed information is the saturation ratio of the chemical in the vehicle v (i.e., $C_{j,v}/S_{j,v}$). The dermal REL, which has units of concentration, could then be calculated as follows:

$$REL = S_{j,v} \frac{(HAID)/(SM)}{M_{in,j,v}\big|_{\text{for } C_{j,v}=S_{j,v}}} \qquad (50)$$

In this equation the HAID and $M_{in,j,v}\big|_{\text{for } C_{j,v}=S_{j,v}}$ are both reported in terms of mass of the chemical, and SM is the safety margin, which is a number larger than 1 and probably at least 10 or 100.

Eq. (50) has been written assuming the thermodynamic activity of solute j in vehicle v is adequately described by the saturation concentration ratio (i.e., $C_{j,v}/S_{j,v}$). If this is not the case, then the thermodynamic activity of solute j in vehicle v that corresponds to the dermal REL ($a_{j,v}|_{REL}$) is calculated using Eq. (51):

$$a_{j,v}\big|_{REL} = \frac{(HAID)/(SM)}{M_{in,j,v}\big|_{\text{for } C_{j,v}=S_{j,v}}} \qquad (51)$$

The dermal REL is then the smallest concentration of solute j in the vehicle v ($C_{j,v}|_{REL}$) that has a thermodynamic activity equal to $a_{j,v}|_{REL}$. The relationship between $C_{j,v}|_{REL}$ and $a_{j,v}|_{REL}$ would need to be calculated from experimental thermodynamic data, if available or from models for estimating phase equilibrium, many of which are available in chemical process design software

72

like the Aspen Engineering Suite from Aspentech, (Cambridge, MA). The BE-water system shown in Figure 12 is an example of using experimental thermodynamic data; the OCT-CYC and TOL-CYC binary mixtures shown in Figure 14 are examples of calculating thermodynamic activity using phase equilibrium models.

The new NIOSH skin notation strategy (NIOSH, 2009) is based on a rearrangement of Eq. (50), where HAID is calculated from the REL for inhalation, and the dermal dose is calculated assuming the skin is exposed to a saturated solution. Furthermore, it is assumed that the dermal dose from any saturated vehicle will be approximately the same as from saturated water (i.e., $M_{in,j,v}\big|_{for\ C_{j,v}=S_{j,v}}$ for a vehicle v is approximately the same as $M_{in,j,w}\big|_{for\ C_{j,v}=S_{j,w}}$ calculated for water, w). Written in the notation of Eq. (50), the new NIOSH skin notation strategy assigns a skin notation for systemic exposure to chemical j if:

$$\frac{\left(M_{in,j,w}\big|_{for\ C_{j,w}=S_{j,w}} \right)}{(HAID)} \geq \frac{1}{(SM)} \tag{52}$$

While a skin notation does indicate the potential for harm, it provides no information on the safety of a solution containing j at less than its saturation concentration. For example, although dermal exposure to phenol at high concentrations in water is certainly toxic, even deadly, exposures at low concentrations in water and other vehicles are safe (in fact, phenol is contained in many cosmetic product designed to be applied to skin). Thus, for chemicals with a skin notation, those charged with protecting human health and safety in the workplace are forced to make judgments about safe or dangerous concentrations, and the type of personal protection required. An important advantage of the dermal REL approach described in Eq. (50) is that it provides guidance on safe concentrations.

The results presented in previous sections of this report support methodologies for: (1) adjusting the saturated dermal dose for concentration of solute j in the vehicle (i.e., by the thermodynamic activity or $C_{j,v}/S_{j,v}$), and (2) estimating the dermal dose of species j from a vehicle v (including mixtures of solvents or solutes) that is saturated with species j (i.e., $M_{in,j,v}\big|_{for\ C_{j,v}=S_{j,v}}$) when the dermal dose is known for another vehicle or it can be estimated for another vehicle. Specifically, the dermal dose from a saturated solution of solute j in vehicle v can be calculated using Eqs. (17) or (18), where the saturated flux and saturated mass from a vehicle y (either known from measurement or by estimation with a QSAR equation) are adjusted by the mass and diffusion ratios ($Rm_{j,v/y}$ and $RD_{j,v/y}$, respectively) as given in Eqs. (23) and (24)

(which were written assuming vehicle y was water). The saturated flux and mass ratio for binary solvent mixtures can be calculated from the saturated mass and saturated flux results for the pure solvents as described by Eqs. (47) through (49). If vehicles v and y do not alter the skin, then $Rm_{j,v/y}$ and $RD_{j,v/y}$ should both be equal to one.

If the saturated flux from a vehicle v ($SF_{j,sclv}$) is known but the saturated mass ($m_{j,sclv}$) is not, then the absorbed dose can be approximated with the following simplification of Eq. (18):

$$M_{in,j,v} = A \, a_{j,v} \, SF_{j,sclv} \, t_{exp} = a_{j,v} \, M_{in,j,v}\big|_{C_{j,v}=S_{j,v}} \tag{53}$$

which has been written in terms of the thermodynamic activity. In appropriate situations, which have been described previously, the thermodynamic activity $a_{j,v}$ can be replaced by ($C_{j,v}/S_{j,v}$). Note that the $M_{in,j,v}\big|_{\text{for } C_{j,v}=S_{j,v}}$ is equal to the mass of solute j that absorbs from a vehicle v when the thermodynamic activity of solute j in v is equal to one (i.e., $M_{in,j,v}\big|_{\text{for } a_{j,v}=1}$).

Electrochemical Impedance Spectroscopy

Characterizing Electrochemical Impedance Spectroscopy (EIS) Data from Skin

Working with Professor Mark Orazem at the University of Florida who is an expert on electrochemical impedance, we have developed a procedure for analyzing EIS skin data to obtain parameters that meaningfully characterizing the resistive and capacitive components of a skin sample. The procedure uses methodology described in the electrochemistry literature for non-skin applications (Agarwal et al., 1995a; Agarwal et al., 1995b; Agarwal et al., 1996; Agarwal, 1992; Brug et al., 1984; Hsu and Mansfeld, 2001; Orazem, 2004; Orazem et al., 1996a; Orazem et al., 1996b), as well as recent developments in the calculation and physical interpretation of the effective capacitance calculated from the parameters of the R-CPE equivalent circuit model (Hirschorn et al., 2009; Huang et al., 2007; Orazem et al., 2006).

Impedance data can include experimental artifacts and other sources of measurement bias that are not obvious without performing an error analysis to assess quality and integrity of the measurements (Agarwal et al., 1995a). Minimizing the systematic experimental error and quantifying the stochastic error in the impedance measurement increases the amount and quality of information that can be obtained from the EIS measurements. Although methods for assessing error in impedance data are described in the literature, these have rarely been applied to measurements of skin.

We have utilized the *Measurement Model Toolbox* for impedance spectroscopy, developed by Mark Orazem (co-PI on this project), to model the stochastic error of the

measurements and to check measurements for Kramers-Kronig consistency (Orazem, 2001). The method summarized here is described in more detail elsewhere (Agarwal et al., 1995a; Agarwal et al., 1995b; Agarwal et al., 1996; Agarwal, 1992; Orazem, 2004; Orazem et al., 1996a; Orazem et al., 1996b).

The residual errors in the impedance scans relative to an equivalent circuit model will vary with frequency. This frequency-dependant residual error (ε_{res}) in the impedance data is defined as:

$$\varepsilon_{res}(f) = Z(f) - \hat{Z}(f) \tag{54}$$

where Z is the measured value of the impedance and $\hat{Z}$ is the model value of the impedance. The residual error (ε_{res}) in turn depends on the systematic error due to lack of fit of the model (ε_{fit}), the systematic experimental (i.e., bias) error (ε_{bias}), and the random stochastic error (ε_{stoch}) as described by Eq. (55) (Orazem, 2004):

$$\varepsilon_{res}(f) = \varepsilon_{fit}(f) + \varepsilon_{bias}(f) + \varepsilon_{stoch}(f) \tag{55}$$

Bias errors arise from instrumental artifacts or inconsistency with the Kramers-Kronig relations as described more below. The measurement model method of error analysis identifies the frequency range of a spectrum that is affected by the bias error, so that these data can be excluded from the data analysis.

The Kramers-Kronig relations are a set of integral equations from which the frequency dependent imaginary component of the impedance can be predicted from the real component and vice versa, as expressed by Eqs. (56) and (57), respectively.

$$Z_j(2\pi f) = -4f \int_0^\infty \frac{Z_r(x) - Z_r(2\pi f)}{x^2 - (2\pi f)^2} dx \tag{56}$$

$$Z_r(2\pi f) = Z_r(\infty) + \frac{2}{\pi} \int_0^\infty \frac{xZ_j(x) - 2\pi f\, Z_j(2\pi f)}{x^2 - (2\pi f)^2} dx \tag{57}$$

where $Z_r(\infty)$ is the real-component of the impedance at an infinitely large frequency. In impedance measurements on skin, $Z_r(\infty)$ corresponds to the resistance of the electrolyte between the electrodes and the skin.

In practice, using the integral form of the Kramers-Kronig relations listed in Eqs. (56) and (57) is problematic, because measurements cannot be performed at infinite frequency. Consequently, in this project, an alternative strategy is used in which data are fit to an equivalent circuit model that is Kramers-Kronig consistent.

Satisfaction of the Kramers-Kronig relations is a necessary but not sufficient requirement of a system that is causal, linear, stable and stationary. A system is causal if the response of the system is caused by a perturbation to the system. A system is stable if the response to a perturbation decays to its un-perturbed value with time. A system is linear if it varies linearly with a perturbation. In the case of EIS, a stationary system means a system that does not change with time. Electrochemical systems that are strictly stationary over the course of the entire experiment are rare. More typically, systems like skin are pseudo-stationary meaning they may change negligibly over the time required to collect impedance data for the frequency spectrum, although they might change significantly over the course of the experiment. To satisfy the Kramers-Kronig relations, changes in the skin barrier must be slow enough to satisfy the pseudo-stationary condition. Non-stationary impedance behavior of human skin may indicate time variations (e.g., in the hydration of the skin, diffusion of charge-carrying ions through the skin, or skin damage) that are rapid relative to the time required to collect the full spectrum of frequencies. Strictly speaking, Kramers-Kronig consistency is not sufficient to prove that the measured spectrum reflects only the properties of the system because some instrument artifacts may result in impedance features that are consistent with the Kramers-Kronig relations (Orazem, 2004).

To evaluate the data for bias errors, the magnitude of the stochastic errors must be known. Because skin impedance measurements are pseudo-stationary rather than strictly stationary, the magnitude of the stochastic error for skin impedance measurements cannot be determined by calculating the standard deviation of replicate measurements because the pseudo-stationary behavior of the skin introduces bias errors to the estimate of the stochastic error. An approach utilizing a *measurement model* enables determination of the magnitude of the stochastic error by using a Kramers-Kronig consistent circuit model as a filter for experimental bias, baseline drift and fitting errors in the impedance measurements. Following Agarwal et al. (Agarwal *et al.*, 1995a; Agarwal *et al.*, 1995b; Agarwal *et al.*, 1996; Agarwal, 1992) and Orazem et al.(Orazem *et al.*, 1996a), the measurement model chosen for this work consists of *n* Voigt elements, composed of a parallel resistor and capacitor, in series with a resistor, representing the solution (i.e., the electrolyte) resistance, as expressed by Eq. (58):

$$Z(f) = R_e + \sum_{k=1}^{n} \frac{R_k}{1 + 2\pi f R_k C_k j} \qquad (58)$$

where R_e is the electrolyte resistance, and R_k and C_k are the resistance and the capacitance of the kth Voigt element.

The stochastic error is determined by fitting the measurement model to several successive EIS scans using a modulus-weighted, complex non-linear least squares regression to Eq. (58). In this approach, each scan must have the same number of data points measured at the same frequencies. Also, each scan must be regressed to the same measurement model (i.e., the value of n in Eq. (58) must be the same in all scans). The value of n is selected to be the maximum number of Voigt elements that can be regressed to all of the scans such that the 95.4 % confidence interval for each fit parameter, R_k and C_k, does not include zero. The value of n is determined by iteratively adding Voigt elements to the measurement model until the fit is no longer improved by the addition of further Voigt elements as determined by the 95.4% confidence interval.

The residual error between the data and the measurement model will not represent the stochastic error because the error due to lack of fit (i.e., ε_{fit}) could be significant. However, the standard deviation of the residual error, as expressed by Eq. (59), is an estimate of the standard deviation of the stochastic error, which will vary with frequency as follows:

$$\sigma_{Z_r}^2(f) = \frac{1}{n-1} \sum_{k=1}^{n} \left(\varepsilon_{res,Z_r,k}(f) - \overline{\varepsilon}_{res,Z_r}(f) \right)^2 \tag{59}$$

where $\varepsilon_{res,Z_r,k}$ is the frequency dependent residual error, as defined by Eq. (54), of the real part of the impedance at frequency f of scan k, $\overline{\varepsilon}_{res,Z_r}(f)$ is the mean of the residual errors at frequency f for n scans. The residual errors of the imaginary parts can be treated in the same way to calculate the standard deviation of the stochastic error in the imaginary component (σ_{Z_i}). For Kramers-Kronig consistent data, the standard deviation of the real and imaginary parts of the stochastic error (σ_{Z_r} and σ_{Z_i}, respectively) are indistinguishable from each other (Durbha et al., 1997). An example comparison of the standard deviation of the real and imaginary components of the stochastic error of eight impedance scans of human split thickness skin is shown in Figure 15. These results were derived from experimental impedance measurements collected (as described in the Materials and Methods section) after the skin had equilibrated for twelve hours in phosphate buffered saline (PBS) solution and then regressed to the measurement model consisting of eight Voigt elements (i.e., n was 8 in Eq. (58)). Because the stochastic error is a characteristic of the impedance instrument, empirical estimates of the stochastic error collected from a series of scans will represent the stochastic error of other impedance scans measured by the same instrument over the same range of frequencies.
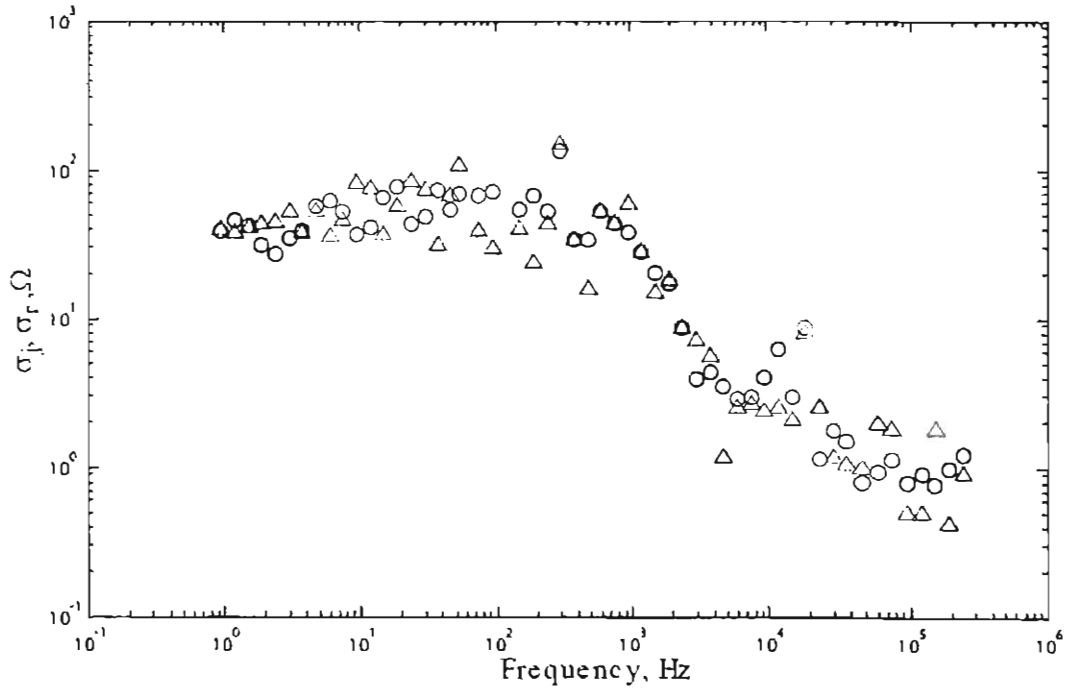
Figure 15. The standard deviation of the real (circles) and imaginary (triangles) residual errors for eight impedance scans of human split-thickness skin plotted as a function of frequency.

Rather than assess Kramers-Kronig consistency by comparing the variance in the real and imaginary components of the stochastic errors (as shown in Figure 15), a more sensitive approach is to fit the measurement model (i.e., Eq. (58)), with the maximum number of statistically significant Voigt elements, to the imaginary component of the impedance data. The resulting regression parameters (i.e., R_k and C_k for each of the Voigt elements and R_e for the solution) are then used to predict the real component of the impedance from which the relative residual errors for the real part of the impedance data can be calculated. The process is then reversed and the measurement model is fit to the real component of the impedance data, from which the imaginary component of the impedance is predicted. Generally, the fit to the imaginary data provides a more sensitive test of the higher frequency data, while the fit to the real component is more sensitive for data collected at lower frequencies.

Examples of the relative residual errors for the real component of the impedance data that are predicted by regression of the measurement model to the imaginary part of the impedance spectrum and vice versa are shown in Figures 16 and 17 for two impedance

spectra. The predicted impedance plane plots are also shown (Figures 16a,b and 17a,b). The dashed curves in the plots of the normalized residuals (defined as the difference in the measurement and model divided by the measurement) represent the 95.4% confidence interval for the model obtained by Monte Carlo simulation using the calculated confidence intervals for the estimated parameters of the measurement model fit to the data (i.e., R_k and C_k for each of the Voigt elements and R_e for the solution). Data that fall outside of the 95.4% confidence interval for the model prediction are considered to be inconsistent with the Kramers-Kronig relations. The impedance spectrum shown in Figure 16 is Kramers-Kronig consistent except for one point at a frequency of 1000 Hz (see Figures 16e and 17f). This point would not be included in further analyses of this spectrum. In contrast, the spectrum shown in Figure 17, which was collected from skin that had become partially exposed to air because the electrolyte solution leaked from the donor chamber, is not Kramers-Kronig consistent. Similar Kramers-Kronig inconsistent data have been observed during hydration of partially dehydrated skin.

Significantly, the impedance plane plot predicted by the fit of the measurement model to the imaginary component of impedance (Figure 17a) appears to be satisfactory. The inconsistency with Kramers-Kronig relations is only evident from the predicted real component (Figure 17e) and the imaginary component and impedance plane plots (Figures 17b and 17d, respectively) predicted from fitting the real component of the impedance data. Based on this analysis, the spectrum shown in Figure 17 was rejected. In some cases (e.g., the data shown in Figure 16), the spectrum satisfies the Kramers-Kronig relations except for one or a few data points. In these cases, the inconsistent data are discarded and the remaining data are regressed to the measurement model. This process is repeated until all data included in the data analysis are demonstrated as being Kramers-Kronig consistent.

For each impedance scan on skin, the four parameters characterizing the R-CPE equivalent model circuit model shown in Figure 8 (i.e., R_e, R_m, Q and α) are determined using all data points shown to be Kramers-Kronig consistent (using the method illustrated in Figures 16 and 17). From these, an effective skin capacitance (C_{eff}) is derived as described in detail elsewhere (Brug et al., 1984; Huang et al., 2007; Orazem et al., 2006).

Briefly, data that are Kramers-Kronig consistent are analyzed using the following procedure. The real and imaginary impedance data from each frequency scan (a spectrum) are fit using non-linear modulus-weighted, complex non-linear least squares regression to the measurement model consisting of n Voigt elements (i.e., a resistor and capacitor in parallel) in series with a resistor (resenting the electrolyte solution) as expressed by Eq.(58). The value of n is the maximum number of Voigt elements that can be fit to all Kramers-Kronig consistent data
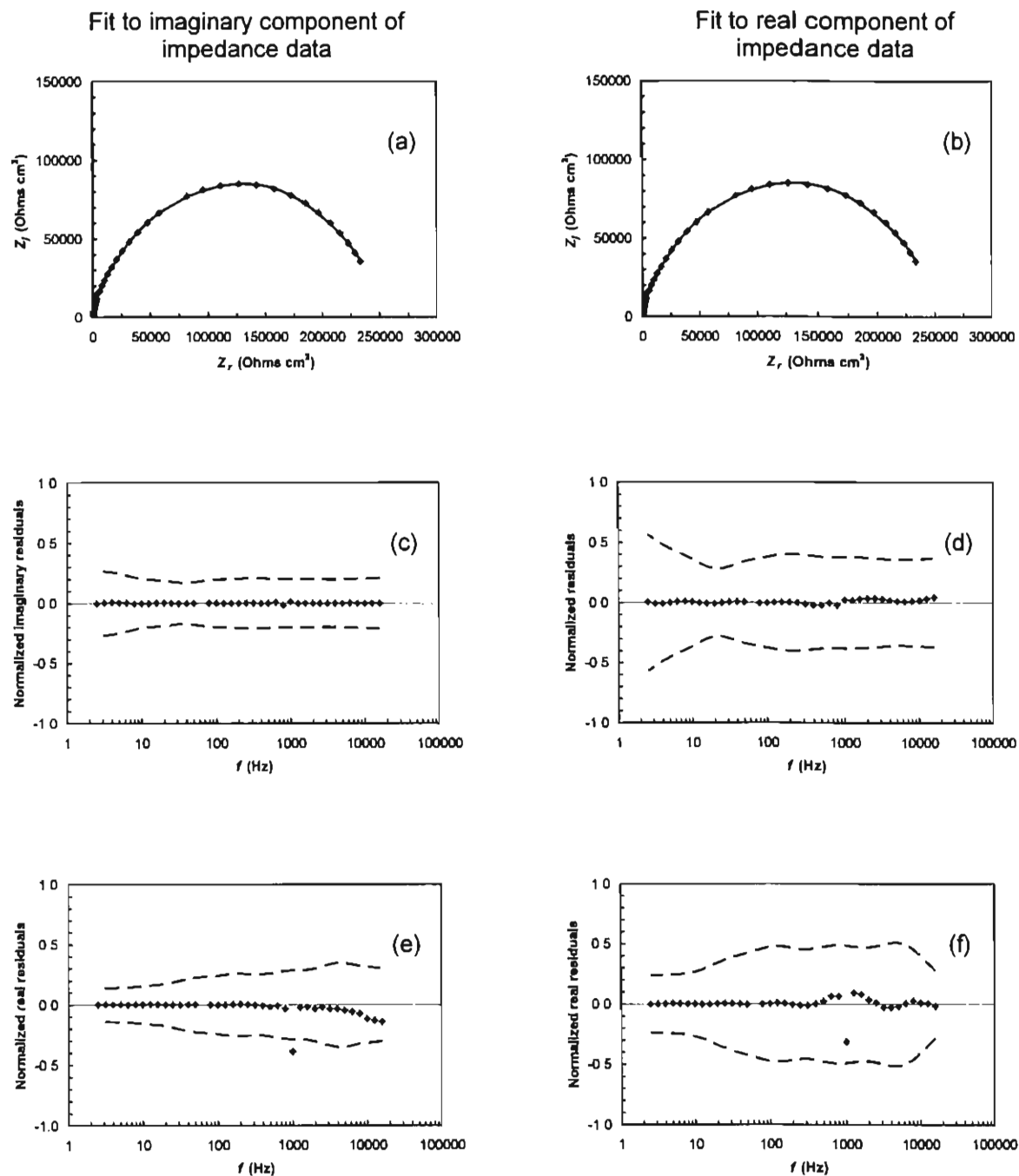
Figure 16. Fit of measurement model to the imaginary component (left hand column) or real component (right hand column) of the impedance data: (a,b) impedance plane plot of data (symbols) compared with model (curve); (c,d) normalized residuals of imaginary component of impedance; (e,f) normalized residuals of real component of impedance. Normalized residuals are the difference between measurement and model divided by the measurement at each frequency. The dashed curves represent the 95.4% confidence interval for the model obtained by Monte Carlo simulation. The data set shown here is Kramers-Kronig consistent except for one point at 1000 Hz.
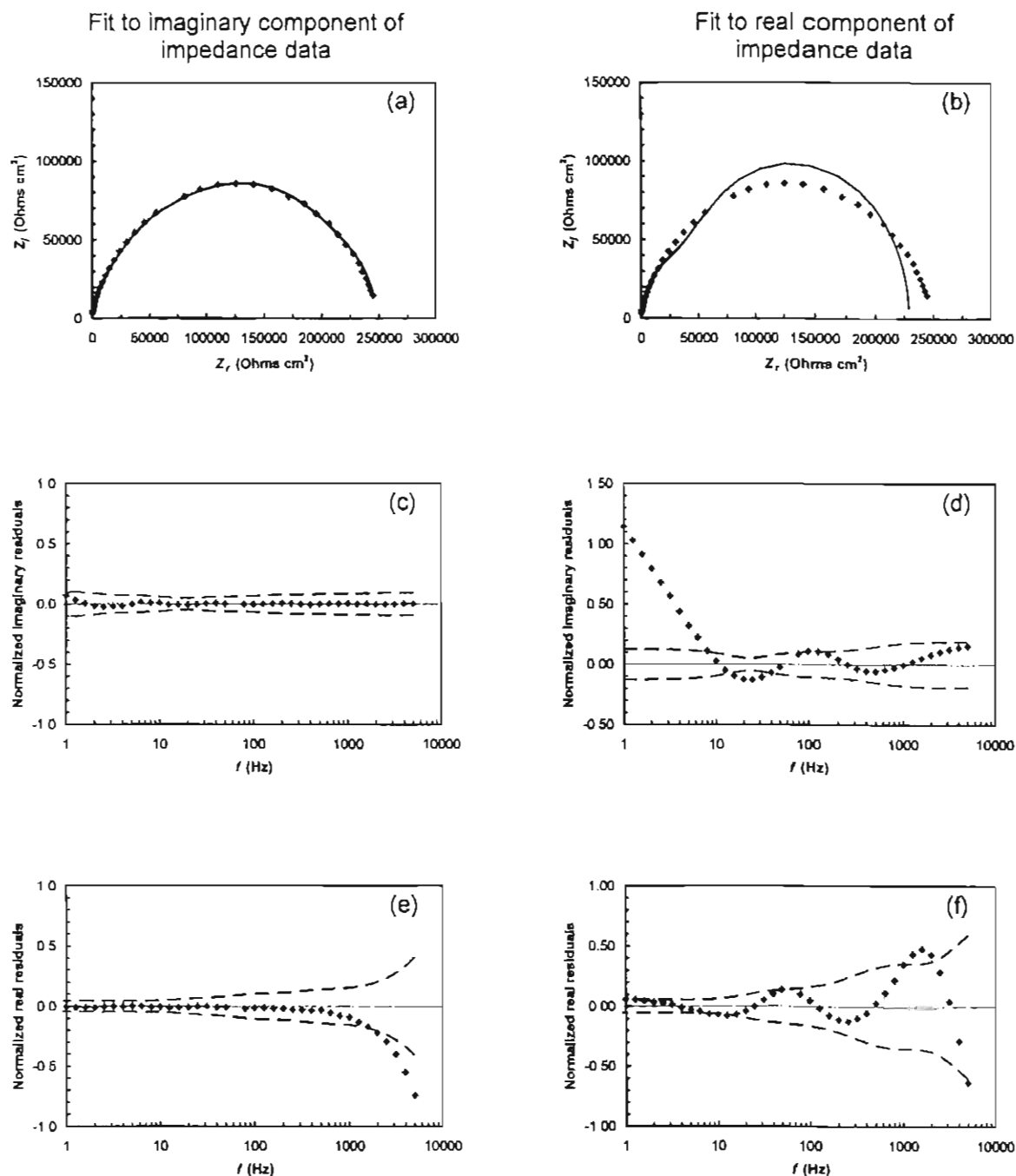
Figure 17. Fit of measurement model to the imaginary component (left hand column) or real component (right hand column) of the impedance data: (a,b) impedance plane plot of data (symbols) compared with model (curve); (c,d) normalized residuals of imaginary component of impedance; (e,f) normalized residuals of real component of impedance. Normalized residuals are the difference between measurement and model divided by the measurement at each frequency. The dashed curves represent the 95.4% confidence interval for the model obtained by Monte Carlo simulation. The data set shown here is not Kramers-Kronig consistent.

from the scan such that the 95.4 % confidence interval for each fit parameter, R_k and C_k, does not include zero. The resulting regression parameters (i.e., R_k and C_k for each of the Voigt elements and R_e for the solution) are then used to estimate the real component of the impedance at the high and low frequency limits. At high frequency, the real component of the impedance approaches a constant that is equal to the solution resistance (R_e); at low frequency, the real component of the impedance approaches a constant equal to the total resistance (R_t). The skin resistance (R_m) is calculated from the difference between R_t and R_e.

The CPE parameter α is then determined from the negative slope of the linear regression of the impedance data to the high frequency, linear portion of $\log(|Z_j|)$ versus $\log(f)$. This value of α is used along with the imaginary component of the impedance to calculate the frequency dependent parameter, Q_{eff}, defined as follows (Brug et al., 1984):

$$Q_{eff}(f) = -\sin\left(\frac{\alpha\pi}{2}\right)\frac{1}{Z_j(2\pi f)^\alpha} \tag{60}$$

At high frequency, Q_{eff} becomes constant and the CPE parameter Q is equal to the high frequency limit of Q_{eff}. Knowing the R-CPE parameters for skin (i.e., R_m, Q and α), an effective skin capacitance, C_{eff}, can then be calculated from Eq. (61):

$$C_{eff} = R_m^{(1-\alpha)/\alpha} Q^{1/\alpha} \tag{61}$$

as described by Hsu and Mansfeld (2001). It follows that the distribution of time constants characterizing ionic conduction through skin can be represented by a single effective characteristic time constant that is equal to the product of R_m and C_{eff}.

Previously Published Impedance and Resistance Results

New skin impedance data have been generated in this study. In addition to this, we have reviewed the skin literature involving measurements of electrical resistance or impedance. Many investigators are using direct current and alternating current measurements to characterize the skin and evaluate skin integrity, including an *in vitro* test for skin corrosivity (OECD, 2004). To compare results collected on various experiments with different areas of skin, the resistance (or impedance) measurement must be normalized with respect to the area. The correct way to do this is multiply the skin resistance or impedance result by the active skin area (i.e., results should be reported as ohms·cm²). However, there are several published papers in which the resistance or impedance results have been divided by the area (i.e., results are reported as ohms/cm²).

The reason ohms/cm^2 is incorrect can be understood by considering chemical permeation through the skin, which is normalize by area (i.e., reported as mass of chemical per area) because the amount of chemical that permeates increases proportional to the permeation area. Electrical conductance, which is reported in units of siemens (S), is analogous to chemical permeation and also increases proportional to increased area. Thus, area normalized conductance should be reported in units of S/cm^2. Electrical resistance is the inverse of conductance and 1 ohm is equivalent to 1/S. Increasing the area through which electrical current transfers causes a proportional decrease in the resistance in the same way that it becomes easier to push water at a fixed flow rate through a pipe with a larger diameter. (That is, the resistance to flud flow in the pipe decreases as the cross-sectional area of the pipe increases.) It follows that area-normalized resistance should be reported as 1/(S/cm^2), which is equal to ohms·cm^2.

Our review of the skin literature reveals that this erroneous reporting of resistance and impedance data is quite common. For example, Davies et al. (2004) recommends using 3.94 kohm/cm^2 as the criterion of acceptable skin integrity for *in vitro* percutaneous absorption studies. Because the exposed skin area in this study was 2.54 cm^2, the correct number should have been 25.4 kohms·cm^2 (which is 3.94 kohm/cm^2 multiplied by 2.54 cm^2 twice). The acceptance criterion of 3.94 kohm/cm^2 from Davies et al. has been used in other studies (e.g., see Larese et al., 2007, 2009). As long as the active skin area is at least as large as in the Davies et al. study, this will lead to rejection of skin samples that should have been judged as acceptable. However, if applied to skin samples with a smaller area (e.g., 0.64 cm^2 is common in many diffusion cells), then skin samples that should be rejected might be used (e.g., using 3.94 kohm/cm^2 for skin in cells with an area of 0.64 cm^2 gives an acceptance criterion of 1.6 kohms·cm^2). This could lead to unrealistically high permeability determinations due to measurement on skin with an inferior barrier.

An additional source of confusion in the skin literature is the reporting of impedance measured at only one frequency. Most commonly, this is 100 or 1000 Hz, although frequencies as large as 120 kHz have been reported (Novotny *et al.*, 2009). As described above in the Background section, impedance varies with measurement frequency. Figure 18 shows a typical impedance spectrum measured in this study (including the real and imaginary components as well as the modulus). At low frequency, the magnitude of the impedance (i.e., the modulus) is equal to the DC-resistance of the skin and electrolyte solution combined; at high frequency the impedance is equal to the DC resistance of the electrolyte solution alone (approximately 220 ohms·cm^2 for the PBS solution in our experiments). For the spectrum shown in Figure 18, the
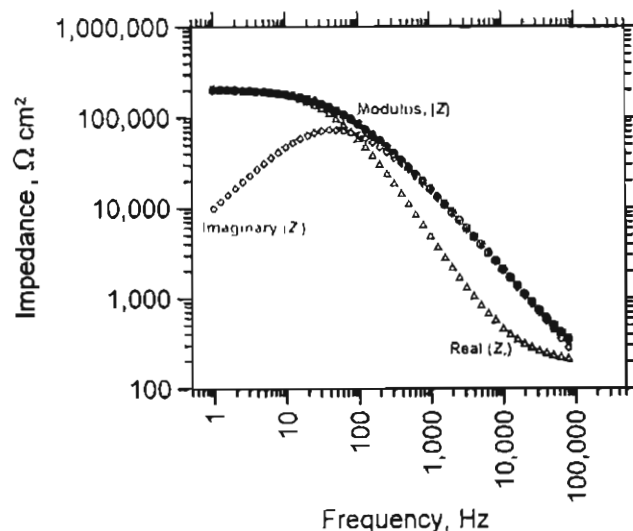
Figure18. A typical example showing the magnitude (i.e., the modulus), and the real and imaginary components of the impedance reported in terms of ohms·cm^2 (Ω·cm^2) plotted as a function of frequency (results are from this work).

impedance modulus determined at 1000 Hz is 5.3-fold smaller than at 100 Hz (i.e., 16 komhs·cm^2 compared with 85 komhs·cm^2). Typically, impedance measurements at frequencies as large as 100 kHz are approximately the same as the resistance of the electrolyte solution alone and therefore, insensitive to the condition of the skin sample. Often, in the skin literature the sensitivity of the skin impedance measurements to frequency has not been considered in comparison of results between studies conducted at different frequencies. Based upon the large body of impedance results collected in this study and the review of the skin literature, we are developing recommendations for the appropriate use of impedance for assessing skin barrier properties for various purposes. This will be included in a paper reviewing the interpretation and use of impedance and resistance data in the study of skin barrier function that is in preparation.

Electrochemical Impedance Spectroscopic (EIS) Data from Skin

Dozens of EIS experiments, most conducted in combination with a skin permeation experiment, have been completed as part of this project. The method for analyzing and interpreting the EIS data has evolved during the project, and the procedure described in this report was only recently finalized. Thus, we are now in the process of reviewing and

reanalyzing all of the EIS data produced during the course of this project to insure that the results from all data sets are reported consistently. In light of this, we will present here some example data, and describe qualitatively the cases we have studied and the main results as we know them at this time.

The initial hypothesis of this project was that the permeability of nonpolar solutes through skin is correlated with the capacitive character of the skin much like skin permeation of polar components are correlated with electrical resistance (e.g., see Figure 3). The test for this is to compare the measured permeability with the effective capacitance (C_{eff}) calculated from the CPE parameters (α and Q) combined with the skin resistance (R_m) as defined by Eq. (61). The permeability of CP was studied extensively in EIS-diffusion cell experiments. Those results have been analyzed to determine α, Q, and R_m, but C_{eff} has not yet been evaluated. In our earlier analysis comparing permeability to α, Q, and R_m, no correlation was found. Since C_{eff} is related to α, Q and R_m in a non-linear fashion, it is possible that a correlation between permeability and C_{eff} will be discovered. However, we do not expect this will be the case.

While the absence of a correlation between permeability and C_{eff} would preclude the ability to reduce skin-to-skin variability by normalizing experimental permeability results to C_{eff}, EIS is still a valuable tool for assessing changes in barrier properties arising from assorted chemical or mechanical insults. Certainly, impedance measurements (usually made at a single frequency) have been used to predict the potential effectiveness of an enhancer chemical (e.g., see Karande et al, 2006; Rachakonda et al, 2008; and Novotny et al, 2009) or chemical corrosion (e.g., see Whittle and Basketter, 1994 and OECD, 2004). Therefore, we have studied in combination with permeation, the effect of various chemical and mechanical insults (e.g., pinholes). Our novel cell design, which holds the skin inside a picture frame, makes it possible to disassemble the EIS-diffusion cells to perform treatments and then reassemble the cell for further EIS and/or permeation measurements.

Figures 19 and 20 show the EIS results for one piece of heat separated human epidermis before and after treatment for 1 hour with 100% DMSO. Specifically, Figure 19 presents the impedance plane results and Figure 20 shows impedance as a function of frequency before and after treatment for 1 hour with 100% DMSO. It is apparent from these results that treatment with DMSO dramatically altered the impedance measurements.

The effect of DMSO compared with control (i.e., the same PBS solution used to initially equilibrate the skin and as the vehicle for the CN permeation measurements) for either 15 or 60-minute treatment times is shown in Table 12. As expected, treatment with PBS had no effect. After 1 hour exposure to DMSO, the skin resistance decreased by a factor of nearly 140.

Furthermore, although the skin resistance before DMSO treatment for 1 hour was highly variable (from 117 k to 177 kΩ cm^2), after treatment the skin resistance was nearly the same for all three samples (the coefficient of variation was only about 3%). As expected, a 15-minute DMSO treatment produced a smaller effect on the skin resistance, which decreased by a factor of only 4. DMSO treatment had a much smaller, although statistically significant effect on C_{eff}, which increased by factors of 4 and 2.4 for treatments 15 minutes and 1 hour, respectively. An increase in C_{eff} is consistent with either an increase in the dielectric constant (as might occur if the lipids become more disorganized) or a reduction in the effective distance across the capacitive elements in the SC. Significantly, the increase in CN flux following DMSO treatment was small (although statistically significantly different from the control) and not statistically different for the 15 minutes and 1-hour treatments. Apparently, the electrical characteristics of the skin barrier, especially resistance, were considerably more sensitive to DMSO treatment than was skin permeation of CN.

As discussed above, impedance measurements made at a single (most often 100 Hz or 1000 Hz) frequency have been used to assess skin integrity. In light of this, the impedance results collected at 100 Hz and 1000 Hz have been highlighted in Figure 20. Before treatment with DMSO, the impedance at 100 Hz is 5.3-fold larger than at 1000 Hz. After treatment, the impedance is the same at 100 and 1000 Hz. The results in Figure 20 are also compared with skin integrity test criteria recommended by Davies et al (2004) and Fasano et al (2002).

Measuring DC resistance, Davies et al (2004) recommended that the electrical resistance "should be equal to or above 3.94 kΩ/cm^2". This was 10 kΩ for their skin area of 2.54 cm^2, which is 25.4 kΩ-cm^2 when written using the correct units. Fasano et al (2002) measured impedance at 1000 Hz and reported that 17.1 kΩ measured across an area of 0.64 cm^2 (i.e., 10.9 kΩ-cm^2) corresponded to tritiated water permeability coefficient of 1.5 x 10^{-3} cm/h. The DC equivalent resistance of the skin impedance data shown in Figure 20 is approximately 200 kΩ cm^2, which is considerably larger than the skin acceptance criteria of 25.4 kΩ-cm^2 recommended by Davies et al (2004). It is interesting that the impedance determined at 1000 Hz which is the same frequency as in the study by Fasano et al (2002), was 16.1 kΩ-cm^2, which was only 1.5-fold larger than the recommended acceptance criteria of 10.9 kΩ-cm^2. Further quantitative assessment of the effect of frequency on measurements to assess skin integrity is needed. We will examine this question as we evaluate the large body of EIS data generated in this project.
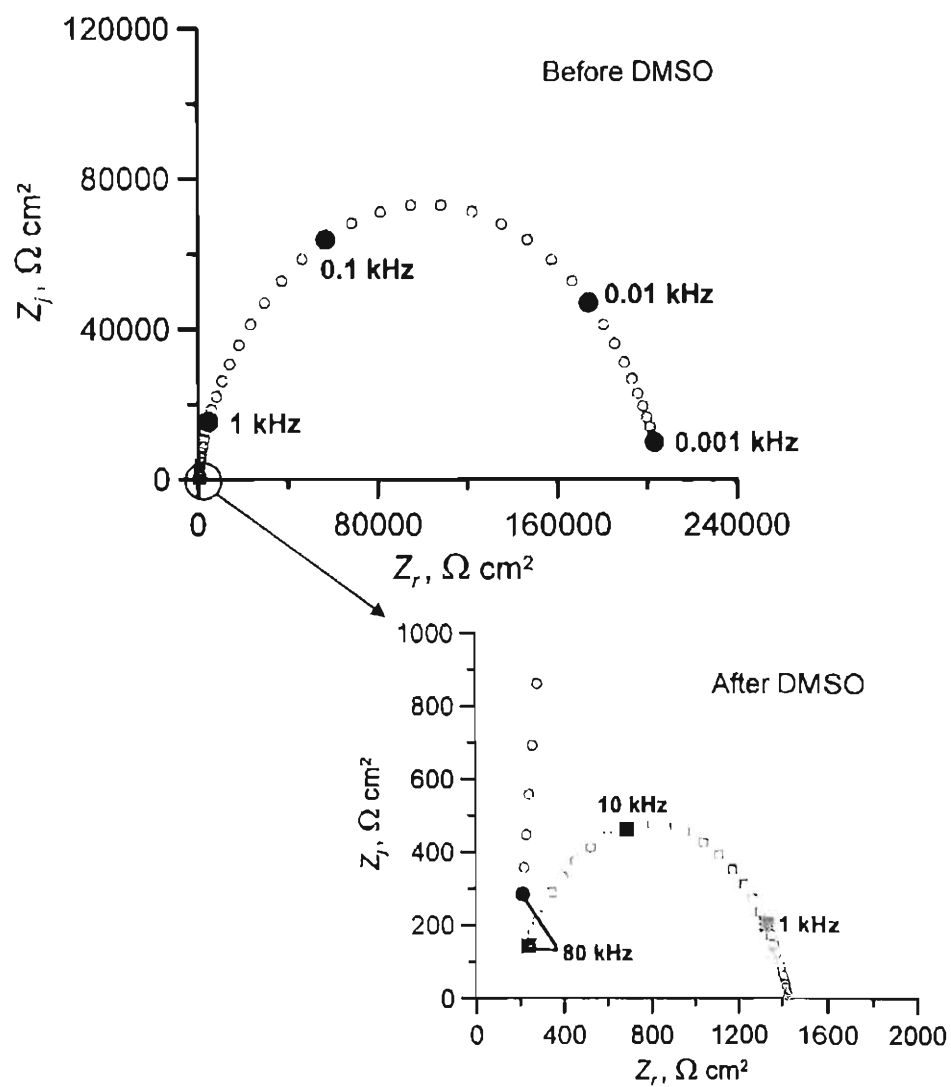
Figure 19. Impedance-plane plot of skin impedance data collected before (circles) and after (squares) treatment with 100% DMSO for 60 minutes. Filled symbols designate measurements collected at the indicated frequencies.
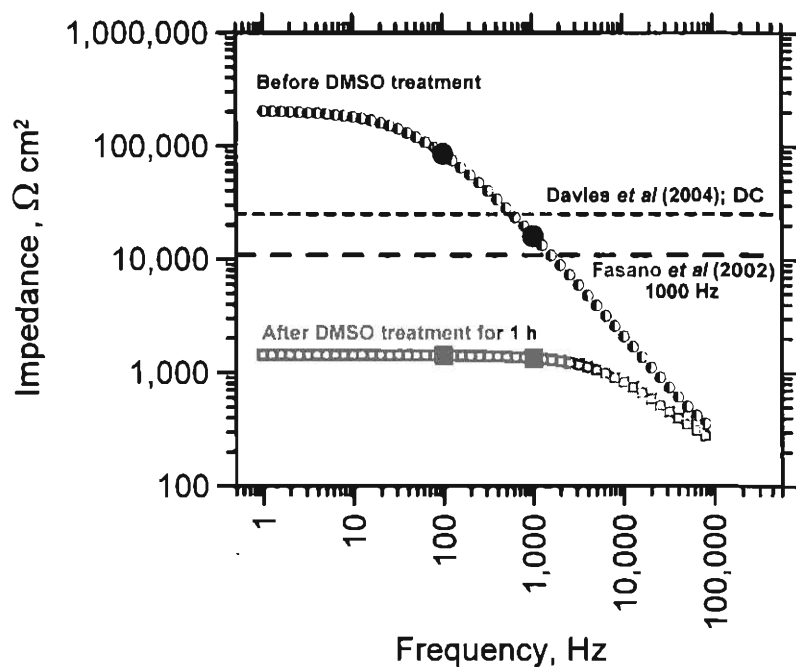
Figure 20. Impedance measurements on split-thickness human skin before and after DMSO treatment for 1 hour compared with the integrity test criteria proposed by Davies et al (2004) and Fasano et al (2002) reported here correctly normalized for area. Measurements at 100 Hz and 1000 Hz have been highlighted. Before treatment, the impedance at 100 Hz is 5.3-fold larger than at 1000 Hz. After treatment, the impedance is the same at 100 and 1000 Hz. Davies et al (2004) measured DC resistance. They recommended that the electrical resistance "should be equal to or above 3.94 $k\Omega/cm^2$". This was 10 $k\Omega$ for their skin area of 2.54 cm^2, which is 25.4 $k\Omega$-cm^2. Fasano et al (2002) measured impedance at 1000 Hz. They reported that 17.1 $k\Omega$ measured across an area of 0.64 cm^2 (i.e., 10.9 $k\Omega$-cm^2) corresponded to tritiated water permeability coefficient of 1.5 x 10^{-3} cm/h .

Table 12. Effect of DMSO treatment compared with control on the steady-state flux of 4-chloronitrobenzene (CN) from a saturated aqueous solution and on the skin resistance (R_m) and effective capacitance (C_{eff}) determined using EIS [a,b]

Treatment→ Parameter	Before[c]	DMSO for 15 min		PBS (control) for 15 min		DMSO for 60 min		PBS (control) for 15 min	
		After	Ratio	After	After	After	Ratio	After	Ratio
$SF_{j,sdv}$ ($\mu g\ cm^{-2} \cdot h^{-1}$)	4.97±21%	5.20±10%	1.18±13%	6.16±32%	1.05±22%	5.98±31%	1.24±8%	5.16±21%	1.04±15%
R_m ($k\Omega \cdot cm^2$)	161±64%	63.8±67%	4.07±45%	64.8±114%	0.95±18%	1.14±2.9%	138±23%	148.6±96%	1.05±17%
C_{eff} ($\mu F\ cm^{-2}$)	0.014±12%	0.115±46%	4.09±45%	0.0146±3.1%	1.08±0.33%	0.0339±5.4%	2.44±15%	0.0138±4%	1.10±3.5%

[a] Results are reported as mean ± one standard deviation (as % of mean) for 3 replicates on skin from the same subject for after treatment and the treatment ratio. All treatments were performed on skin from the same subject (identified as subject AS). Before treatment results are reported all four treatments combined (n = 12; 3 replicates for each of 4 treatments). Ratios were calculated as after treatment divided by before treatment for the steady-state saturated flux ($SF_{j,sdv}$) and effective capacitance (C_{eff}), and as before treatment divided by after treatment for the skin resistance (R_m). All measurements were at 32°C.

[b] EIS results were determined from PBS containing no CN at 10 mV root-mean-squared amplitude for frequencies from 1 Hz to 100 kHz

[c] Skin resistance (R_m) before treatment was larger than 25 $k\Omega \cdot cm^2$ for all but one sample, which was 15.8 $k\Omega \cdot cm^2$. The saturated flux of CN through this low resistance sample was 5.29 $\mu g\ cm^{-2}\ h^{-1}$, which is not statistically different from the mean of all 12 skin samples. The range of R_m values for the other samples before treatment was 27.0 to 358 $k\Omega \cdot cm^2$. Before treatment the range of effective capacitance values (C_{eff}) was 0.0119 to 0.0173 $\mu F/cm^2$ and the range of steady-state saturated flux of CN was 3.41 to 6.95 $\mu g\ cm^{-2}\ h^{-1}$.

References Cited

ACGIH (2009). *2009 TLVs (Threshold Limit Values) and BEIs (Biological Exposure Indices)*, Seventh/Ed., ACGIH, Cincinnati, OH, http://www.acgih.org/TLV/ (accessed 07/28/2009).

Agarwal, P., Crisalle, O., Orazem, M.E. and Garcia-Rubio, L. (1995a). Application of measurement models to impedance spectroscopy, II. Determination of the stochastic contribution to the error structure. *J Electrochem Soc*, 142:4149-4158.

Agarwal, P., Orazem, M.E. and Garcia-Rubio, L. (1995b). Application of measurement models to impedance spectroscopy, III. Evaluation of consistency with Kramers-kronig relations. *J Electrochem Soc*, 142:4159-4168.

Agarwal, P., Orazem, M.E. and Garcia-Rubio, L.H. (1996). The influence of error structure on interpretation of impedance spectra. *Electrochemica Acta*, 41:1017-1022.

Agarwal, P., Orazem, M. E. & Garcia-Rubio, L. H. (1992). Measurement models for electrochemical impedance spectroscopy I. Demonstration of applicability. *Journal of Electrochemical Society*, 139:1917-1926.

Barry, B.W. (1999). Reflections on transdermal drug delivery. *Pharmaceutical Science & Technology Today*, 2:41-43.

Barry, B.W. and Bennett, S.L. (1987). Effect of penetration enhancers on the permeation of mannitol, hydrocortisone and progesterone through human skin. *J Pharm Pharmacol*, 39:535-546.

Barry, B.W., Harrison, S.M. and Dugard, P.H. (1985a). Correlation of thermodynamic activity and vapour diffusion through human skin for the model compound, benzyl alcohol. *J Pharm Pharmacol*, 37:84-90.

Barry, B.W., Harrison, S.M. and Dugard, P.H. (1985b). Vapour and liquid diffusion of model penetrants through human skin; corrleation with thermodynamic activity. *J Pharm Pharmacol*, 37:226-235.

Bogen, K.T., Keating, G.A., Meissner, S. and Vogel, J.S. (1998). Initial uptake kinetics in human skin exposed to dilute aqueous trichloroethylene *in vitro*. *J Expos Anal Environ Epidemiol*, 8:253-271.

Bond, J.R. and Barry, B.W. (1988). Hairless mouse skin is limited as a model for assessing the effects of penetration enhancers in human skin. *J Invest Dermatol*, 90:810-813.

Booth, E.D., Loose, R.W. and Watson, W.P. (1999). Effects of solvent on DNA adduct formation in skin and lung of CD1 mice exposed cutaneously to benzo(a)pyrene. *Arch Toxicol*, 73:316-322.

Bronaugh, R.L. and Franz, T.J. (1986). Vehicle effects on percutaneous absorption: in vivo and in vitro comparisons with human skin. *Br J Dermatol*, 115:1-11.

Bronaugh, R.L. and Maibach, H.I. (1985). Percutaneous absorption of nitroaromatic compounds: in vivo and in vitro studies in the human and monkey. *J Invest Dermatol*, 84:180-183.

Bronaugh, R.L., Stewart, R.F. and Simon, M. (1986). Methods for in vitro percutaneous absorption studies. VII. Use of excised human skin. *J Pharm Sci*, 75:1094-1097.

Brug, G.J., van den Eeden, A.L.G., Sluyters-Rehbach, M. and Sluyters, J.H. (1984). The analysis of electrode impedances complicated by the presence of a constant phase element. *Journal of Electroanalytical Chemistry*, 176:275.

Bunge, A.L. (2006). Why skin permeation data from neat and aqueous solutions of 2-butoxyethanol are not surprising. (K.R. Brain and K.A. Walters, eds.), Vol. 10a, STS Publishing, Perspectives in Percutaneous Penetration (PPP), La Grande Motte, France April 19-22, 2006.

Bunge, A.L. and Cleek, R.L. (1995). A new method for estimating dermal absorption from chemical exposure. 2. Effect of molecular weight and octanol-water partitioning. *Pharm Res*, 12:87-94.

Bunge, A.L., Cleek, R.L. and Vecchia, B.E. (1995a). A new method for estimating dermal absorption from chemical exposure. 3. Compared with steady-state methods for prediction and data analysis. *Pharm Res*, 12:972-982.

Bunge, A.L., Cleek, R.L. and Vecchia, B.E. (1995b). A new method for estimating dermal absorption from chemical exposure. 3. Compared with steady-state methods for prediction and data analysis. *Pharm Res*, 12:972-982.

Bunge, A.L., Flynn, G.L. and Guy, R.H. (1994). A predictive model for dermal exposure assessment. In: *Drinking Water Contamination and Health: Integration of Exposure Assessment, Toxicology and Risk Assessment*, (R.G.M. Wang, ed.), Marcel Dekker, New York, NY, pp. 347-374.

Bunge, A.L. and McDougal, J.N. (1999). Dermal uptake. In: *Exposure to Contaminants in Drinking Water: Estimating Uptake through the Skin and by Inhalation*, (S. Olin, ed.), CRC Press, Boca Raton, FL, pp. 137-181.

Bunge, A.L. and Parks, J.M. (1997). Predicting dermal absorption from chemically contaminated soils. In: *Environmental Toxicology and Risk Assessment: Modeling and Risk Assessment*, (F.J. Dwyer, T.R. Doane and M.L. Hinman, eds.), Vol. 6, ASTM STP 1317, ASTM, W. Conshohocken, PA, pp. 227-244.

Bunge, A.L. and Parks, J.M. (1998). Soil contamination: Theoretical descriptions. In: *Dermal Absorption and Toxicity Assessment*, (M.S. Roberts and K.S. Walters, eds.), Marcel Dekker, New York, NY, pp. 669-696.

Chiang, C.M., Flynn, G.L., Weiner, N.D. and Szpunar, G.J. (1989). Bioavailability assessment of topical delivery systems: effect of inter-subject variability on relative In vitro deliveries of minoxidil and hydrocortisone from solution and ointment formulations. *Int J Pharm*, 50:21-26.

Cleek, R.L. and Bunge, A.L. (1993). A new method for estimating dermal absorption from chemical exposure. 1. General approach. *Pharm Res*, 10:497-506.

Curdy, C., Kalia, Y.N., Falson-Rieg, F. and Guy, R.H. (2000). Recovery of human skin impedance in vivo after iontophoresis: Effect of metal ions. *AAPS Pharmsci*, 2:article 23.

Davies, D.J., Ward, R.J. and Heylings, J.R. (2004). Multi-species assessment of electrical resistance as a skin integrity marker for in vitro percutaneous absorption studies. *Toxicol In Vitro*, 18:351.

DeNuzzio, J.D. and Berner, B. (1990). Electrochemical and iontophoretic studies of human skin. *J Controlled Release*, 11:105-112.

Dugard, P.H., Walker, M., Mawdsley, S.J. and Scott, R.C. (1984). Absorption of some glycol ethers through human skin in vitro. *Environ Health Perspect*, 57:193-197.

Durbha, M., Orazem, M.E. and Garcia-Rubio, L.H. (1997). Spectroscopy Applications of the Kramers-Kronig Transforms: Implications for Error Structure Identification. *J Electrochem Soc*, 144:48-55.

Essa, E.A., Bonner, M.C. and Barry, B.W. (2002). Human skin sandwich for assessing shunt route penetration during passive and iontophoretic drug and liposome delivery. *J Pharm Pharmacol*, 54:1481-1490.

Fiserova-Bergerova, V., Pierce, J.T. and Droz, P.O. (1990). Dermal absorption potential of industrial chemicals: criteria for skin notation. *Am J Ind Med*, 17:617-635.

Fiserova, B.V. (1993). Relevance of occupational skin exposure. *Ann Occup Hyg*, 37:673-685.

Flynn, G.L. (1990). Physicochemical determinants of skin absorption. In: *Principles of Route-to-Route Extrapolation for Risk Assessment*, (T.R. Gerrity and C.J. Henry, eds.), Vol. 12, Elsevier, New York, NY, pp. 93-127.

Ghanem, A.-H., Mahmoud, H., Higuchi, W.I., Rohr, U.D., Borsadia, S., Liu, P., Fox, J.L. and Good, W.R. (1987). The effects of ethanol on the transport of beta-estradiol and other permeants in hairless mouse skin II. A new quantitative approach. *J Controlled Release*, 6:75-83.

Grandjean, P., Berlin, A., Gilbert, M. and Penning, W. (1988). Preventing percutaneous absorption of industrial chemicals: The "skin" denotation. *Am J Ind Med*, 14:97-107.

Green, D.M. and Brain, K.R. (2006). Does pre-study water permeability correlate with subsequent test compound permeation and what is a suitable limit for water Kp? (K.R. Brain and K.A. Walters, eds.), STS Publishing, Cardiff, UK, Perspectives in Percutaneous Penetration (PPP) 2006, La Grande Motte, France, pp. 45.

Hadgraft, J., Beutner, D. and Wolff, H.M. (1993). In vivo-in vitro comparisons in the transdermal delivery of nitroglycerin. *Int J Pharm*, 89:R1-R4.

Hadgraft, J., Hadgraft, J.W. and Sarkany, I. (1972). The effect of glycerol on the percutaneous absorption of methyl nicotinate. *Br J Dermatol*, 87:30-36.

Hadgraft, J., Hadgraft, J.W. and Sarkany, I. (1973). The effect of thermodynamic activity on the percutaneous absorption of methyl nicotinate from water glycerol mixtures. *J Pharm Pharmacol*, 25:122P-123P.

Hadgraft, J. and Ridout, G. (1987). Development of model membranes for percutaneous absorption measurements: I. Isopropyl myristate. *Int J Pharm*, 39:149-156.

Hadgraft, J. and Wolff, H.M. (1998). *In vitro/in vivo* correlations in transdermal drug delivery. In: *Dermal Absorption and Toxicity Assessment*, (M.S. Roberts and K.A. Walters, eds.), Drugs and the Pharmaceutical Sciences, Vol. 91, Marcel Dekker, New York, pp. 269-279.

Hirschorn, B., Orazem, M.E., Tribollet, B., Vivier, V., Frateur, I. and Musiani, M. (2009). Dermination of effective capacitance and film thickness from CPE parameters. *Electrochimica Acta*, submitted.

Hsu, C.H. and Mansfeld, F. (2001). Technical note: Concerning the conversion of the constant phase element parameter Y_0 into a capacitance. *Corrosion*, 57:747-748.

Huang, V.M.-W., Vivier, V., Orazem, M.E., Pebere, N. and Tribollet, B. (2007). The Apparent Constant-Phase-Element Behavior of an Ideally Polarized Blocking Electrode: A Global and Local Impedance Analysis. *J Electrochem Soc*, 154:C81-C88.

Islam, M.S., Zhao, L., McDougal, J.N. and Flynn, G.L. (1995). Uptake of chloroform by skin during short exposures to contaminated water. *Risk Anal*, 15:343-352.

Islam, M.S., Zhao, L., Zhou, J., Dong, L., McDougal, J.N. and Flynn, G.L. (1996). Systemic uptake and clearance of chloroform by hairless rats following dermal exposure. I. Brief exposure to aqueous solutions. *Risk Anal*, 16:349-357.

Jakasa, I., Mohammadi, N., Krüse, J. and Kezic, S. (2004). Percutaneous absorption of neat and aqueous solutions of 2-butoxyethanol in volunteers. *Int Arch Occup Environ Health*, 77:79-84.

Johanson, G., Boman, A. and Dynesius, B. (1988). Percutaneous absorption of 2-butoxyethanol in man. *Scand J Work Environ Health*, 14:101-109.

Johanson, G. and Fernstrom, P. (1988). Influence of water on the percutaneous absorption of 2-butoxyethanol in guinea pigs. *Scand J Work Environ Health*, 14:95-100.

Kasting, G.B., Smith, R.L. and Cooper, E.R. (1987). Effect of lipid solubility and molecular size on percutaneous absorption. In: *Skin Pharmacokinetics*, (B. Shroot and H. Schaefer, eds.), Karger, Basel, pp. 138-153.

Kim, H.S. and Oh, S.Y. (2000). Effect of nonionic surfactants on the transdermal flux of ketoprofen. American Association of Pharmaceutical Scientists (AAPS) Annual Meeting, Indianapolis, IN Oct. 29 - Nov. 2, 2000.

Koga, Y. (1991). Vapor pressures of aqueous 2-butoxyethanol solutions at 25°C: Transition in mixing scheme. *J Phys Chem*, 95:4119-4126.

Kontturi, K. and Murtomaki, L. (1994). Impedance Spectroscopy in Human Skin. A Refined Model. *Pharm Res*, 11:1355-1357.

Korinth, G., Schaller, K.H. and Drexler, H. (2005). Is the permeability coefficient K_p a reliable tool in percutaneous absorption studies? *Arch Toxicol*, 79:155-159.

Larese, F., Gianpietro, A., Venier, M., Maina, G. and Renzi, N. (2007). In vitro percutaneous absorption of metal compounds. *Toxicol Lett*, 170:49-56.

Larese, F.F., D'Agostin, F., Crosera, M., Adami, G., Renzi, N., Bovenzi, M. and Maina, G. (2009). Human skin penetration of silver nanoparticles through intact and damaged skin. *Toxicology*, 255:33-37.

Liron, Z., Wright, R.W. and McDougal, J.N. (1994a). A mathematical model for water vapor sorption kinetics in porcine stratum corneum. *J Pharm Sci*, 83:692-698.

Liron, Z., Wright, R.W. and McDougal, J.N. (1994b). Water diffusivity in porcine stratum corneum measured by a thermal graivemetric analysis (TGA) technique. *J Pharm Sci*, 83:457-462.

Macdonald, J.R., ed. (1987). *Impedance Spectroscopy: Emphasizing Solid Materials and Analysis,* John Wiley & Sons, New York.

McCarley, K.D. and Bunge, A.L. (1998). Physiologically relevant one-compartment pharmacokinetic models for skin. 1. Development of models. *J Pharm Sci*, 87:470-481.

McCarley, K.D. and Bunge, A.L. (2000). Physiologically relevant two-compartment models for skin. *J Pharm Sci*, 89:1212-1235.

McCarley, K.D. and Bunge, A.L. (2001). Pharmacokinetic models for skin -- A review. *J Pharm Sci*, 90:1699-1719.

Moghimi, H.R., Williams, A.C. and Barry, B.W. (1996). A lamellar matrix model for stratum corneum intercellular lipids. II. Effect of geometry of the stratum corneum on permeation of model drugs 5-fluorouracil and oestradiol. *Int J Pharm*, 131:117-129.

Nakai, J., Chu, I., Moir, D. and Moody, R.P. (1995). Dermal absorption of chemicals into freshly-prepared and frozen human skin.

NIOSH (2000). National Occupational Research Agenda (NORA) Developing Dermal Policy Based on Laboratory and Field Studies. DHHS (NIOSH) Publication NO. 2000-142, origin.cdc.gov/niosh/topics/skin/pdfs/NORADermal-2.pdf, accessed 07/28/2009.

NIOSH (2007a). Evidence for the National Academies' Review of the NIOSH Personal Protective Technology Program. CDC/NIOSH, www.cdc.gov/niosh/nas/ppt/pdfs/PPT_EvPkg_090707_FinalR.pdf, accessed 07/28/2009.

NIOSH (2007b). NIOSH Pocket Guide to Chemical Hazards. NIOSH Publication 2005-149, September 2007 (with minor technical changes from September 2005), http://www.cdc.gov/niosh/npg/, accessed 07/28/2009.

NIOSH (2009). Current Intelligence Bulletin 61: A Strategy for Assigning New NIOSH Skin Notations. DHHS (NIOSH) Publication No. 2009-147, http://www.cdc.gov/niosh/docs/2009-147/default.html (accessed 07/28/2009).

Novotny, J., Kovarikova, P., Novotny, M., Janusova, B., Hrabalek, A. and Vavrova, K. (2009). Dimethylamino acid esters as biodegradable and reversible transdermal permeation enhancers: Effects of linking chain length, chirality and polyfluorination. *Pharm Res*, 26:811-821.

OECD (2004). *OECD Guideline for the Testing of Chemicals. Guidline 430: In Vitro Skin Corrsion: Transcutaneous Electrical Resistance Test (TER)*, (adopted 13th April 2004).

Oh, S.Y., Leung, L., Bommannan, D., Guy, R.H. and Potts, R.O. (1993). Effect of current, ionic strength and temperature on the electrical properties of skin. *J Controlled Release*, 27:115-125.

Orazem, M.E. (2001). *User Manual for the Measurement Model Toolbox for Impedance Spectroscopy*, University of Florida, Gainesville, FL.

Orazem, M.E. (2004). A systematic approach toward error structure identification for impedance spectroscopy. *Journal of Electroanalytical Chemistry*, 572:317-327.

Orazem, M.E., Agarwal, P., Deslouis, C. and Tribollet, B. (1996a). Application of Measurement Models to Electrohydrodynamic Impedance Spectroscopy. *J Electrochem Soc*, 143:948-960.

Orazem, M.E., Moustafid, T.E., Deslouis, C. and Tribollet, B. (1996b). The Error Structure of Impedance Spectra for Systems with a Large Ohmic Resistance with Respect to the Polarization Impedance. *J Electrochem Soc*, 143:3880-3890.

Orazem, M.E., Pebere, N. and Tribollet, B. (2006). Enhanced Graphical Representation of Electrochemical Impedance Data. *J Electrochem Soc*, 153:B129-B136.

Ostrenga, J., Haleblian, J., Poulsen, B., Ferrell, B., Mueller, N. and Shastri, S. (1971a). Vehicle design for a new topical steroid fluocinonide. *J Invest Dermatol*, 56:392-399.

Ostrenga, J., Steinmetz, C. and Poulsen, B. (1971b). Significance of vehicle composition I: Relationship between topical vehicle composition, skin permeability, and clinical efficacy. *J Pharm Sci*, 60:1175-1179.

Ostrenga, J., Steinmetz, C., Poulsen, B. and Yett, S. (1971c). Significance of vehicle composition II: Prediction of optimal vehicle composition. *J Pharm Sci*, 60:1180-1183.

Parry, G.E., Bunge, A.L., Silcox, G.D., Pershing, L.K. and Pershing, D.W. (1990). Percutaneous absorption of benzoic acid across human skin. I. In vitro experiments and mathematical modeling. *Pharm Res*, 7:230-236.

Peck, K.D., Ghanem, A.H. and Higuchi, W.I. (1995). The effect of temperature upon the permeation of polar and ionic solutes through human epidermal membrane. *J Pharm Sci*, 84:975-982.

Peck, K.D., Ghanem, A.H., Higuchi, W.I. and Srinivasan, V. (1993). Improved stability of the human epidermal membrane during successive permeability experiments. *Int J Pharm*, 98:141-147.

Pirot, F., Kalia, Y.N., Stinchcomb, A.L., Keating, G., Bunge, A. and Guy, R.H. (1997). Characterization of the permeability barrier of human skin in vivo. *Proc Nat Acad Sci USA*, 94:1562-1567.

Potts, R.O. and Guy, R.H. (1992). Predicting skin permeability. *Pharm Res*, 9:663-669.

Potts, R.O. and Guy, R.H. (1995). A predictive algorithm for skin permeability: The effects of molecular size and hydrogen bond activity. *Pharm Res*, 12:1628-1633.

Poulsen, B.J. (1972). Diffusion of drugs from topical vehicles: An analysis of vehicle effects. In: *Pharmacology and the Skin*, (W. Montagna, E.J. Van Scott and R.B. Stoughton, eds.), Advances in Biology of Skin, Vol. 12, Meredith Corporation, New York, N Y, pp. 495-509.

Poulsen, B.J. (1973). Design of topical drug products: Biopharmaceutics. In: *Drug Design*, (E.J. Ariëns, ed.), Vol. Volume IV, Academic Press, New York, London, pp. 149-192.

Prausnitz, J.M. (1969). *Molecular Thermodynamics of Fluid-Phase Equilibria*, Prentice-Hall, Englewood Cliffs, NJ.

Reddy, M.B., McCarley, K.D. and Bunge, A.L. (1998). Physiologically relevant one-compartment pharmacokinetic models for skin. 2. Comparison of models when combined with a systemic pharmacokinetic model. *J Pharm Sci*, 87:482-490.

Reddy, M.B., Stinchcomb, A.L., Guy, R.H. and Bunge, A.L. (2002). Determining dermal absorption parameters *in vivo* from tape stripping data. *Pharm Res*, 19:292-297.

Rigg, P.C. and Barry, B.W. (1990). Shed snake skin and hairless mouse skin as model membranes for human skin during permeation studies. *J Invest Dermatol*, 94:235-240.

Roberts, M.S. and Walters, K.A. (1998). The relationship between structure and barrier function of skin. In: *Dermal Absorption and Toxicity Assessment*, (M.S. Roberts and K.A. Walters, eds.), Drugs and the Pharmaceutical Sciences, Vol. 91, Marcel Dekker, New York, pp. 1-42.

Romonchuk, W.J. and Bunge, A.L. (2006). Enhanced dermal permeation of 4-cyanophenol and methyl paraben from saturated aqueous solution containing both solutes. (K.R. Brain and K.A. Walters, eds.), Vol. 10a, STS Publishing, Perspectives in Percutaneous Penetration (PPP), La Grande Motte, France April 19-22, 2006.

Romonchuk, W.J. and Bunge, A.L. (2009). Mechanism of enhanced dermal permeation of 4-cyanophenol and methyl paraben from saturated aqueous solutions containing both solutes. *Skin Pharmcol Physiol*, in revision.

Scanseti, G., Pilatto, G. and Rubino, G.F. (1988). Skin notation in the context of workplace exposure standards. *Am J Ind Med*, 14:725-732.

Scheuplein, R.J. and Blank, I.H. (1973). Mechanism of percutaneous absorption. IV. Penetration of nonelectrolytes (alcohols) from aqueous solutions and from pure liquids. *J Invest Dermatol*, 60:286-296.

Scott, R.C., Batten, P.L., Clowes, H.M., Jones, B.K. and Ramsey, J.D. (1992). Further validation of an in vitro method to reduce the need for in vivo studies for measuring the absorption of chemicals through rat skin. *Fundam Appl Toxicol*, 19:484-492.

Scott, R.C. and Ramsey, J.D. (1987). Comparison of the in vivo and in vitro percutaneous absorption of a lipophilic molecule (cypermethrin, a pyrethroid insecticide). *J Invest Dermatol*, 89:142-146.

Silcox, G.D., Parry, G.E., Bunge, A.L., Pershing, L.K. and Pershing, D.W. (1990). Percutaneous absorption of benzoic acid across human skin. II. Prediction of an in vivo, skin-flap system using in vitro parameters. *Pharm Res*, 7:352-358.

Sims, S.M., Higuchi, W.I. and Srinivasan, V. (1991). Skin alteration and convective solvent flow effects during iontophoresis: I. Neutral solute transport across human skin. *Int J Pharm*, 69:109-121.

Theeuwes, F., Gale, R. and Baker, R. (1976). Transference: A comprehensive parameter governing permeation of solutes through membranes. *J Membr Sci*, 1:3-16.

Tojo, K. and Lee, A.C. (1989). A method for predicting steady-state rate of skin penetration in vivo. *J Invest Dermatol*, 92:105-108.

Traynor, M.J., Wilkinson, S.C. and Williams, F.M. (2007a). Corrigendum to "The influence of water mixtures on the dermal absorption of glycol ethers". *Toxicol Appl Pharmacol*, 221:129.

Traynor, M.J., Wilkinson, S.C. and Williams, F.M. (2007b). The influence of water mixtures on the dermal absorption of glycol ethers. *Toxicol Appl Pharmacol*, 218:128-34.

Twist, J.N. and Zatz, J.L. (1986). Influence of Solvents on Paraben Permeation Through Idealized Skin Model Membranes. *J Soc Cosmet Chem*, 37:429-444.

US EPA (1992). *Dermal Exposure Assessment: Principles and Applications*, EPA/600/8-91/011B, Exposure Assessment Group, Office of Health and Environmental Assessment, Office of Research and Development, Washington, DC.

US EPA (1998a). *Guidelines for Nuerotoxicity Risk Assessment*, EPA/630/R-95/001F, Risk Assessment Forum, Washington, DC.

US EPA (1998b). *Guidelines for Reproductive Toxicity Risk Assessment*, EPA/630/R-96/009, Washington, DC.

US EPA (1998c). *Risk Assessment Guidance for Superfund, Volume I: Human Health Evaluation Manual, Supplemental Guidance, Dermal Risk Assessment, Interim Guidance*, NCEA-W-0364/External Review Draft, Office of Emergency and Remedial Response, Washington, DC.

US EPA (2004). In vitro dermal absorption rate testing of certain chemicals of interest to the occupational safety and health administration, pp. 22402-22441. Federal Register, Volume 69, Number 80, April 26, 2004.

US EPA (2005). *Guidelines for Carcinogen Risk Assessment,* EPA/630/P-03/001F, Risk Assessment Forum, US Environmental Protection Agency, Washington, DC.

Vecchia, B.E. (1997). *Estimating Dermal Absorption: Data Analysis, Parameter Estimation, and Sensitivity to Parameter Uncertainties.* M.S. Thesis, Colorado School of Mines, Golden, Colorado.

Vecchia, B.E. and Bunge, A.L. (2002a). Evaluating the transdermal permeability of chemicals. In: *Transdermal Drug Delivery Systems,* 2nd, (J. Hadgraft and R.H. Guy, eds.), Marcel Dekker, New York, pp. 25-55.

Vecchia, B.E. and Bunge, A.L. (2002b). Partitioning of chemicals into skin: Results and prediction. In: *Transdermal Drug Delivery Systems,* 2nd, (J. Hadgraft and R.H. Guy, eds.), Marcel Dekker, New York, pp. 143-198.

Vecchia, B.E. and Bunge, A.L. (2002c). Skin absorption databases and predictive equations. In: *Transdermal Drug Delivery Systems,* 2nd, (J. Hadgraft and R.H. Guy, eds.), Marcel Dekker, New York, pp. 57-141.

Warner, K.S., Li, S.K. and Higuchi, W.I. (2001). Influences of alkyl group chain length and polar head group on chemical skin permeation enhancement. *J Pharm Sci,* 90:1143-1153.

Wertz, P.W. (2000). Lipids and barrier function of the skin. *Acta Derm Venereol Suppl,* 208:7-11.

Wertz, P.W. and van den Bergh, B. (1998). The physical, chemical and functional properties of lipids in the skin and other biological barriers. *Chem Phys Lipids,* 91:85-96.

Wilkinson, S.C. and Williams, F.M. (2002). Effects of experimental conditions on absorption of glycol ethers through human skin in vitro. *Int Arch Occup Environ Health,* 75:519-27.

Williams, A.C. and Barry, B.W. (1998). Chemical penetration enhancement: Possibilities and problems. In: *Dermal Absorption and Toxicity Assessment,* (M.S. Roberts and K.A. Walters, eds.), Drugs and the Pharmaceutical Sciences, Vol. 91, Marcel Dekker, New York, pp. 297-312.

Yamamoto, T. and Yamamoto, Y. (1976). Electrical properties of the epidermal stratum corneum. *Med Biol Eng,* 14:151-158.

Publications

Beach JD, Bunge AL, Orazem ME: [2006] Evidence that pores are the primary conductive pathway in human skin. Paper no. 1174, Published proceedings. The Electrochemical Society (ECS) 209th Meeting, Denver, CO, May 7-12.

JD Beach JD, Orazem ME, Bunge AL: [2006] Evidence that pores are the primary conductive pathway in human skin. Perspectives in Percutaneous Penetration (PPP), 2006, Vol 10A, Eds. KR Brain and KW Walters, STS Publishing, Cardiff, UK. Conference Proceedings, la Grande Motte, France, April 18-22.

Bunge AL:[2006] Why skin permeation data from neat and aqueous solutions of 2-butoxyethanol are not surprising. Perspectives in Percutaneous Penetration (PPP), 2006, Vol 10A, Eds. KR Brain and KW Walters, STS Publishing, Cardiff, UK. Conference Proceedings, la Grande Motte, France, April 18-22.

Romonchuk WJ, Bunge AL: [2006] Enhanced dermal permeation of 4-cyanophenol and methyl paraben from saturated aqueous solutions containing both solutes. Perspectives in Percutaneous Penetration (PPP), 2006, Vol 10A, Eds. KR Brain and KW Walters, STS Publishing, Cardiff, UK. Conference Proceedings, la Grande Motte, France, April 18-22.

Bunge AL: [2006] Skin exposure to chemicals: The effect of vehicle and why concentration might not be a good indicator of skin permeation. Australian Institute of Occupational Hygienists (AIOH) Annual Conference, Surfers Paradise Marriott Resort, Queensland, December 2-6.

Bunge AL: [2006] Contributing Author, Environmental Health Criteria 235, Dermal Absorption., International Programme on Chemical Safety, World Health Organization.

Bunge AL: [2007] Explaining skin permeation of 2-butoxyethanol from neat and aqueous solutions, A.L. Bunge, Occupational and Environmental Exposure of Skin to Chemicals (OEESC)-2007, Golden, CO, June 17-20.

Bunge AL: [2007] Estimating dermal absorption from finite volume exposures. Occupational and Environmental Exposure of Skin to Chemicals (OEESC)-2007, Golden, CO, June 17-20, 2007.

Romonchuk WJ, Bunge AL: [2007] Mechanisms of enhanced dermal permeation of 4-cyanophenol and methyl paraben from saturated aqueous solutions containing both solutes. Occupational and Environmental Exposure of Skin to Chemicals (OEESC)-2007, Golden, CO, June 17-20.

Bunge AL: [2007] Skin delivery of drugs: Basic principles, A.L. Bunge, Proc. 6th International Congress of Pharmaceutical Sciences, University of Sao Paolo, Ribeirão Preto, Sao Paolo, Brazil, September 2-5.

Inclusion of Gender and Minority Study Subjects

Human skin used in these studies was collected post mortem and acquired through the National Disease Research Interchange (NDRI). The diversity of skin sources depended on what was available to NDRI. Approximately half of the skin was from females; during the study period of this research we received no skin from minority subjects.

Inclusion of Children

No skin used in these studies was collected from children.

Materials Available for Other Investigators

All data, protocols and computational algorithms developed as part of this grant will be shared with other investigators. These resources will be made available through refereed publications, conference abstracts and presentations, and upon direct request by interested investigators.